

See discussions, stats, and author profiles for this publication at: <https://www.researchgate.net/publication/7911030>

About Supramolecular Assemblies of π -Conjugated Systems

ARTICLE *in* CHEMICAL REVIEWS · MAY 2005

Impact Factor: 46.57 · DOI: 10.1021/cr030070z · Source: PubMed

CITATIONS

1,878

READS

442

4 AUTHORS, INCLUDING:



Pascal Jonkheijm

University of Twente

131 PUBLICATIONS 6,924 CITATIONS

[SEE PROFILE](#)



Albertus P H J Schenning

Technische Universiteit Eindhoven

295 PUBLICATIONS 14,158 CITATIONS

[SEE PROFILE](#)

About Supramolecular Assemblies of π -Conjugated Systems

Freek J. M. Hoeben, Pascal Jonkheijm, E. W. Meijer,* and Albertus P. H. J. Schenning

Laboratory of Macromolecular and Organic Chemistry, Eindhoven University of Technology, P.O. Box 513, 5600 MB Eindhoven, The Netherlands

Received June 24, 2004

Contents

1. Introduction	1491
2. Chemical Structures of π -Conjugated Systems	1492
3. Self-Assembly Principles of π -Conjugated Systems	1493
4. Nature's Design of Multicomponent Systems	1494
5. Polymers versus Oligomers	1495
6. Supramolecular Organization of π -Conjugated Polymers	1496
6.1. Self-Assembly of Homopolymers	1496
6.1.1. Thermotropic Liquid Crystallinity	1496
6.1.2. Solvatochromism and Thermochromism	1496
6.1.3. Chirality	1496
6.1.4. Ionochromism	1498
6.2. Self-Assembly of Block Copolymers	1499
6.2.1. Polydisperse π -Conjugated Blocks	1499
6.2.2. Monodisperse Main-Chain π -Conjugated Blocks	1501
6.2.3. Monodisperse Side-Chain π -Conjugated Blocks	1504
6.3. Aided-Assembly of π -Conjugated Polymers	1505
7. Supramolecular Organization of π -Conjugated Oligomers	1508
7.1. Self-Assembly of Liquid-Crystalline Materials	1508
7.1.1. Thermotropic Rodlike Molecules	1508
7.1.2. Thermotropic Discotic Molecules	1509
7.1.3. Lyotropic Liquid Crystals	1512
7.2. Self-Assembly by Specific Interactions in Solution	1515
7.2.1. Assembly by $\pi-\pi$ Interactions	1515
7.2.2. Assembly by Amphiphilic Interactions	1516
7.2.3. Assembly by Hydrogen Bonding	1518
8. Supramolecular Organization of Multicomponent Systems	1521
8.1. Assembly in Organic Devices	1523
8.2. Assembly by Liquid Crystallinity	1525
8.2.1. Mixed Liquid Crystals	1525
8.2.2. Covalent Donor–Acceptor Liquid Crystals	1527
8.3. Assembly in Mixed Gels	1530
9. Supramolecular Organization of Nanoscopic Multicomponent Systems in Solution	1531
9.1. Assembly by $\pi-\pi$ Interactions	1532
9.2. Aided-Assembly Using DNA, RNA, or PNA	1533
9.3. Assembly of Mixed Porphyrins	1533
9.4. Assembly by Hydrogen Bonding	1535
10. Conclusions and Prospects	1538
11. Acknowledgment	1538
12. Note Added after ASAP Publication	1538
13. References	1538

1. Introduction

With the introduction of π -conjugated systems in electronic devices and the dream to arrive at molecular electronics based on these systems, the detailed understanding of the supramolecular interactions between the individual π -conjugated molecules has become one of the most challenging scientific research areas. As a result, nanoscience and nanotechnology are logically merged and academic and industrial endeavors are moving hand in hand. In an unprecedented way, the synthesis of new molecules is guided by the results of device physicists, while devices show improved performance due to progress in the synthesis of new materials. However, the different hierarchies of organization going from molecules to devices have been addressed to a much lesser extent, while it is generally accepted as being the most critical issue. For electronic devices made out of π -conjugated systems the interchain electronic coupling will determine the device performance. Not only is a perfect fit between the π -conjugated elements required, but also the anisotropy of the electronic coupling is equally important for a macroscopic performance of these mainly two-dimensional (semi-)conductors. It is an enormous challenge to obtain monodomain ordered structures in the micrometer regime. Only in that way control over all length scales in organic electronic devices is achieved. In general, the average size of crystalline-like domains is within the range of a few hundreds of nanometers. Knowledge of this scope and limitations of the ordering of π -conjugated systems at the different length scales has brought the area of supramolecular electronics¹ to the fore: electronic devices based on individual supramolecular objects in the 5–100 nm regime. This is an area between devices based on thin films of organic materials and molecular electronics based on single molecules.

The aim of this review is to bring together the areas of supramolecular assembly and π -conjugated systems. Both polymers and oligomers are reviewed but only in their relation to achieving supramolecular organization of more than a few molecules. Therefore, this review focuses on the self-assembly and properties of nanoscopic structures of π -conjugated systems.

* To whom correspondence should be addressed. Fax: +31-40-2451036. E-mail: E.W.meijer@tue.nl.



Freek J. M. Hoeben (second from right) received his M.Sc. degree in Chemical Engineering and Chemistry at the Eindhoven University of Technology in 2001, where he did his undergraduate work in the group of Prof. Dr. E. W. Meijer on energy transfer in oligomeric π -conjugated assemblies. His current research interests lie in the use of supramolecular chemistry to obtain functional nanoscopic objects for artificial photosynthesis and supramolecular electronics. He is currently completing his Ph.D. research in the group of Prof. Dr. E. W. Meijer, which is focused on energy and electron transfer in supramolecular π -conjugated architectures.

Pascal Jonkheijm (left) studied Chemical Engineering and Chemistry at the University of Eindhoven from 1996 to 2001. After finishing his undergraduate thesis he stayed in the group of Prof. Dr. E. W. Meijer, Laboratory of Macromolecular and Organic Chemistry, to complete his Ph.D. research. During these years his research interests have been in macromolecular engineering of π -conjugated oligomers via supramolecular interactions into nanoscopic objects. He is a laureate of the DSM awards for chemistry and technology. His thesis will focus on developing guidelines to program π -conjugated oligomers into supramolecular architectures in solution. A stay in the groups of Prof. R. Lazzaroni and Prof. F. C. DeSchryver enabled him to study scanning-probe techniques, allowing him to investigate the supramolecular assemblies in the solid state in great detail.

E. W. "Bert" Meijer (right) is professor of Macromolecular and Organic Chemistry at Eindhoven University of Technology, The Netherlands. He received his Ph.D. degree in Organic Chemistry at the University of Groningen in 1982 with Prof. Hans Wynberg. He was a research scientist in the area of optoelectronic materials at Philips Research Laboratories from 1982 to 1989 and group leader of new polymeric materials at DSM Research from 1989 to 1992. Since 1992 he has been a full professor in Eindhoven, and since 1995 he has also been an adjunct professor at the University of Nijmegen. His research interests are in dendrimers, supramolecular systems, and organic materials for electronics. For further information, consult the www.chem.tue.nl/smo website of the laboratory of Macromolecular and Organic Chemistry.

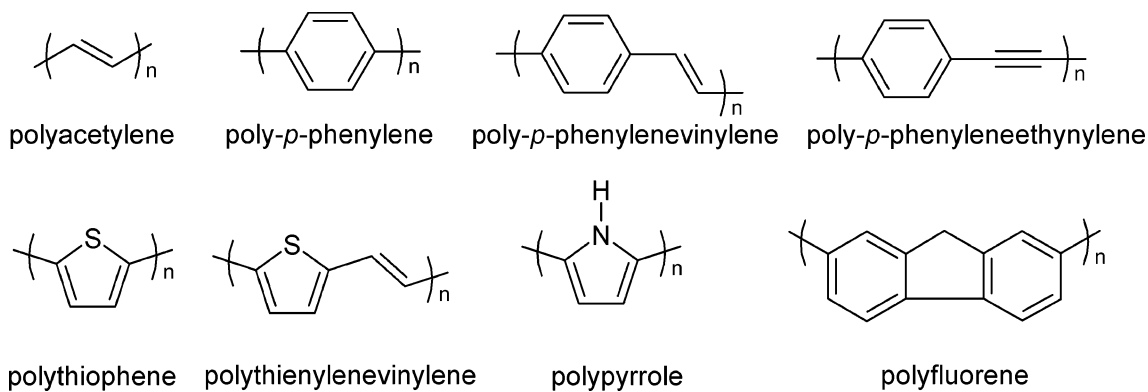
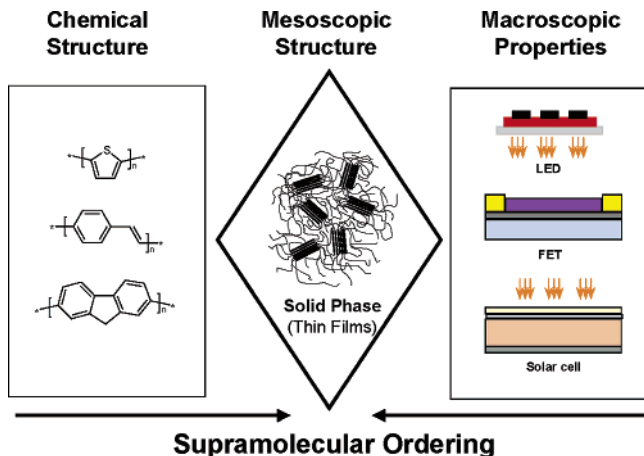
Dr. Albert P. H. J. Schenning (second from left) is an assistant professor in the Laboratory of Macromolecular and Organic Chemistry at Eindhoven University of Technology. His research interests center on plastic and supramolecular electronics. He received his Ph.D. degree at the University of Nijmegen in 1996 on supramolecular architectures based on porphyrin and receptor molecules with Dr. M. C. Feiters and Prof. Dr. R. J. M. Nolte. Between June and December 1996 he was a postdoctoral fellow in the group of Prof. Dr. E. W. Meijer at Eindhoven University of Technology working on dendrimers. In 1997 he joined the group of Prof. Dr. F. Diederich at the ETH in Zurich, where he investigated π -conjugated oligomers and polymers based on triacetylenes. From 1998 until 2002 he was a KNAW fellow at Eindhoven University of Technology (Laboratory of Macromolecular and Organic Chemistry), active in the field of the supramolecular organization of π -conjugated oligomers. In 2004 he received the European Young Investigators Award from the European Heads of Research Councils and the European Science Foundation.

2. Chemical Structures of π -Conjugated Systems

π -Conjugated (semiconducting) polymers are by far the most promising functional polymers in view of applications in less expensive and flexible electronic devices. Prototype field-effect transistors (FET)s,² light-emitting diodes (LED)s,^{3,4} photovoltaic cells,⁵ and related devices have already been fabricated, and Philips introduced the first commercial LED based on polymer technology in 2002. Nowadays a plethora of conjugated polymers exists having a base structure of alternating single and double/triple bonds of which some parent structures are shown in Figure 1.⁶

The performance of organic devices is mainly determined by the chemical structure, purity, and supramolecular organization or morphology of the π -conjugated material. This dependence is not unique for semiconducting materials but also valid for functional polymers in general. However, the importance of control of structure at every structural hierarchy is by far the most delicate for semiconducting polymers. Going from isolated chains to an intermolecular hierarchy, charge transfer between chains is required for conduction in a "microcrystalline" or mesoscopic phase. To arrive at controlled microcrystallinity, it is necessary to have (latent) solubilizing groups, and nowadays a number of ways to control solubility are known. Whereas side chains are useful at the mesoscopic level of microcrystallization, they are sometimes detrimental for the macroscopic ordering. It is evident that materials research in the area of semiconducting polymers is only useful when macromolecular engineering by organic synthesis is combined with investigations to control molecular architecture at all levels of hierarchy (Figure 2).

The versatility of substituted conjugated polymers has led to tunable physical properties (color, emission efficiency, etc.) by major improvements in polymer synthesis.⁷ Improved purity and a decreasing number of defects, such as tetrahedral carbon centers that interrupt conjugation, photodamage, or end groups, have a positive influence on the conformational freedom of conjugated chains.^{8–14} Side-chain variation on the polymer backbone has been studied in terms of steric hindrance and electronic effects and related to morphology and charge-carrier mobility.^{15–20} For instance, bulky alkyl substituents directly linked to the conjugated rod hampers a planar conformation.^{21–24} Systems employing linear or branched side-chain substituents have been compared based on their photophysics and charge transport, the linear substituents showing emission at higher wavelength due to formation of π -stacked aggregates, while the branched substituents show blue-shifted emission lacking higher order.^{25,26} The effects of the chemical composition of conjugated polymers on the supramolecular organization, i.e., the morphology of the active layer, are of major concern to further optimize the performance of the devices. This feature can nicely be illustrated with poly(3-alkylthiophene)s. Since polymerization procedures for regioregular poly(3-substituted-thiophene)s have improved considerably, it is clear that many functional properties are more pronounced for the regioregular material, being either head-to-tail^{27–29} or head-to-head/tail-to-

**Figure 1.** Chemical structures of several conjugated polymers.**Figure 2.** Schematic representation on how the properties of optoelectronic devices such as LEDs, FETs, and solar cells are related to chemical structure and supramolecular organization. Chemists and materials scientists have aimed for control of supramolecular organization of π -conjugated polymers by using chemical modification or various preparation methods.

tail,³⁰ due to an improved ordering of the planar conformation compared to the regioirregular polythiophene. The latter polymer, without defined inter-chain interactions, gave rise to low charge-carrier mobilities ($10^{-5} \text{ cm}^2/\text{V s}$), whereas the former, with lamellar arrays of polythiophene rods, gave significant higher mobilities ($0.01\text{--}0.1 \text{ cm}^2/\text{V s}$).^{31,32} However, the molecular weight of regioregular polythiophene has a substantial effect on the way that the chains pack with each other. As recently found by McGehee et al., low molecular weight polythiophene films have more defined grain boundaries, by rodlike crystalline features, than the isotropic nodules of the high molecular weight films, thereby creating a continuous pathway for charge carriers. This difference in morphology causes the mobility to rise by at least 4 orders of magnitude in a FET.^{33–35} In an engineering approach, variations in processing conditions³⁶ of the conjugated polymeric materials have realized tremendous progress in controlling the morphology of the active layer, also by introduction of alignment layers^{37,38} and thermal^{39–42} and mechanical⁴³ treatments. Nonetheless, most polymeric films are highly amorphous and inhomogeneous, resulting in small domains of 15–30 nm for polyfluorenes,⁴⁴ while for polypyridylvinylene,⁴⁵ polythiophenes,⁴⁶ and poly-*p*-phenylenevinylene⁴⁷ par-

tially aligned regions of the film of typically 200–300 nm in size are found. However, dimensions of devices are roughly in the micrometer regime. Therefore, additional instruments to control the morphology of the active layers are highly requested to improve performance. In the next section the ensemble of supramolecular interactions that may occur in π -conjugated polymers will be discussed with emphasis on preorganizing these polymers in mesoscopic domains. This ordering can be studied in solution, and these results can be extrapolated to polymeric thin films.

3. Self-Assembly Principles of π -Conjugated Systems

π -Conjugated systems built up from repeating units can roughly be divided into oligomers and polymers. The self-assembly of these systems has mainly been approached from both a materials and a supramolecular chemistry point of view.

Programmed self-assembly of π -conjugated oligomers has been achieved using supramolecular design rules. Supramolecular chemistry, a term introduced by Jean-Marie Lehn, is ‘chemistry beyond the molecule’, that is the chemistry of molecular assemblies using noncovalent bonds.⁴⁸ While a covalent bond normally has a homolytic bond dissociation energy that ranges between 100 and 400 kJ mol^{−1}, noncovalent interactions are generally weak and vary from less than 5 kJ mol^{−1} for van der Waals forces, through approximately 50 kJ mol^{−1} for hydrogen bonds, to 250 kJ mol^{−1} for Coulomb interactions (Table 1).

Two important secondary interactions in the design of supramolecular materials are π – π ⁵⁰ and hydrogen-bond interactions. Logically, π – π interactions often

Table 1. Strength of Several Noncovalent Forces⁴⁹

type of interaction or bonding	strength (kJ mol ^{−1})
covalent bond	100–400
Coulomb	250
hydrogen bond	10–65
ion–dipole	50–200
dipole–dipole	5–50
cation– π	5–80
π – π	0–50
van der Waals forces	<5
hydrophobic effects	difficult to assess
metal–ligand	0–400

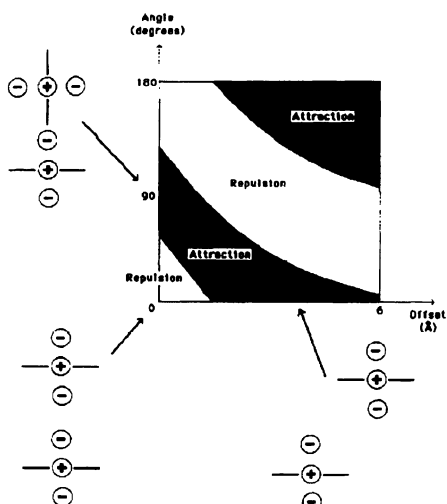


Figure 3. Interaction between two idealized p atoms as a function of orientation: two attractive geometries and the repulsive face-to-face geometry are illustrated. (Reprinted with permission from ref 51. Copyright 1990 American Chemical Society.)

exist in π -conjugated materials. The strength as well as the causes of these interactions, however, varies strongly. In water the stacking interaction between aromatic molecules is mainly caused by the hydrophobic effect. Water molecules solvating the aromatic surface have a higher energy than bulk water, resulting in stacking of the aromatic surfaces, which reduces the total surface exposed to the solvent. In solvents other than water the interactions between solvent molecules are weaker, and therefore, solvophobic forces play a minor role. Hunter and Sanders developed a practical model for $\pi-\pi$ interactions.⁵¹ In their model, which is entirely electrostatic, three point charges are assigned to the atoms in an aromatic molecule, one at the site of the atom (often a positively charged carbon atom) and one above and below the plane of the π system (π point charges of $-1/2$ each) (Figure 3). One of the important outcomes of this model is that geometries different from face-to-face have hardly been recognized in the design of supramolecular architectures.

Hydrogen bonds are ideal secondary interactions to construct supramolecular architectures since they are highly selective and directional. In nature, beautiful examples of these properties are present in DNA and proteins. Hydrogen bonds are formed when a donor (D) with an available acidic hydrogen atom is interacting with an acceptor (A) carrying available nonbonding electron lone pairs. The strength depends largely on the solvent and number and sequence of the hydrogen bonds.⁵²

The morphology of polymers has been mainly controlled using block copolymers.⁵³ The microphase separation of diblock polymers depends on the total degree of polymerization, the Flory–Huggins χ parameter, and the volume fraction of the constituent blocks. The segregation product χN determines the degree of microphase separation, and higher values give stronger segregation. By replacing one of the segments by a π -conjugated rigid unit, a rod–coil diblock polymer is obtained. The self-assembly of these polymers is also affected by the aggregation of

the π -conjugated segments. Furthermore, the stiffness asymmetry present in rod–coil diblock polymers results in an increase in the Flory–Huggins χ parameter. As a consequence, phase separation can already occur at lower molecular weights and for rigid segments consisting of a π -conjugated oligomer. For example, when a good solvent for both the rod and coil block is used during the processing, microphase separation will continuously compete with crystallization of the rod segment. If a solvent is used that is a good solvent for one of the blocks exclusively, the polymers will readily assemble in solution and this superstructure will determine the final morphology of the deposited film.

4. Nature's Design of Multicomponent Systems

Multicomponent systems are highly important in optoelectronic devices. For example, in solar cells the active layer consists of electron-donor and electron-acceptor components, while in LEDs the emissive wavelength can be tuned in a multicomponent fashion. In all these devices the organization of the different components will largely determine the macroscopic properties.

The way nature has mastered the art of ordering large numbers of molecules into functional systems remains unmatched. The light-harvesting photosynthetic system of higher plants is merely one example in which individual protein-bound pigments are organized into a highly efficient pathway for the transfer of excitation energy.^{54,55} A highly symmetrical organization of chromophores is also observed in the photosystem of purple bacteria (Figure 4).^{56,57} In this case, the photosynthetic complexes are comprised of ring-like structures of chlorophyll molecules. The continuously overlapping pigments inside these rings serve as light-harvesting antennae, ensuring a high absorption of sunlight.⁵⁸ Coherent transfer then funnels the absorbed energy to a reaction center, around which another ring of bacteriochlorophylls is organized, having red-shifted absorption.⁵⁹ This transfer pathway eventually leads to a charge-separated state inside the reaction center.

Photosynthetic ring-like structures have been mimicked in various clever ways by synthetic chemists,^{62–64} and mimicking of natural photosynthetic systems⁶⁵ using a covalent or a supramolecular^{66–68} approach is a flourishing area of science.^{69–71} Elegant examples from the groups of Müllen⁷² and Fréchet⁷³ comprise multichromophoric dendrimers displaying directional, near quantitative energy transfer to a central acceptor moiety. These are but examples of scientific efforts to obtain control of multichromophoric functionality and ordering in space, as encountered in natural systems.

Another photosynthetic antennae system is employed by green bacteria.^{74–76} Instead of employing chlorophyll molecules that are embedded in a protein matrix, the positioning of light-harvesting chromophores occurs primarily by means of supramolecular interactions between the individual porphyrin rings with little use of protein support. In this way huge chlorosomes arise, comprised of stacked pigments, which incorporate up to tens of thousands

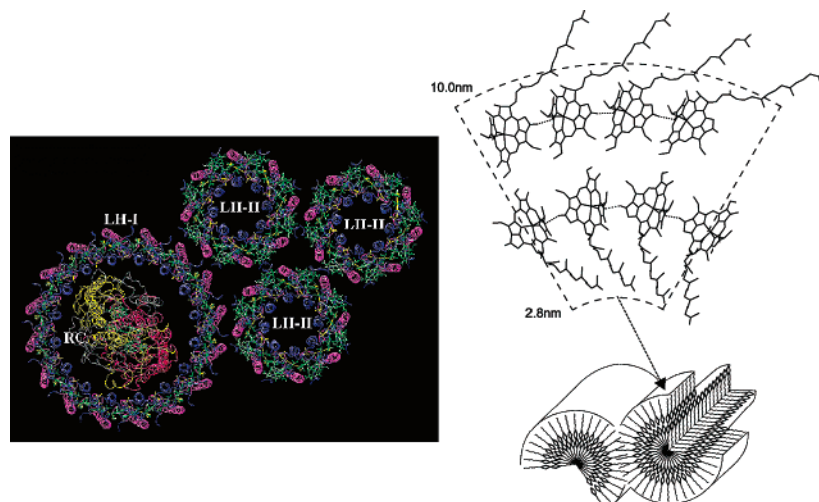


Figure 4. High degree of organization in the light-harvesting photosynthetic system of purple bacteria (left, courtesy of the Theoretical Biophysics Group, Beckman Institute, University of Illinois at Urbana–Champaign) and chlorosome organization in green bacteria (right).^{60,61} (Reprinted with permission from refs 60/61. Copyright 2000/2001 American Chemical Society.)

of chlorophyll moieties and literally reach for the sky to satisfy their light-harvesting purpose. Recently, accessibility to the characterization of these complex systems was greatly enhanced by implementation of powerful NMR techniques (Figure 4).⁷⁷ Combined with molecular modeling, elucidation of the structural assembly of a modified bacteriochlorophyll *d* yielded a valuable model for extended chromophore aggregation in green bacteria. The chlorosome superstructure is especially appealing to supramolecular chemists working in electronics since it cleverly combines cooperative supramolecular interactions into a functional object, approaching directional, one-dimensional energy transport.

Complexity resulting from self-assembly of individual building blocks and the resulting long-distance, directional energy and electron transfer is appealing to scientists working in the field of organic electronics. Noncovalently assembling multiple components into large, well-defined architectures in which the different chromophores exhibit various functionalities remains a challenging task for chemists.

5. Polymers versus Oligomers

Due to the viscosity of polymer solutions, π -conjugated polymers can be easily processed from solution and therefore feature low-cost manufacture. Ink-jet printing is, for instance, highly suitable to process semiconducting polymers.⁷⁸ The processing of the polymers dictates morphology and interchain interactions and is difficult to tune. Moreover, small impurities in the polymer backbone can have a negative influence on the performance of optoelectronic devices.

Plastic electronic devices can also be constructed from small molecules, i.e., π -conjugated oligomers, which have a well-defined chemical structure and can be purified relatively easily. Highly ordered layers can be obtained by using vapor deposition techniques,^{79,80} and mobilities are generally 1 order of magnitude higher than those of solution processed

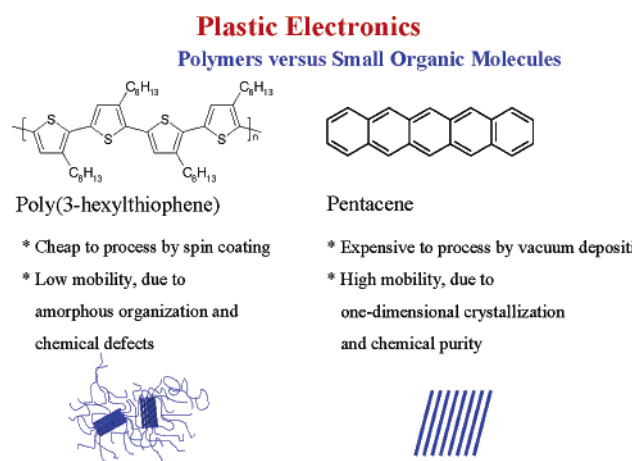


Figure 5. Advantages and disadvantages of π -conjugated polymers compared to that of small organic molecules.

devices.² Especially for large area electronics, solution processing is preferred since vacuum deposition techniques are more expensive (Figure 5).⁸¹

Exciting results have been obtained in plastic electronic devices based on polymers and small organic molecules. As discussed, both semiconducting material classes have their own pros and cons in which the processability of polymers and the high ordering of organic thin layers are the unique features of both systems. It is a dream for many scientists to bring together these two features within one class of materials, leading to highly ordered easy-to-process molecular systems. Hence, an attractive approach would be to use the principles of supramolecular chemistry in organizing conjugated oligomers via programmed information within the molecule into well-defined polymeric structures.

This review will focus on π -conjugated systems and discusses their supramolecular organization. The first section starts with the use of polymers and polydisperse systems, and examples will be given on how these systems have been organized. The section ends with supramolecular architectures based on monodisperse, oligomeric building blocks. In the next

two sections architectures composed of two or even more different types of π -conjugated units will be discussed. Special attention will be paid to systems in which electron and energy transfer occurs since these processes are essential in optoelectronic devices.

6. Supramolecular Organization of π -Conjugated Polymers

6.1. Self-Assembly of Homopolymers

6.1.1. Thermotropic Liquid Crystallinity

π -Conjugated polymer chains obviously act as rigid chains that could function as a mesogenic unit for liquid-crystalline properties. Rigid-rod main-chain polymers such as poly(2,5-dialkoxyphenylenevinylene), poly(2,5-dialkoxy-1,4-phenylene-2,5-thiophene), poly(2,5-dialkylphenyleneethynylene), and poly(9,9-dialkylfluorene) show liquid-crystalline behavior. Polarizing microscopy reveals birefringent fluid melts above their melting temperature defined as a nematic phase. The liquid-crystalline range is tunable by proper choice of the side chains.^{82–85} PPVs substituted with dendritic side chains show liquid crystallinity with high photoluminescence yield as further aggregation is prohibited by the bulky side chains.⁸⁶ A correlation between the microscopic morphology and photoluminescence in polyfluorenes has been established by Lazzaroni et al. Linear alkyl substituents allow for a close packing of the conjugated chains into very long, regular π stacks, resulting in a red shift of the photoluminescence and green emission. On the contrary, bulkier substituents on the polyfluorenes result in unorganized structures and retain the blue emission in the solid state.⁸⁷

6.1.2. Solvatochromism and Thermochromism

Solvatochromic and thermochromic behavior has been reported for conjugated polymers. Their spectral features vary as a consequence of the conformational changes of the backbone, which are coupled with aggregation processes. In a poor solvent or at low temperature chain planarization and concomitant interchain π – π stacking interactions take place, generating an increase of the conjugation length.⁸⁸ As a result, a bathochromic shift in the UV-vis absorption spectra and the appearance of vibronic fine structures are generally observed (Figure 6). The

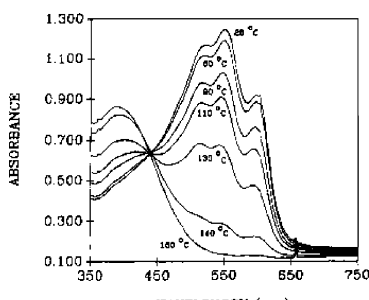


Figure 6. Thermochromism of poly(3-octyloxy-4-methyl)-thiophene in the solid state between 150 (disordered phase) and 25 °C (ordered phase). (Reprinted with permission from ref 93. Copyright 1992 American Chemical Society.)

original studies on organization processes of polythiophenes in solution attributed the spectral changes either to the existence of two distinct phases, disordered polymers, and ordered polymers in the form of microcrystalline aggregates⁸⁹ or to intramolecular conformational transitions.^{90–93} Similar inter-^{94–96} and intramolecular^{97–99} effects have also been reported for polydiacetylene.¹⁰⁰

McCullough,²⁸ Yamamoto,¹⁰¹ and Leclerc^{102,103} extensively studied the self-organization of poly(3-alkylthiophene)s in solution and in the solid state, exploring the effect of temperature, regioregularity, and solvent by means of spectroscopy and light-scattering techniques. Similar studies on polymer chain aggregation of poly(methoxy-ethylhexyloxy-phenylenevinylene)s and poly(*p*-phenyleneethynylene)s have been reviewed by Schwartz³⁶ and Bunz,¹⁰⁴ respectively. Most of these studies rule out that these spectral transitions are purely based on intramolecular conformations. A high number of substituents can prevent π stacking between polymeric chains, resulting in a wormlike cylindrical conformation. When the concentration of the side chains is reduced, an increase of the planarity of the polymeric chain will result in stronger π stacking, leading to lamellar arrangements. These solution properties were compared to the optical properties of the same polymers in thin films. The aggregates formed in a nonsolvent are comparable to those found in the solid state, although the ordering is a little less in the solid state.

6.1.3. Chirality

Chiroptical techniques, which were commonly used to probe the secondary and tertiary structure in biopolymers, have become a highly sensitive tool for investigating the degree of (helical) order in synthetic conjugated polymer assemblies as disordered coil conformations are optically inactive.¹⁰⁵ An important contribution to the discussion of the coexistence of two phases was given by the work on the aggregation behavior of a series of polythiophenes bearing chiral substituents (Figure 7).¹⁰⁶ Meijer et al. found that chiral substituents can induce strong optical activity in the π – π^* transition of the backbone, though only when the polymer is in its aggregated state. It is proposed that strong chiroptical effects in the aggregated phases result from an intermolecular chiral orientation of the rigid polymer chains in ordered crystalline domains. Regioregular polythiophene **1** shows a more pronounced chiroptical effect compared to regiorandom polythiophene **2** due to the enhanced crystallinity of **1**, revealing the importance of a well-defined structure in the helical self-assembly process.

The presence of an isosbestic point in the temperature-dependent CD spectra confirms that the induction of supramolecular chirality with preferred

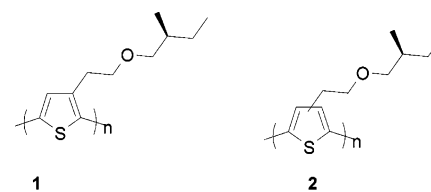


Figure 7. Optically active polythiophenes.

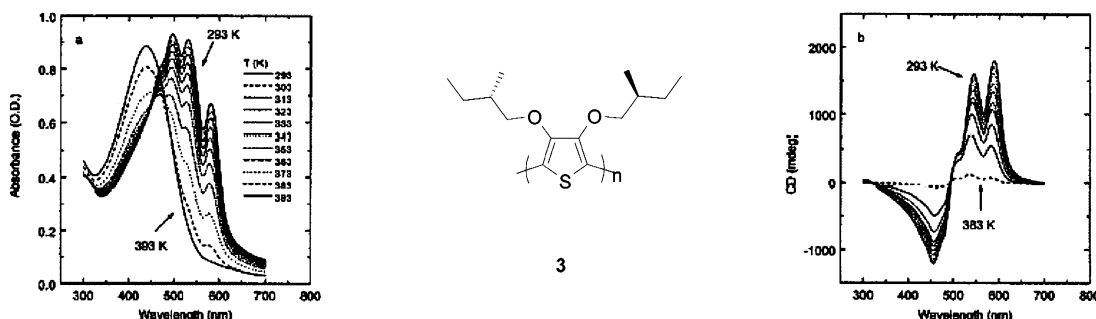


Figure 8. Thermochromic UV–vis absorption and CD spectra of **3** in 1-decanol. (Reprinted with permission from ref 107. Copyright 1996 American Chemical Society.)

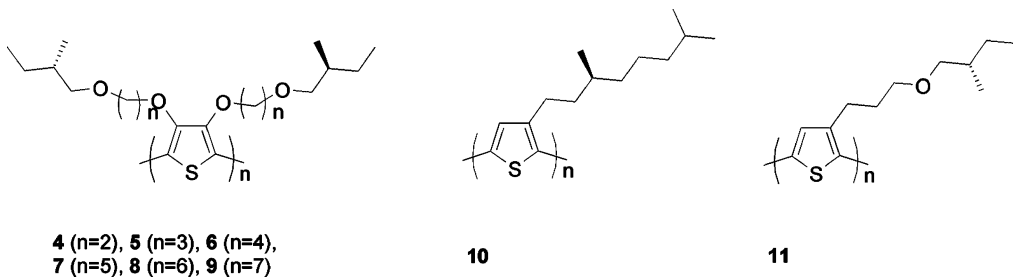


Figure 9. Several chiral polydialkoxythiophenes and poly(3-alkoxythiophenes).

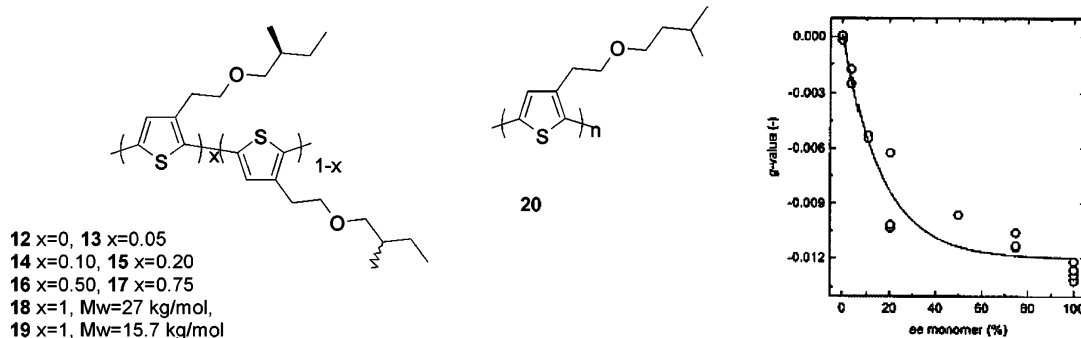
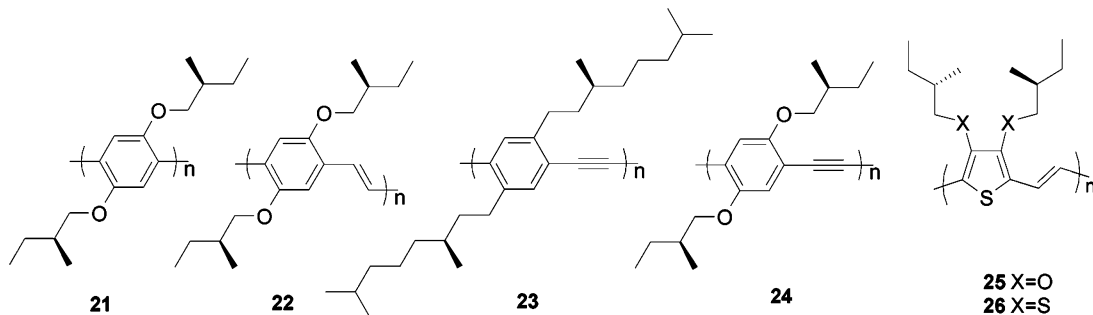
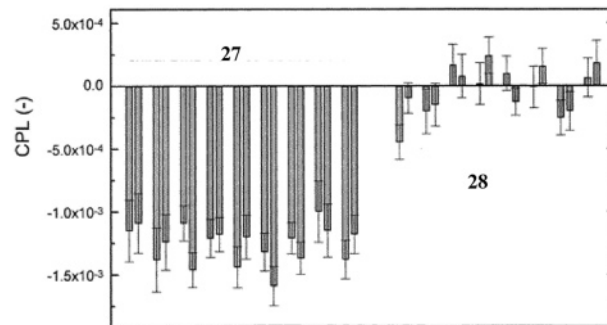
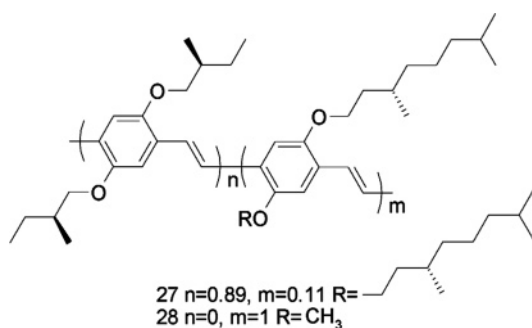


Figure 10. Chiral copolymers **12–19** used to explore majority rules and sergeant and soldiers principles and their achiral analogue **20**. The anisotropy value g is plotted as function of the monomer enantiomeric excess. (Reprinted with permission from ref 113. Copyright 1999 American Chemical Society.)

handedness takes place upon aggregation of polythiophene **3** (Figure 8).¹⁰⁷ The cholesteric packing of chiral polythiophenes is dependent not only on the absolute configuration of the stereocentra but also on their distance to the rigid core. In the aggregated phase the sign of the induced optical activity in the $\pi-\pi^*$ transition alternates with the parity of the number of atoms in the spacer in a series of poly(dialkoxythiophene)s **4–9**.^{108,109} The same group reported circularly polarized photoluminescence of chiral polythiophene **3** in an aggregated phase in solution.¹⁰⁷ Stereomutation in optically active regioregular polythiophene **1** has been reported as well.¹¹⁰ The authors show that optically inactive films at 160 °C give a restored Cotton effect upon slow cooling whereas an inverted Cotton effect is obtained upon fast cooling. By adjusting the cooling rate it was even possible to produce films with no optical activity. Opposite optical activity has also been observed for regioregular polythiophene **10** by Sorokin et al. in chloroform–methanol mixtures of different composition¹¹¹ and two other chiral polythiophenes **1** and **11** by changing the solvent during aggregation, Figure 9.¹¹²

A cooperative behavior of the chiral side chains in the aggregation process was found in line with the majority rules principle for a series of polythiophenes (**12–19**) in which the ratio between (R) and (S) stereocenters in the side chain varies. For aggregates in poor solvents, a nonlinear relation exists between the chiral anisotropy factor and the enantiomeric excess of the optically active substituents, e.g., for **14** with (S)-ee of 10%, g_{abs} is already one-third of that of the enantiomerically pure polymer **18** (Figure 10).¹¹³ The same authors revealed an increased optical activity after cooling a blend of chiral **19** and achiral polythiophene **20** in poor solvent. This sergeants and soldiers principle is strongly related to the molecular weight of the sergeant; nucleation starts with the longest polymer chains of **18** that determine the further chiral or achiral aggregation of the shorter chains.¹¹³

Sergeants and soldiers principle has also been observed for chiral poly(*p*-phenylene) copolymer by Scherf et al., where a small percentage of chiral side groups is able to induce optical activity when the polymer chains aggregate in poor solvents.^{114,115} Aggregation-induced Cotton effects have also

**Figure 11.** Various chiral π -conjugated polymers.**Figure 12.** Reproducible results of the measurements of the CPEL effect for nine independent polymer LEDs having an enantiomerically pure polymer layer (**27**) and eight LEDs with a racemic layer (**28**). Error bars indicate the standard error of the experimental result. (Reprinted with permission from ref 127. Copyright 1997 American Chemical Society.)

been reported for chiral polydiacetylenes,^{116,117} poly(*p*-phenylenevinylene)s,^{118,119} poly(*p*-phenyleneethynylene)s,^{120,121} poly(terthiophene)s,¹²² and poly(*p*-thiophenevinylene)s, Figure 11.^{123–125}

For all these polymers the chiroptical properties are associated with an exciton-coupled CD effect. This means that the electronic coupling between different conjugated chromophores is attributed as resulting from a helical packing of the polymer chains in the aggregated phases. Model compounds were used to investigate the angle between the molecules in the helical orientation in the aggregates.¹²⁶ Control over the organization of π -conjugated polymers over macroscopic length scales can lead to new applications, such as a circularly polarized electroluminescent device (CPEL) (Figure 12). The observation of a CPEL effect in a LED constructed from chiral PPV and PPE derivatives illustrates that molecular chirality can result in a net macroscopic optical activity of a working device. Differences in the degree of circular polarization could be related to the optical purity of the polymer backbone.^{127–130} The highest dissymmetry factors have been reported for polyfluorenes and PPE derivatives, probably due to their thermotropic behavior.^{131–133}

6.1.4. Ionochromism

Ionochromic effects were initially reported for regioregular head-to-head disubstituted polythiophenes bearing crown ether or calixarene side chains. These polymers undergo dramatic conformational changes upon coordination with alkali-metal ions, creating interesting sensory systems as reviewed by Swager et al.¹³⁴ The conformational changes are dependent on the size of the ions and its binding strength with the host material.^{135–138} Leclerc et al. studied the thermochromic and ionochromic proper-

ties of regioregular polythiophene **29** with pendant oligo(ethyleneoxide) chains. This polymer has thermochromic properties in solution; at low temperature in methanol the polymer exhibits an absorption maximum at 550 nm, which shifts to 426 nm upon heating. Addition of potassium shifts the equilibrium from an ordered to a disordered form of the polymer through potassium complexation.^{102,103,139} Substitution of polymer backbones with binding sites for ionic guests also creates a tool to control polymer aggregation. Most elegant is the induced aggregation of polythiophene **30** by adding sodium, which already favors interchain aggregation in a good solvent. Swager et al. extended this concept to crown-ether-functionalized poly(*p*-phenyleneethynylene) **31** that π - π stacks upon adding potassium, whereas upon adding sodium a planar nonaggregated polymer backbone was obtained that is highly emissive (Figure 13).

PPV **32** with crown ether substituents could form wormlike nanoribbons through complexation with potassium in dilute chloroform solution. The growth of nanoribbons is enhanced by longer exposure times to potassium. TEM and AFM revealed that these nanoribbons are 15 nm in diameter and a few micrometers long (Figure 14).^{140,141}

Acid–base interactions can also^{142,143} be used to influence the conformation of the polymeric backbone in polythiophene derivatives **33–35**, resulting in spectral changes.^{144–146} Schwartz et al. extended this concept to PPV **36** substituted with dialkylamino chains (Figure 15). Protonation of just a few percent of the amino side groups leads to coiled polymers that in turn result in a blue-shifted absorption. At higher concentration, however, protonation of the side groups increases the charge density along the polymeric

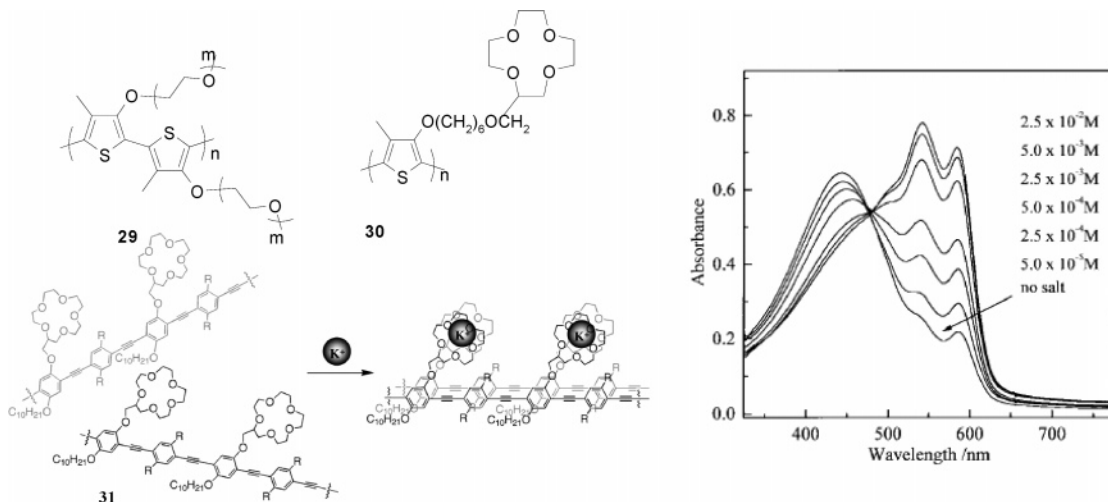


Figure 13. Polythiophenes **29** and **30** substituted with ion-coordinating groups. UV-vis absorption spectra of polythiophene **30** in acetone upon addition of NaCF_3SO_3 . (Reprinted with permission from ref 140. Copyright 1999 Royal Society of Chemistry.) The cartoon represents the induced aggregation of poly(*p*-phenyleneethynylene) **31** upon addition of potassium. (Reprinted with permission from ref 137. Copyright 2000 John Wiley & Sons, Inc.)

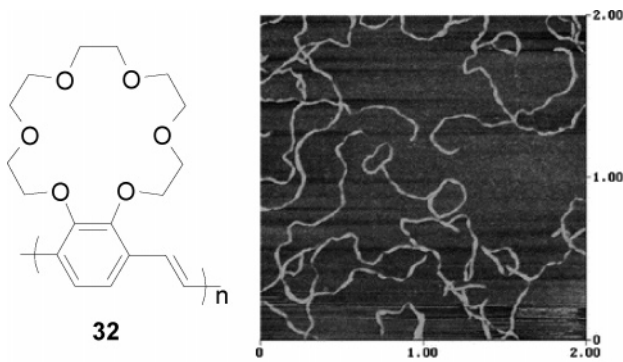


Figure 14. AFM picture showing wormlike morphologies obtained from poly(*p*-phenylenevinylene) **32** with pendant crown ethers in the presence of potassium. (Reprinted with permission from ref 141. Copyright 2003 American Chemical Society.)

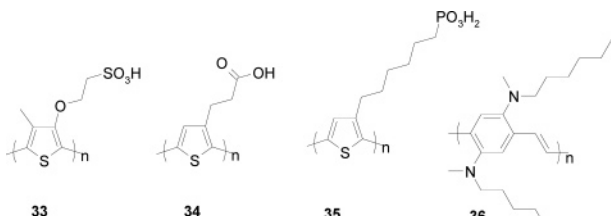


Figure 15. Various π -conjugated polymers with pH-sensitive side groups.

backbone. This causes the coil to collapse in order to minimize exposure of both the backbone charges and counterions to the nonpolar environment, resulting in red-shifted emission. The degree of side-group protonation varies directly with the surface topography of the PPV films, demonstrating the ability to transfer the degree of interchain interactions from solution to films.¹⁴⁷

6.2. Self-Assembly of Block Copolymers

An alternative methodology to physical blending of different polymers is to synthetically link the oligo- or polymeric conjugated building blocks to other blocks that are able to enhance the positioning of the

conjugated blocks in the active layer and improve the mechanical and processing properties (see also section 3).

6.2.1. Polydisperse π -Conjugated Blocks

The block copolymer approach can display phase separation, and therefore, a rich variety of nanoscopic organizations are available ranging from lamellar, spherical, cylindrical, to vesicular morphology.¹⁴⁸ Micelle formation by evaporating the solvent CS_2 resulted in regular pores arranged in a hexagonal array.¹⁴⁹ This honeycomb morphology discovered by François et al. was made from rod-coil poly(*p*-phenylene)-polystyrene block copolymer **37** (Figure

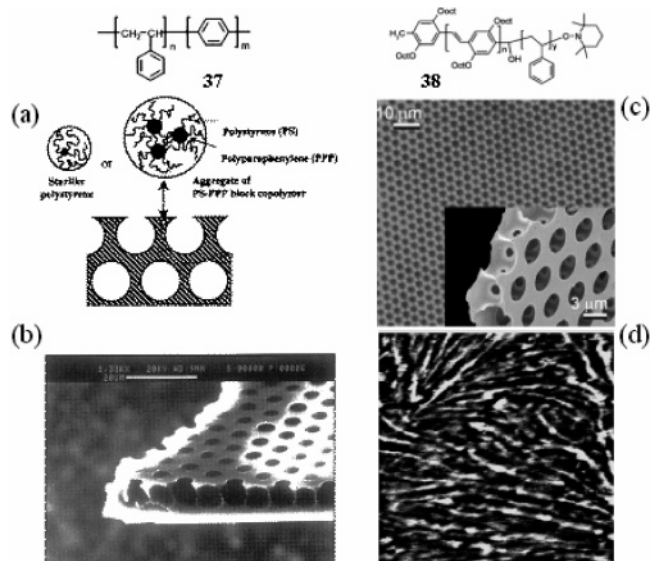


Figure 16. (a) Schematic representation for the cross section and (b) SEM image of a honeycomb structure of polymer **37**. (Reprinted with permission from *Nature* (<http://www.nature.com>), ref 149. Copyright 1994 Nature Publishing Group.) (c) Fluorescence and SEM (inset) images of a honeycomb-structured film of PPV-*b*-PS **38** obtained by drop casting from CS_2 and (d) lamellar morphology as obtained by drop casting from dichlorobenzene. (Reprinted with permission from ref 152. Copyright 2001 Elsevier.)

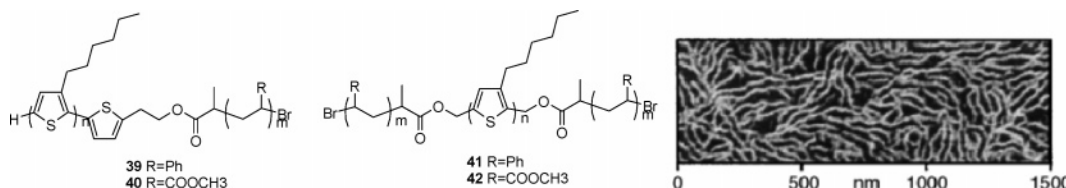


Figure 17. Nanowire morphology in poly(3-hexylthiophene) copolymers **39–42**, solvent-cast from toluene and visualized with tapping-mode AFM. (Reprinted with permission from ref 156. Copyright 2002 John Wiley & Sons, Inc.)

16). Interestingly, the high number of defects in the PPP backbone did not affect the morphology.^{150,151} Similarly, Hadzioannou et al. reported a honeycomb morphology for block copolymers of polystyrene and poly(*p*-phenylenevinylene) **38** when cast from CS₂, a poor solvent (Figure 16). However, when cast from a good solvent dichlorobenzene, a bilayered lamellar morphology was observed of stacked PPV blocks.^{77,152} The honeycomb morphology could also be reproduced by François et al. with block copolymers of polystyrene and polythiophene.^{153–155}

McCullough et al. were able to self-assemble regioregular poly-3-hexylthiophenes (**39–42**) copolymerized with polystyrene, polymethacrylate, and polyurethane into cylindrical morphologies (Figure 17). These high molecular weight materials, with polydispersities of 1.4 on average, showed good mechanical properties, for example, elastic polyurethane films. Nanowire morphologies of the di- and triblock copolymers were obtained by slow evaporation from toluene. These films showed conductivities correlated to the ratio of the conducting and nonconducting blocks present in the block copolymers. Interestingly, the long-range order induced by balanced π stacking and phase separation is lacking when the films were cast from chloroform, and as a result, the conductivity drops.¹⁵⁶

Also, the syntheses of block copolymers of polystyrene or poly(methyl methacrylate) with polypyrrole and poly(3-alkylpyrroles) have been reported.¹⁵⁷ The synthesis of block copolymers **43–49** consisting of polydimethylsilane or poly(ethyleneoxide) as coil segment with rod segments as poly(*p*-phenyleneethynylene),¹⁵⁸ poly(*p*-phenylene),^{159,160} and polyfluorenes¹⁶¹ were carried out by Müllen et al. and François et al. Optical measurements showed the influence of the coil blocks on the optoelectronic properties of the rod segments by induced phase separation, Figure 18.

Lazzaroni et al. showed the strong tendency of block copolymers containing PPP, PPE, and PF segments to spontaneously assemble into stable, ribbonlike fibril morphologies, irrespective of the nature of the coil segment, when coated on substrates (Figure 19). The ribbonlike structure was proposed to result from the head-to-tail packing of the conjugated segments.^{162–164}

Poly(phenylquinoline) (PPQ) is a well-known n-type semiconductor and used as an electron-transport and emission layer in LED's.^{165,166} Its poor solubility attracted Jenekhe et al. to explore the block copolymer approach to improve the PPQ processability. The authors studied the self-assembling behavior of rod-coil copolymer **50** consisting of PPQ as the rod block and polystyrene as the coil block. This block copoly-

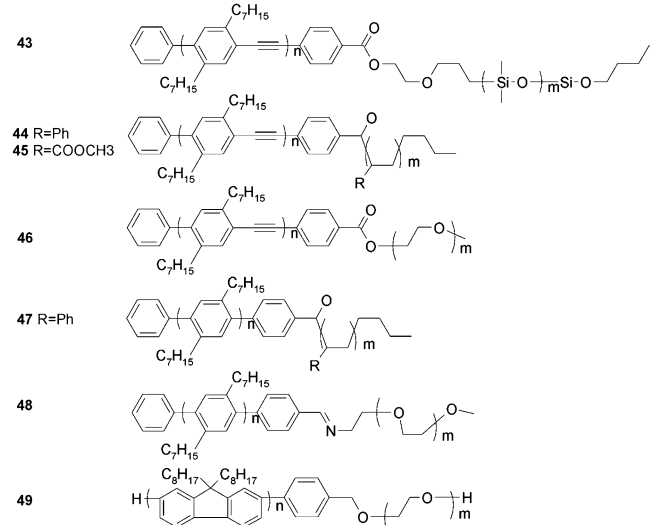


Figure 18. Several π -conjugated block copolymers.

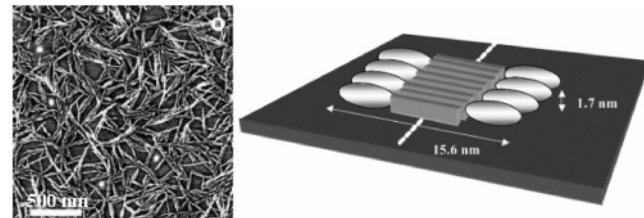


Figure 19. AFM image of the ribbonlike morphology and the proposed stacking model of block copolymer **49**. The conjugated parts are represented by gray bricks, while the nonconjugated parts are represented by light gray ellipsoids. (Reprinted with permission from ref 164. Copyright 2002 Elsevier.)

mer was found to self-assemble into diverse supramolecular structures (Figure 20) in which the amide linkage at the rod-coil interface provides a self-organized scaffold by strong intermolecular hydrogen bonding. The heterocyclic PPQ block allows tuning of its amphiphilicity by addition of trifluoroacetic acid, which protonates the imine-like nitrogens. For example, fast drying at 25 °C from 9:1 TFA:dichloromethane leads to polydisperse cylinders 1–3 nm in diameter and 5–25 nm in size that decreased with the decreasing fraction of the rigid-rod block. Excimer-like emission suggests close packing of the PPQ block chains in a J-type fashion. Fluorescence images of the cylinders reveal that the fluorescent PPQ block is located at the outer shells of the aggregates together with a hollow cavity and closed ends of the cylinder. Also, because of three-dimensional symmetry and uniformity of emission, the authors concluded that micellar bilayered supramolecular cylinders are formed.^{167,168} In extension, the same authors reported the self-assembly of triblock copoly-

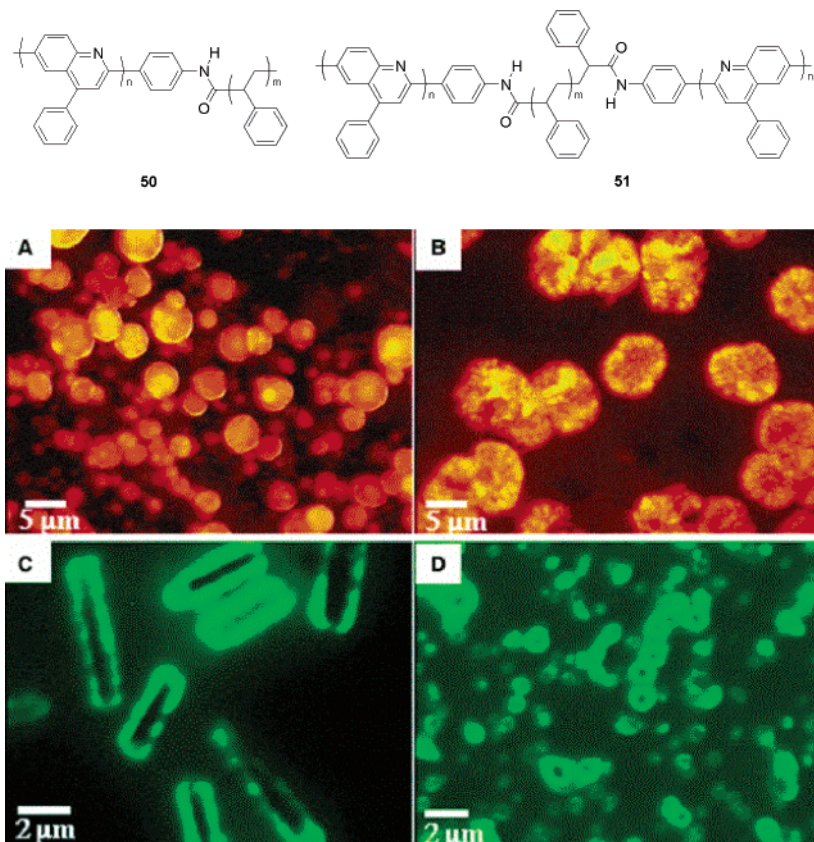


Figure 20. Fluorescence photomicrographs of the aggregates formed by **50** being (a) spherical (1:1 TFA:DCM v/v, 95 °C), (b) lamellar (1:1 TFA:DCM, 25 °C), (c) cylindrical (9:1 TFA:DCM, 25 °C), and (d) vesicular (1:1–1:4 TFA:DCM, 25 °C). (Reprinted with permission from ref 167. Copyright 1998 American Association for the Advancement of Science.)

mer **51** comprised of PPQ–PS–PPQ. In contrast to the diblock copolymers with multiple morphologies, the triblock copolymers were found to spontaneously and exclusively form spherical vesicles.¹⁶⁹

Complexation of block copolymers with amphiphiles is a new strategy for the formation of self-organized supramolecular polymeric materials developed by Ikkala and ten Brinke et al.¹⁷⁰ A combination of a diblock copolymer, proton transfer, and hydrogen bonding yields hierarchical structures of different length scales as analyzed with SAXS and TEM. Poly(4-vinylpyridine) (P4VP) was stoichiometrically protonated with methane sulfonic acid, which was then hydrogen bonded to pentadecylphenol (PDP). At temperatures below 100 °C a protonated polystyrene-[poly(4-vinylpyridine)pentadecylphenol] diblock copolyelectrolyte complex separates into microphases with a lamellar-within-lamellae structure. Alternating layers 35 nm in width consisting of polystyrene and poly(4-vinylpyridine)pentadecylphenol were obtained. The domains of the latter phase are further phase separated into a bilayered hydrogen-bonded structure of pentadecylphenol moieties with a 4.8 nm periodicity. Protonic conductivity was found to take place in one direction of the nanoscale poly(4-vinylpyridine) compartments only.¹⁷¹ The temperature-induced self-organization is schematically depicted in Figure 21.

Further known hydrogen-bonded structure-within-structure morphologies for P4VP are lamellar-within-spherical, lamellar-within-cylindrical, cylindrical-within-lamellar, and spherical-within-lamellar struc-

tures and are dependent on the hydrogen-bonded poly(4-vinylpyridine) complex weight fraction.¹⁷² Imposing shear can lead to considerable alignment of cylinders and lamellae. The cylinders align along the shear flow with the normal plane parallel with respect to the shear plane. The matrix layers align perpendicular to the cylinders, transverse to the flow.^{173,174} Cleavage of the pentadecylphenol leads to nanorods containing polystyrene cores and poly(4-vinylpyridine) coronas.¹⁷⁵ These nanorods show high dichroism and polarized photoluminescence (Figure 22).¹⁷⁶

6.2.2. Monodisperse Main-Chain π -Conjugated Blocks

Miller et al. prepared block copolymers **52**–**53** having alternating bi-, quarter-, or octathiophenes and a polyester chain,^{177,178} and Jenekhe et al.¹⁷⁹ connected terthiophenes **54** via alkyl tails. Leclerc et al. prepared block copolymers having a range of well-defined oligothiophene blocks and polyester chains (**55**–**62**). The polyester with pentathiophene segments showed increased conductivity up to 0.4 S/cm due to favorable π stacking, Figure 23.¹⁸⁰

The block copolymer approach has been adopted by Feast et al. for the organization of hydrophobic oligothiophene blocks that alternate with hydrophilic poly(ethylene oxide) blocks ($M_n = 2000$, 1000, and 600) (**63**–**66**).¹⁸¹ Aggregation of the oligothiophenes occurs in dioxane–water mixtures, which was manifested by a blue shift of the UV–vis absorption maximum and quenching of the fluorescence. An oligothiophene length of three thiophenes was neces-

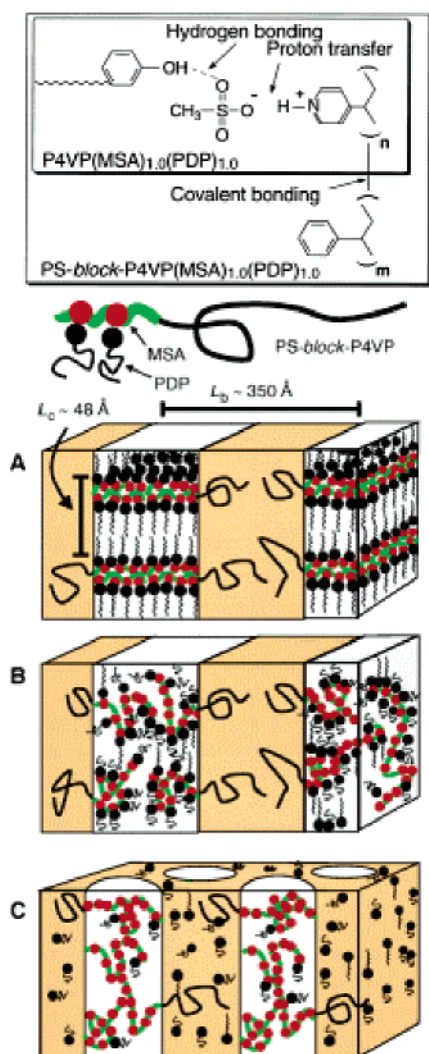


Figure 21. Schematic illustration of the temperature-induced hierarchical self-organization of PS-block-P4VP- $(\text{MSA})_{1.0}(\text{PDP})_{1.0}$. (a) Alternating PS layers and layers consisting of alternating one-dimensional compartments of P4VP($\text{MSA})_{1.0}$ and PDP for $T < 100^\circ\text{C}$. (b) Alternating two-dimensional PS and disordered P4VP($\text{MSA})_{1.0}(\text{PDP})_{1.0}$ lamellae for $100^\circ\text{C} < T < 150^\circ\text{C}$. (c) One-dimensional disordered P4VP($\text{MSA})_{1.0}(\text{PDP})_x$ cylinders within the PS matrix for $T > 150^\circ\text{C}$. (Reprinted with permission from ref 171. Copyright 1998 American Association for the Advancement of Science.)

sary to observe aggregation.¹⁸² When a sexithiophene is alternated with well-defined chiral undeca(ethyleneoxy) blocks (**67**), aggregation also occurs in dioxane itself. However, no helicity was found in this aggregate, which was in contrast with the monodis-

perse chiral monomeric unit. It illustrates that although the processability and mechanical robustness of block copolymers may be superior to those of analogous oligomers, the degree of self-assembled order found in oligomer-based systems may be lost in alternating polymers.¹⁸³ Oligo(ethylene oxide) can also be used in alternation with distyrylbenzene units (**68**), providing efficient light-emitting diodes, presumably by efficient ion-conducting pathways.^{184,185} Polymers consisting of alternating perylene bisimide chromophores and flexible polytetrahydrofuran segments of different length (**69**) have been studied using absorption and (time-resolved) photoluminescence spectroscopy. In poor solvents the chromophores self-organize into H-type aggregates, which were enhanced by shortening the flexible spacer.^{186,187}

Yu et al. reported the synthesis of a polystyrene-nonathiophene diblock copolymer (**70**) without specifying phase separation.¹⁸⁸ Hempenius et al. used the same units by synthesizing a triblock copolymer of polystyrene-undecathiophene-polystyrene (**71**, polydispersity of 1.1), and phase separation was observed in a poor solvent. TEM and AFM show that the copolymer is self-assembled into irregular, spherical, micellar structures having an average diameter of 12 nm (Figure 24). This value corresponds to about 60 block copolymer molecules per aggregate. The optical properties are in agreement with aggregated unsubstituted oligothiophenes. Electrochemical doping was hampered by the polystyrene shell; however, chemical doping afforded small nanoscopic charged aggregates that are soluble in organic solvents.¹⁸⁹

The triblock copolymer approach has been expanded to other conjugated blocks such as oligo(*p*-phenylenethynylene) **72**, and here, phase separation was observed also in poor solvents.^{190,191} In the case of oligofluorene-polystyrene block copolymer **73**, nano-wire morphologies were observed. The polymers can be applied in LEDs displaying stable blue light emission, Figure 25.¹⁹²

Stupp et al. reported the synthesis and characterization of triblock rod-coil molecules **74–78** consisting of diblock coil segments of polystyrene and polyisoprene and oligo(*p*-phenylenevinylene)s (OPVs) as rod segments. On the basis of TEM and X-ray diffraction data, **75–78** formed self-organized nanostructures (Figure 26) whereas **74** lacked any order, showing that π aggregation of OPV units is not the dominant factor in the self-assembly process. The regularity of the nanostructures depends on rod-to-coil volume fraction. If the diblock coil segments are

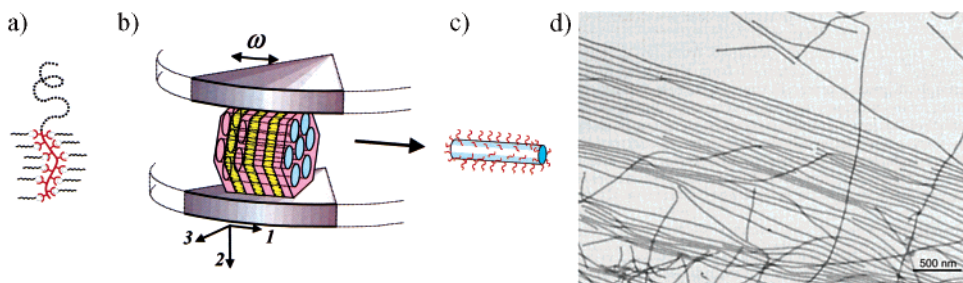


Figure 22. (a and b) Applying shear to hexagonally organized PS cylinders within the layered background consisting of P4VP(PDP) and (c and d) subsequent cleavage of the PDP amphiphiles results in nanorods that can be visualized with TEM. (Reprinted with permission from ref 174. Copyright 2003 American Chemical Society.)

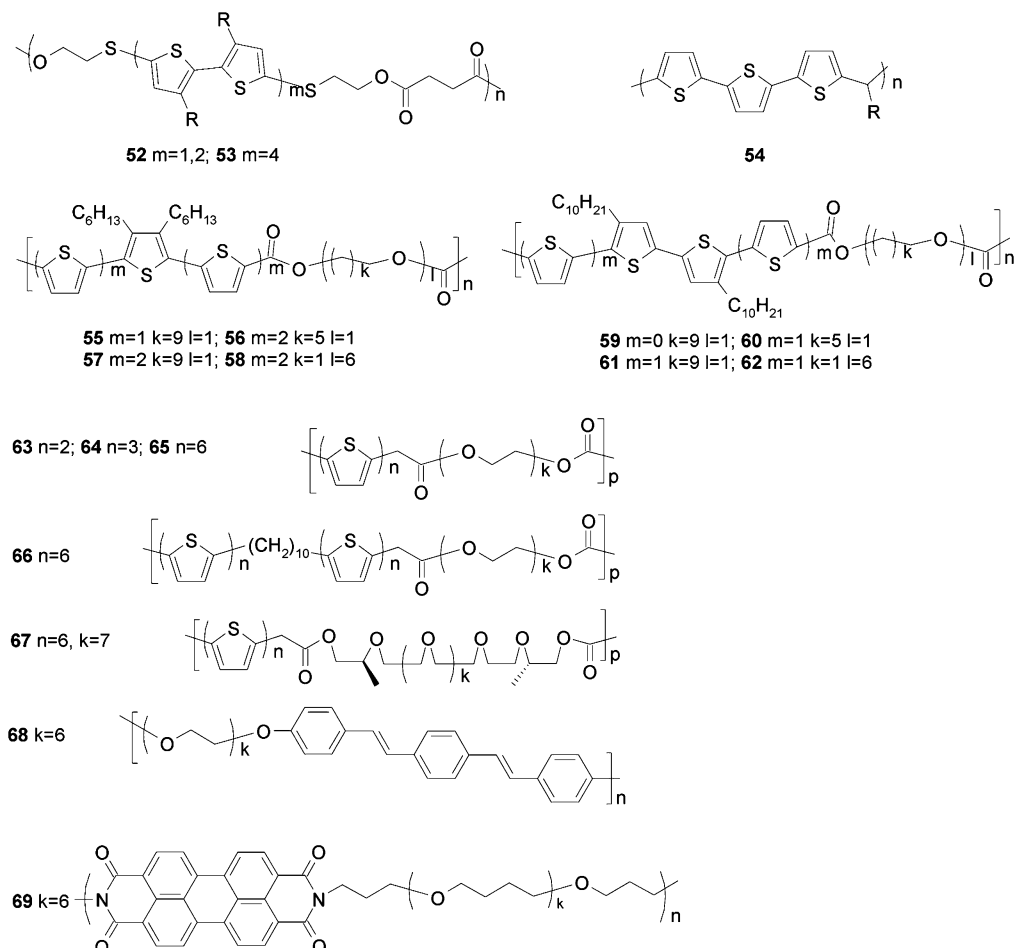


Figure 23. Amphiphilic block copolymers containing monodisperse conjugated blocks.

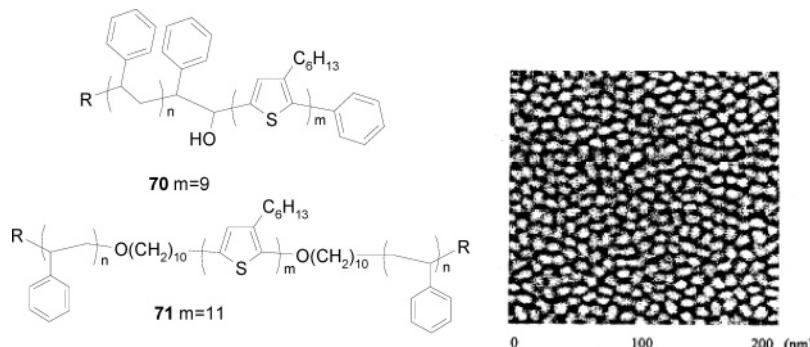


Figure 24. Di- and tri-block copolymer of polystyrene and oligothiophene blocks. The AFM image shows that **71** phase separates into micellar aggregates. (Reprinted with permission from ref 189. Copyright 1998 American Chemical Society.)

still solvated during rod block crystallization, the steric forces among the coil segments will be larger, stabilizing smaller nanostructures. Long-range order is disrupted in systems **77** and **78**, resulting in polydisperse nanostructures, whereas for **76** a regular strip morphology was observed. The latter is possibly the result of a more favorable enthalpy of aggregation for OPV rod segments relative to those in **77** and **78**. The supramolecular strips arranged further into antiparallel sheets. Absorption and emission spectra showed strong photoluminescence facilitated by the herringbone packing of the chromophores.^{193,194a} The self-assembled macroscopic material **77** is polar, and the authors showed films with piezoelectric activity.¹⁹⁵ Very recently, the same

group synthesized dendron rod-coil molecules containing conjugated oligothiophene, OPV, or oligo(*p*-phenylene) segments.^{194b} All three molecules self-assembled into high aspect ratio ribbonlike nanostructures on mica, which could be aligned using an electric field. Interestingly, for the oligothiophene molecule a 3 orders of magnitude increase in the conductivity of iodine-doped films was observed.

The influence of the nature of the coil on the phase behavior was studied in rod-coil molecules **79–83** consisting of a monodisperse oligo(*p*-phenylenevinylene) (OPV)¹⁹⁶ and a coil segment of poly(ethylene oxide) (PEO), poly(propylene oxide) (PPO),^{197–199} or polyisoprene²⁰⁰ (PI) of varying length. All block copolymers showed a polydispersity of less than 1.1.

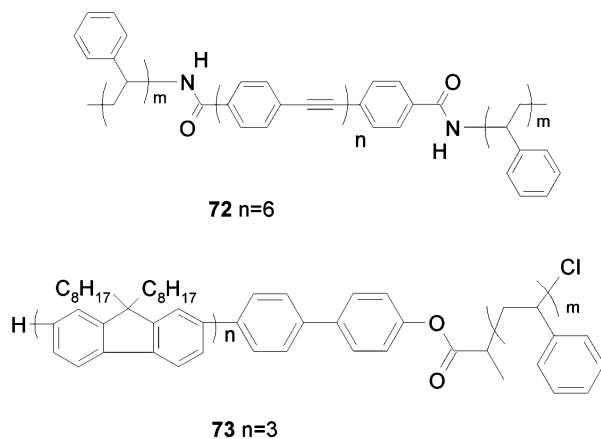


Figure 25. Block copolymers based on oligo(*p*-phenyleneethynylene) and oligofluorene.

SANS data of the copolymers based on PEO or PPO in water revealed a strong tendency to self-assemble into cylindrical micelles in which the cylindrical OPV core is surrounded by the PEO or PPO corona. In the case of the PI-based polymer, a layered phase of alternated PI and OPV was observed. In addition, the semiflexible character of PI blocks dramatically decreases the processability of the molecule, hence limiting the length of the OPV segment. In the case of the hydrophilic blocks, the supramolecular structure could be manipulated by changing the ratio of poor and good solvent (Figure 27). Stable and ordered cylinders are formed in the case of long PPO coil segments. At higher ratios of poor solvent, initial swelling of the corona occurs, followed by aggregation among cylinders into a hexagonal closed packing. This phase is stable upon further increasing the amount of poor solvent. In the case of the PEO-based systems, however, regular and interwoven fibers micrometers long and diameters around 10 nm were observed (Figure 27).

6.2.3. Monodisperse Side-Chain π -Conjugated Blocks

Another approach to create block copolymers is to introduce pendant conjugated oligomers to nonconjugated polymers. It is expected that these polymers

form films that exhibit unique properties characteristic of the pendant oligomer. Shirota et al. studied the correlation between the length of pendant oligothiophenes and electrical properties of the resulting vinyl and methacrylate polymers (**84**, **85**).^{201–203} The electrical conductivity of films of these polymers increased with increasing conjugation length of the oligothiophene segment. Furthermore, films of longer oligothiophene polymers exhibited a reversible color change upon doping which could be of interest for applications in the field of electrochromic materials. By replacing the pendant oligomers, with, e.g., perylene bisimides,²⁰⁴ the emission could be tuned. Soluble polyacetylenes with dangling terfluorenes (**86**)²⁰⁵ and tetra(*p*-phenylenevinylene)s (**87**) have also been prepared. The latter system could be applied in a photovoltaic device when blended with a C₆₀ derivative, Figure 28.²⁰⁶

The full potential of pendant oligomers to construct functional organized materials was recently shown by Hayakawa et al., who created extremely regular hierarchical structures from low polydisperse copolymers of coiled polystyrene blocks with semirigid polyisoprene segments bearing terthiophene side chains (**88**) (Figure 29). Self-organization at three different length scales occurred on films cast from CS₂ solution. SEM and POM images showed single layers of hexagonally packed micropores with a narrow size distribution: 1.5 μ m in diameter having walls as thin as 100 nm. A sulfur-distribution TEM image of cross-sectional films indicated a 50 nm spacing of lamellar layers of polystyrene and polyisoprene blocks perpendicular to the substrate. DSC and X-ray data showed characteristics of a liquid-crystalline smectic mesophase of the π -stacked oligothiophene blocks. Annealing changed the direction of the cylinders from perpendicular to parallel at the bottom of the film, while the upper side of the film remained the same. The depth of the pores could be adjusted by the annealing conditions and their diameter by polymer concentration.²⁰⁷

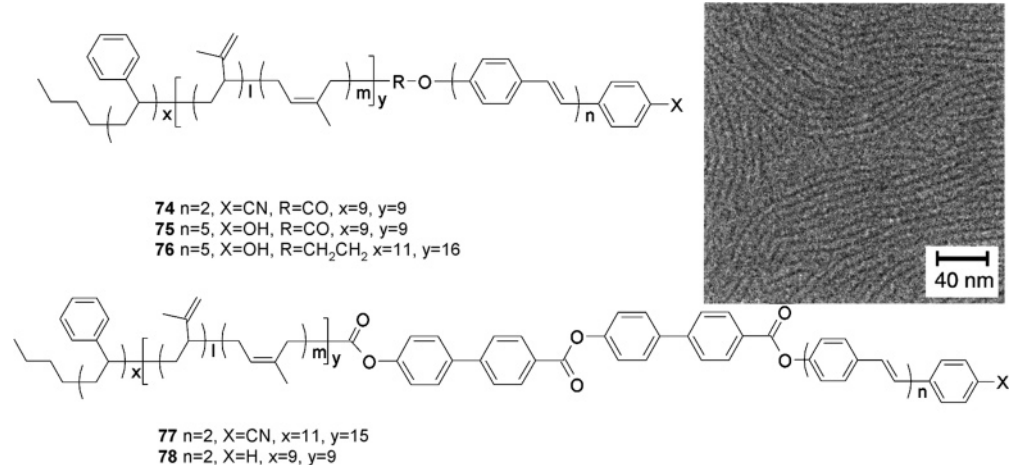


Figure 26. Rod–coil triblock copolymers **74–78** containing oligo(*p*-phenylenevinylene) units. TEM micrograph of **76** revealing the formation of strips with nanoscale dimensions. The strips are about 8 nm in width and approximately 80 nm in length, and rod segments are perpendicular to the plane of the micrograph. (Reprinted with permission from ref 194. Copyright 1999 American Chemical Society.)

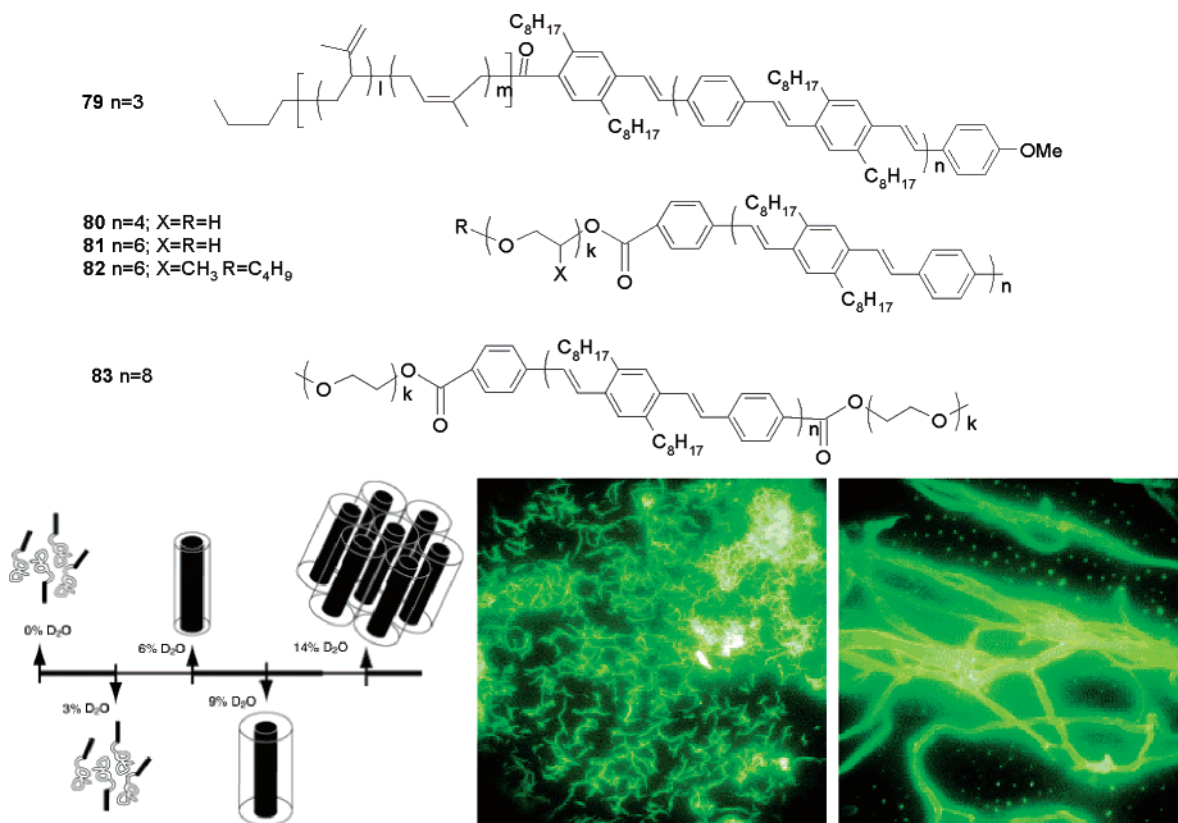


Figure 27. Schematic representation of the self-assembly of block copolymers **80–83** in aqueous solution and fluorescence micrographs of **82** with short (left) and long (right) PPO blocks. (Reprinted with permission from ref 197. Copyright 2004 John Wiley & Sons, Inc.)

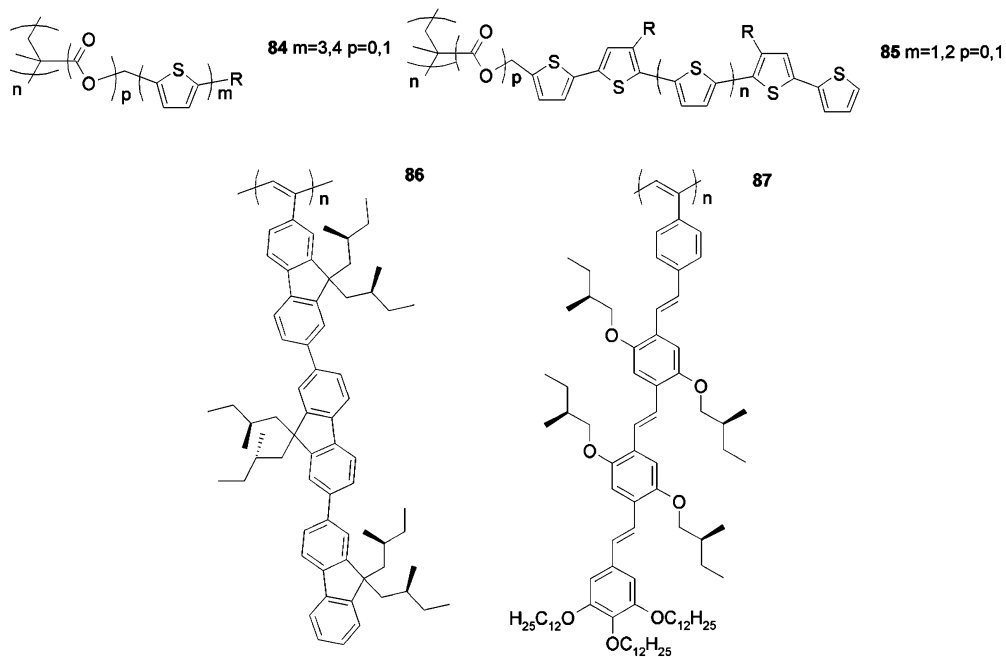


Figure 28. Graft copolymers with pendant π -conjugated oligomers.

6.3. Aided-Assembly of π -Conjugated Polymers

Templating organic synthetic methodologies have been applied to control the superstructure of conjugated polymers using anionic synthetic lipid assemblies as a template. The anionic template assemblies harbor the cationic intermediates produced by oxidative polymerization of the monomer, e.g., pyrrole. A SEM image of the resulting poly(pyrrole) films

showed fibrous structures with a left-handed helical motif, similar to the structure of the organic templates (Figure 30).²⁰⁸

Gin et al. prepared electroactive materials by columnar self-assembly of an amphiphilic polymerizable liquid crystal and a water-soluble precursor of PPV. A stable hexagonal arrangement was created through self-assembly (Figure 31) in which the PPV

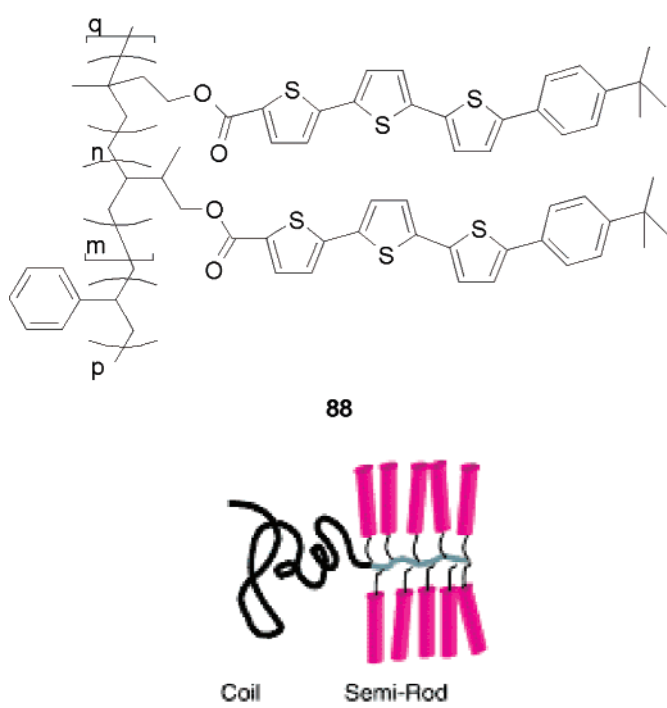


Figure 29. Schematic representation of hierarchical, self-organized structures of **88** bearing pendant oligothiophenes. (a) Centimeter-sized film. (b) Microsized porous structure. (c) Nanosized phase-separated structure of polystyrene and polyisoprene-oligothiophene blocks. (d) Oligothiophene with molecularly orientated structure in polyisoprene-oligothiophene nanophase-separated domains. (e) Cartoon representing **88**. (Reprinted with permission from ref 207. Copyright 2003 John Wiley & Sons, Inc.)

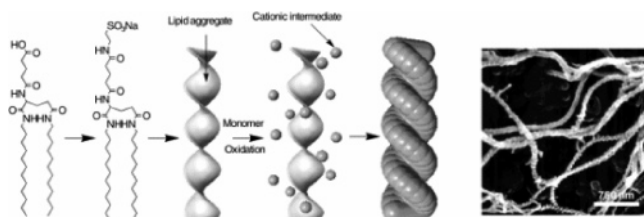


Figure 30. SEM image of a poly(pyrrole) composite film obtained by a templating method as schematically depicted. (Reprinted with permission from ref 208. Copyright 2004 John Wiley & Sons, Inc.)

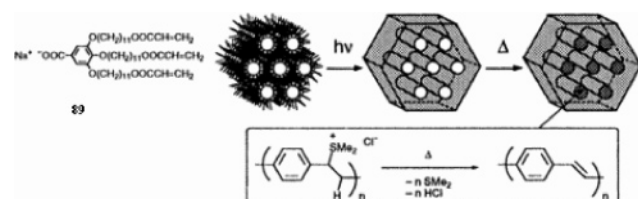


Figure 31. Schematic route to obtain a conductive PPV nanocomposite. (Reprinted with permission from ref 209. Copyright 1997 American Chemical Society.)

precursor is one-dimensionally aligned in the hexagonal matrix. After polymerization of the amphiphilic molecules and heat treatment of the precursor, a conductive nanocomposite was obtained.²⁰⁹

This amphiphilic template approach was also used by Grady et al. to construct nanowires of polyaniline and polypyrrole in a three-step process. In the first stage the monomer and amphiphile were allowed to aggregate on the surface of a substrate creating the preferred cylindrical morphology. In the second stage polymerization took place, and in the third stage the

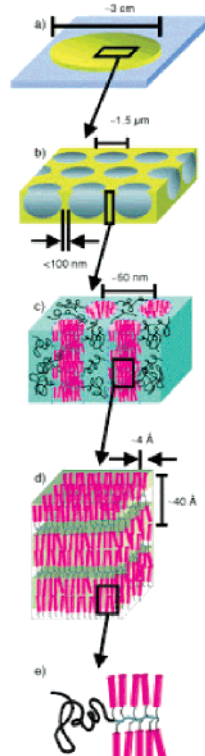


Figure 32. $2 \times 2 \mu\text{m}^2$ AFM image of polyaniline wires on HOPG using surfactant templates. (Reprinted with permission from ref 210. Copyright 2003 American Chemical Society.)

substrate was rinsed. Nanowires in aligned arrays were constructed from polyaniline with a diameter of 45 nm and a few 100 nm long (Figure 32).²¹⁰

To avoid polymerization reactions on surfaces, membranes such as filter membranes can be used to furnish conjugated materials with an engineered nanoshape. These membranes have pores of defined size and diameter. Using this technique PPE derivatives were deposited into these pores, and the membrane was dissolved in dilute base or acid to produce solid nanotubes. The width of the tubes ranged from 200 to 300 nm, corresponding to the filter pore dimensions. The length of the tubes reached 43 μm , which was slightly shorter than the depth of the pores (60 μm) (Figure 33).²¹¹

Frisbie et al. showed a mild way to produce thin wires of poly(3-hexylthiophene) by applying a drop-casting procedure—a small droplet of a diluted polymer solution is deposited over the electrodes. After

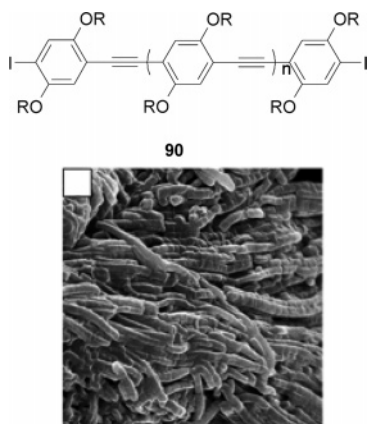


Figure 33. SEM image ($6 \times 6 \mu\text{m}^2$) showing poly(*p*-phenyleneethynylene) **90** wires constructed using a membrane. (Reprinted with permission from ref 211. Copyright 2003 American Chemical Society.)

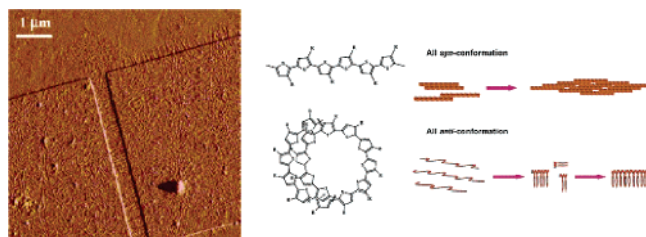


Figure 34. Polythiophene nanowires 3–7 nm in diameter aligned by an electric field (Reprinted with permission from ref 213. Copyright 2004 IOP.) together with the suggested mechanism that can lead to formation of such structures. (Reprinted with permission from ref 214. Copyright 2003 American Chemical Society.)

slow evaporation of the solvent, the authors could determine the conductivity of these wires.²¹² Hadley et al. applied an ac voltage during this drop-casting procedure resulting in the formation of aligned poly-(3-hexylthiophene) nanowires along the electric field lines (Figure 34). The wires show mobilities as high as $0.04 \text{ cm}^2/\text{V s}$.²¹³ The organization of the nanowires, which are 3–7 nm in diameter and a few micrometers long, is unclear. Both an extended syn conformation of the thiophene units leading to face-to-face aggregation as well as the anti conformation of the thiophene units in the polymer chain could result in tubes having a diameter of a few nanometers (Figure 34).²¹⁴

Controlled deposition of nanowires was also accomplished by a scanned-tip electrospinning deposition method by Craighead et al. using a polyaniline/poly(ethylene oxide) mixture (ratio 72/1) (Figure 35). In this method a droplet of a polymer solution was placed on a tip acting as a scanned electrospinning source. The polymer jet, electrostatically extracted from the tip, dried in transit to a substrate on a slow rotating electrode. This process produced oriented nanowires over electrode patterns micrometers long and 190 nm in diameter and showed a conductivity of up to 0.5 S/cm upon doping.²¹⁵

The Langmuir–Blodgett (LB) technique offers a unique possibility to study supramolecular assemblies and internal order of conjugated systems. Monolayers on the air–water interface can be transferred onto solid substrate by several methods such

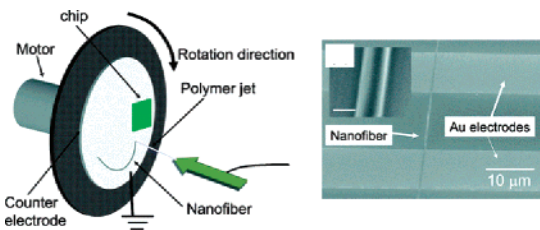


Figure 35. Scanned electrospinning nanofiber deposition system consisting of an arrow-shaped silicon tip source and a rotating counter electrode to which a silicon chip is attached. SEM image of a polyaniline/poly(ethylene oxide) (72/1) nanowire deposited on gold electrodes with a diameter of 190 nm. (Reprinted with permission from ref 215. Copyright 2004 Royal Chemical Society.)

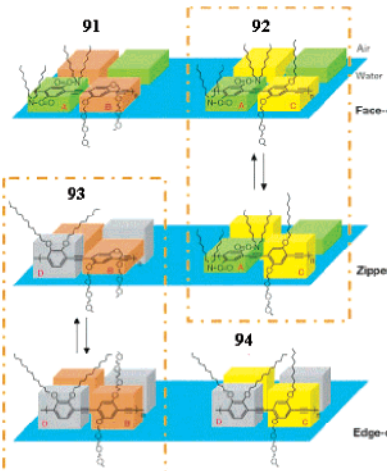


Figure 36. Conformations and spatial arrangements of polymers **91–94** at the air–water interface and their reversible conversions between face-on, zipper, and edge-on structures. (Reprinted with permission from *Nature* (<http://www.nature.com>), ref 220. Copyright 2001 Nature Publishing Group.)

as vertical dipping or horizontal lifting. High-quality multilayer LB films from alkyl-substituted polythiophenes can be obtained by dispersing the polymer in amphiphilic molecules,^{216,217} PPVs²¹⁸ or PPEs²¹⁹ using different amphiphilic building blocks displayed preferential orientations at the air–water interface. Swager et al. showed that the isolated polymer chain's morphology and interchain interactions in PPE polymers (**91–94**) can be controlled.²²⁰ These PPE polymers display face-on, alternating face-on, or edge-on (zipper) orientation depending upon the chemical structure and surface pressure (Figure 36).²²⁰ One monolayer formed by substituted PPE could be reconstructed into nanoscopic-aligned networks of fibrils tens of nanometers in diameter.²²¹

Bjørnholm et al. studied the formation of nanowires of polythiophene which were substituted by alternating hydrophilic and hydrophobic side groups.²²² Isothermic compression leads to densely packed monolayers in which the polythiophene backbones are homogeneously π stacked parallel to the water surface, the oligo(ethylene oxide) tails stick into the water, and the alkyl tails point into the air (Figure 37). Horizontal dipping created a monolayer surface consisting of highly ordered domains. These domains are connected by soft, more disordered boundaries.

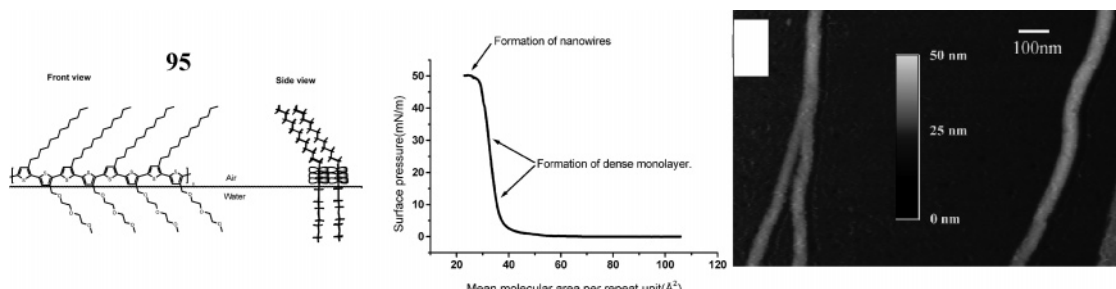


Figure 37. Orientation of amphiphilic polythiophene **95** at the air–water interface. Upon dipping in the upper regime of the Langmuir isotherm, nanowires of **95** can be transferred to a silicon oxide substrate. (Reprinted with permission from ref 223. Copyright 1999 John Wiley & Sons, Inc.)

The order-dependent conductivity of the monolayer was measured by a four-point probe method. Exceptionally high conductivities were observed on the single-domain level, while the disordered regions exhibited much poorer conductivity. This indicated that the in-plane alignment of polymer molecules in a monolayer is a crucial parameter for the electrical properties. When compressed beyond the collapse point on the LB trough, the polythiophene spontaneously folds into wire-like structures (Figure 37), which could be horizontally lifted onto a substrate. The wires are micrometers long, 60 nm wide, and 15 nm high. Bundles of these nanowires could be placed between gold electrodes showing a high conductivity of 40 S/cm upon doping.^{46,222–225}

7. Supramolecular Organization of π -Conjugated Oligomers

Synthetic procedures to produce monodisperse π -conjugated oligomers have considerably improved during the past decades,^{226,227} and relationships have been established between chemical structure and charge-carrier mobility.²²⁸ A continuous film with intermolecular π overlap is beneficial to increase the charge-carrier mobility. Instead, if the charges reside in local potential minima, or traps, they will be stuck and relatively high voltages will be needed to dislodge them. Such traps can be due to oxidizable or reducible chemical impurities, grain boundaries, inhomogeneities at the dielectric interface, or crystallographic defects, resulting in low mobility. Despite the possibility to obtain well-ordered two-dimensional monolayers on graphite of oligo(thiophene)s,²²⁹ oligo(*p*-phenyleneethynylene)s,²³⁰ or oligo(*p*-phenylenevinylene)s,²³¹ as studied with STM, and the ability to vacuum evaporate these oligomers to gain crystalline films,^{16,232–237} it is a challenge to increase control over the mesoscopic order of such oligomers into larger domains by less expensive means. This section surveys the tools that are available nowadays to organize oligomers by self-assembly (see also section 3). The first part deals with the self-assembly of oligomers in the solid state, liquid crystals, and the second part covers the influence of the different supramolecular interactions on the self-assembled structures of oligomers in solution.

7.1. Self-Assembly of Liquid-Crystalline Materials

Liquid-crystalline molecules combine the properties of mobility of liquids and orientational order of

crystals. The mesophases and their temperature regimes provide insight into the internal organization of liquid crystals. Different degrees of orientational order arise from the relative anisotropy of the molecules and can be controlled by varying the rigid segment, its size, and the peripheral side chains. Liquid crystals may be thermotropic, being a state of matter between the solid and liquid phase, or lyotropic, that is ordering induced by the solvent. In the latter case the solvent usually solvates a certain part of the molecule while the other part of the molecule helps induce aggregation, leading to mesoscopic assemblies.

7.1.1. Thermotropic Rodlike Molecules

In the field of optoelectronic applications it is important to produce films that are less expensive and easy to produce without forfeiting the high charge-carrier mobility that is common in crystal structures obtained via vacuum evaporation. Charge transport in smectic systems is generally considered to be two-dimensional. Terthiophene **96** forms a highly ordered smectic SmG phase with a charge-carrier mobility of $0.01 \text{ cm}^2/\text{V s}$.²³⁸ End substitution of oligo(thiophene)s **97–105** (Figure 38) with varying alkyl chain length leads to highly soluble conjugated oligomers, which exhibit smectic mesophases with two spacings that increase with temperature.^{239–242} This result was interpreted by a model involving alkyl-chain movements, yielding shrinkage in spacing, whereas the thiophene units remained at typical van der Waals distances. The liquid-crystal-like structural organization of, e.g., **103** resulted in a high-field-effect carrier mobility for cast films on the order of $0.03 \text{ cm}^2/\text{V s}$.²⁴³ The electron-diffraction pattern of the crystals indicated two-dimensional side-by-side and end-to-end packing of the molecules. However, when oxygen substituents are introduced (**106–107**), the mobilities deteriorated. Smectic phases could be stabilized by additional hydrogen bonding as shown by naphthalene,²⁴⁴ triphenylene,^{245,246} and terthiophene²⁴⁷ derivatives bearing carboxylic acids, carboxamide, or oxyethylenes. Long-range order in oligo(*p*-phenylenevinylene)s was studied as a function of the conjugation length (**108–110**). It was found that only strong π – π interactions in the longest oligomer could phase separate from the tridodecyl chains.^{248,249} Columnar order in OPV derivatives was also reached using hydrogen-bonded dimers between carboxylic acids aided by strong phase separation of the tridodecyloxyphenyl groups (**112, 114**).²⁵⁰ Also,

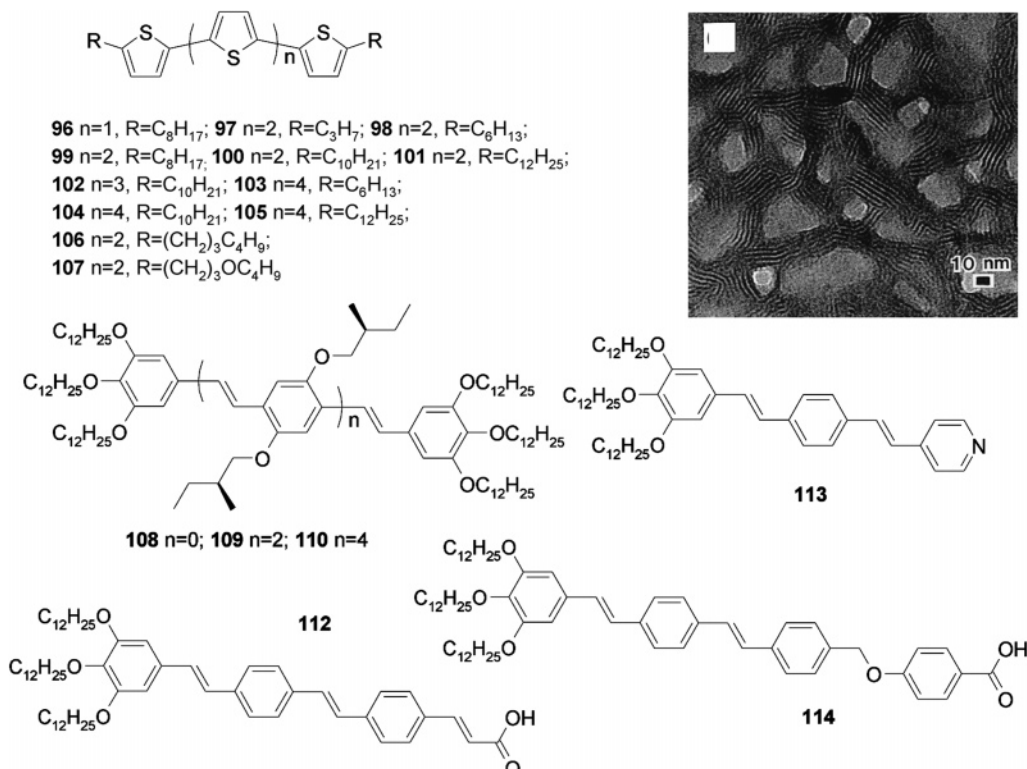


Figure 38. Rodlike π -conjugated oligomers **96–114**. TEM micrograph of a cast film of **103** showing a network morphology of interconnected crystals with random orientations and lattice fringes having a periodicity of 3.6 nm, consistent with the thickness of end-to-end molecular layers. (Reprinted with permission from ref 242. Copyright 1998 American Chemical Society.)

dimerization of OPVs by coordination (**113**), ionic, and fluorophilic interactions have led to discrete liquid-crystalline supramolecular structures that further organize into columnar mesophases.²⁵¹

7.1.2. Thermotropic Discotic Molecules

Whereas rodlike molecules predominantly form smectic phases, discotic molecules preferably form columnar mesophases. Since the first discotic liquid crystal was discovered in 1977,²⁵² a phenylene derivative that exhibited a columnar mesophase, factors that influence the short-range intracolumnar order and long-range intercolumnar order have intensively been studied by varying the substituents on the core. Although columnar stacking was observed by Chandrasekhar et al., the N_{col} mesophase lacked a 2D lattice structure, which was further studied by Destrade et al. to arrive at a semiconducting columnar mesophase.^{253–255} The exchange of the oxygens for sulfur atoms in the side chains resulted ultimately in two mesophases with intracolumnar liquid order, Col_{hd} , and intracolumnar fixed order, Col_{ho} . The latter consisted of hexagonal arrays of columns with a periodic, positional, and helical columnar order due to the steric bulk of the sulfur atoms limiting the rotation of disks but preserving $\pi-\pi$ interactions. The effects of the different degrees of order on the photoconduction were shown by Haarer et al., who injected charges into discotic liquids sandwiched between transparent conducting electrodes. The transient time-of-flight (TOF) measurement for **115** showed increasing charge-carrier mobilities with decreasing temperature in the Col_{hd} , which correlates

with an increase in short-range interactions. A 2 orders of magnitude jump in the charge-carrier mobility up to $0.1 \text{ cm}^2/\text{V s}$ is observed around the transition to the Col_{ho} phase (Figure 39).²⁵⁶ The high mobility and the time dependence of the currents evidence an efficient short-range transport mechanism provided by the face-to-face π stacking of the triphenylene units. Moreover, these values are representative of the bulk sample conductivity since they correspond well with high-frequency time-resolved microwave conduction studies (TRMC).²⁵⁷ Cooling further into the glassy matrix, high mobilities are still present but defects are locked in, causing a significant number of traps.

The thermodynamic stability of the columnar mesophase can be stabilized by introducing additional aromatic interactions (**116**, **118**) at room temperature, giving similar high mobilities.^{258–262} The charge-carrier mobility is determined by the extent of electronic overlap between the triphenylene cores.^{262–264} Short side chains (**117**, $n = 3, 10^{-2} \text{ cm}^2/\text{V s}$) allow for better interaction of the cores resulting in higher mobilities in comparison with long side chains (**117**, $n = 11, 10^{-4} \text{ cm}^2/\text{V s}$).²⁶⁵ Not only the size of the peripheral side chains, but also the nature of the aromatic core affects the charge-carrier mobility. Larger aryl cores such as hexabenzocoronenes (HBCs, **119–121**) give rise to both higher mobilities ($0.7 \text{ cm}^2/\text{V s}$)^{257,266–268} due to the large overlap integral and more efficient charge injection due to the low band gap as pioneered by Müllen et al. (Figure 40).²⁶⁹ The larger aryl cores also widen the mesophase, and the phase-transition temperatures can be easily

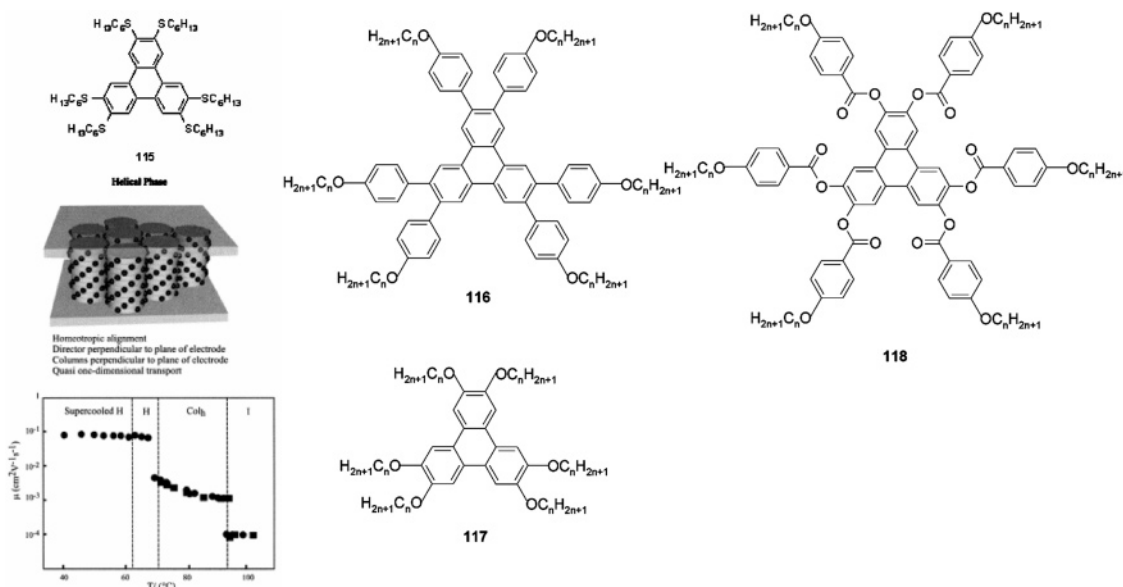


Figure 39. Structural formula of triphenylenes **115–118** and schematic representation of the helical phase formed by **115** and its orientation with respect to the electrode surface. Variation of the TOF charge-carrier mobility as a function of temperature for **115**. (Reprinted with permission from *Nature* (<http://www.nature.com>), ref 256. Copyright 1994 Nature Publishing Group.)

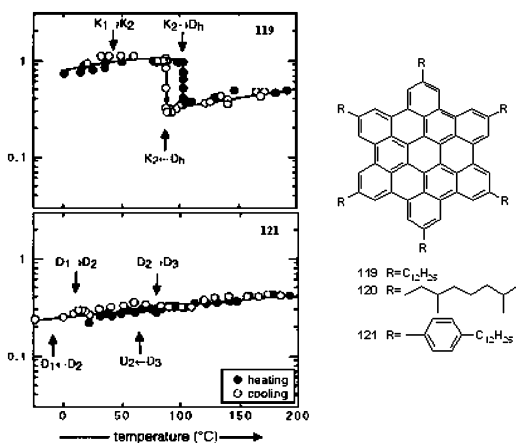


Figure 40. Hexabenzocoronenes **119–121** with temperature-dependent TRMC intracolumnar charge-carrier mobility data for **119** and **121**. (Reprinted with permission from ref 268. Copyright 1999 John Wiley & Sons, Inc.)

engineered by the length, degree of branching, and aromaticity of the side chains.^{270–272}

The HBC molecules can be easily processed from the melt or from solution into columns of high persistence length, and it is a challenge to align them macroscopically. Films with isotropically distributed columns yield numerous grain boundaries. Solid-state NMR studies revealed that the HBC disks can rotate uniaxially within the columns and mobility gradients along the alkyl chains can exist,²⁷³ thereby allowing the dynamic nature of liquid crystals to self-repair defects on the mesoscopic scale. Therefore, a variety of methods to induce macroscopic uniform films were studied.

Annealing at the isotropic transition temperature can induce a reorientation in mechanically deformed films.²⁷⁴ The deposition of HBC molecules in the channel of organic transistors coated with alignment layers generated micrometer long columns extending from source to drain with charge mobilities ap-

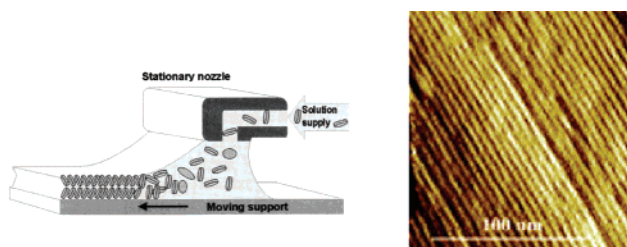


Figure 41. Schematic representation of the zone-casting process with gray disks representing HBC **119** and AFM image of the resulting aligned film. (Reprinted with permission from ref 277. Copyright 2003 American Chemical Society.)

proaching $10^{-3} \text{ cm}^2/\text{V}$.^{275,276} X-ray diffraction confirmed that the columnar stacks were indeed oriented parallel to the underlying PTFE chains. The charge-carrier mobility is lower than that measured by TRMC, indicating polycrystallinity. In a LED configuration it was shown that the onset of the current decreases in homeotropically aligned columns.

Uniaxially aligned thin films of HBC could also be prepared by a simple solution zone-casting method as developed by Müllen et al. (Figure 41). Deposition of a HBC solution from a stationary nozzle onto a moving substrate produces concentration and temperature gradients, dictating uniaxial columnar growth driven by π -stacking interactions. AFM together with X-ray diffraction data reveals large uniform domains with slight columnar defects presumably caused by the folding of columns during final evaporation.²⁷⁷

The additional aromatic interactions in **122** and the out-of-plane orientation of the peripheral phenyl rings induces a helical orientation of the HBC cores giving a helical crystalline phase with a higher persistence length.²⁷⁸ Spin-cast films of **122** revealed arrays of uniform parallel nanoribbons with lengths of 300 nm as studied by AFM (Figure 42). Slow evaporation of the solvent resulted in long, isolated

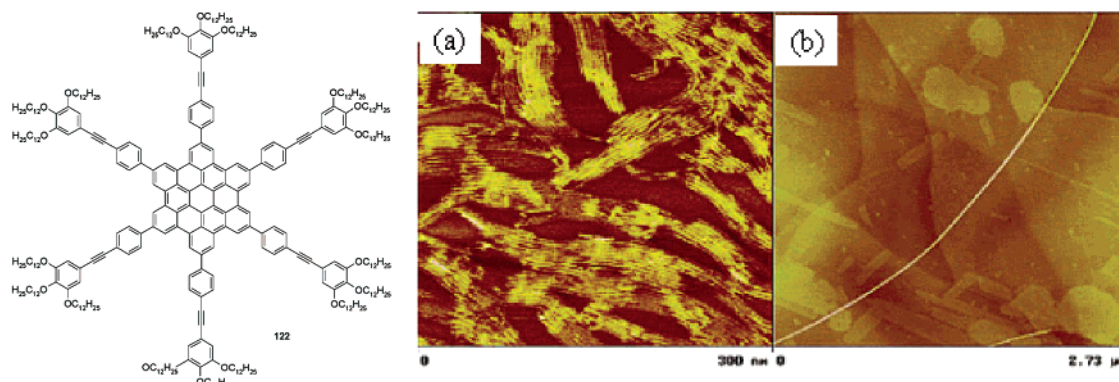


Figure 42. AFM images showing nanoribbons of **122** of 21 nm wide and 3.8 nm high, obtained from (a) spin-cast and (b) drop-cast solutions. (Reprinted with permission from ref 279. Copyright 2004 American Chemical Society.)

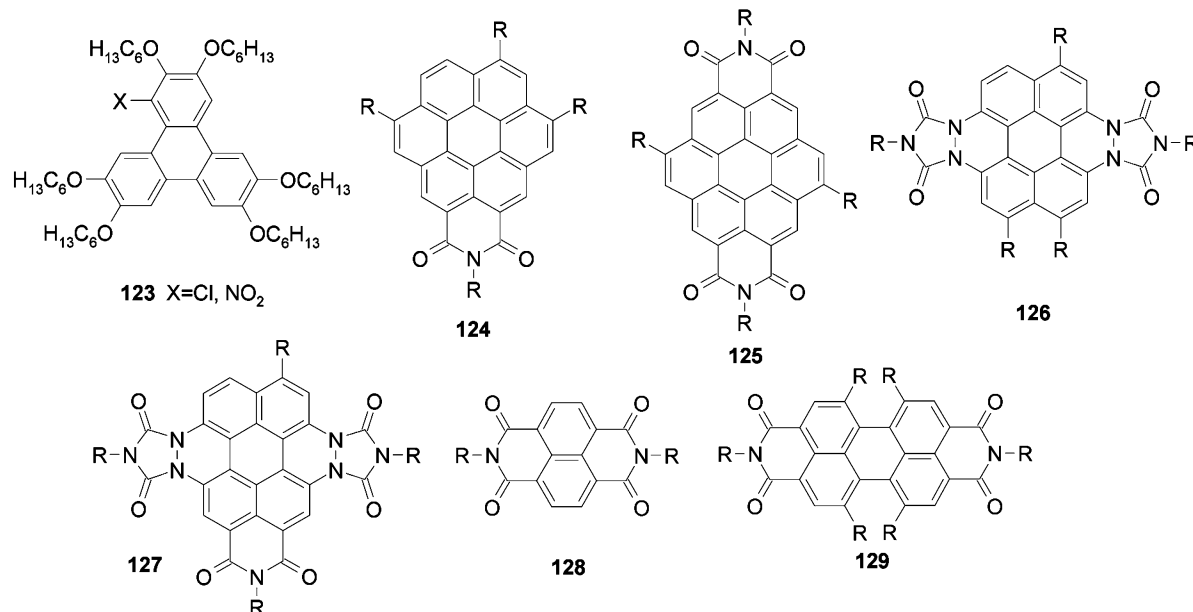


Figure 43. Several general chemical structures of n-type liquid-crystalline materials bearing electron-withdrawing substituents.

regular ribbons 3.8 nm in height and 21 nm in width representing parallel single columns with the columnar axis oriented parallel to the substrate.²⁷⁹ The increased tendency of **122** to spontaneously aggregate is supported by the red-shifted emission solution spectra compared to the alkyl-substituted HBC **119**.

Most columnar liquid crystals are electron-rich aromatic systems that are good hole transporters: p-type materials. Electron-poor aromatic systems are needed to provide electron-transporting n-type materials (**123**), Figure 43. Such compounds are obtained when coronene derivatives were functionalized with carboximide groups. These compounds give rise to mesophases depending on the substitution pattern (**124–127**).^{280–284} Coronenemonoimide **124** showed a large intracolumnar charge-carrier mobility of 0.2 cm²/V s with room-temperature liquid crystallinity.²⁸⁵ Related compounds such as alkyl-substituted naphthalene bisimides **128** and perylene bisimides **129** also formed columnar mesophases^{286–289} with similar high electron charge-carrier mobilities measured by TRMC²⁹⁰ and in FET devices.²⁹¹ Recently, Faul et al.²⁹² showed that complexation of a cationic perylene bisimide derivate **130** with anionic aliphatic surfactants in water also led to a regular hexagonal packing

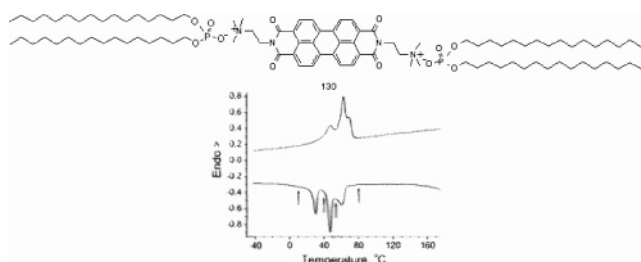


Figure 44. Chemical structure of the complex of ammonium-derivatized perylene bisimide **130** with dihexadecyl phosphate. The DSC trace shows three transitions corresponding to different mesophases. (Reprinted with permission from ref 292. Copyright 2003 Royal Chemical Society.)

of the perylene bisimides that, by shearing, produced uniform birefringent films with high dichroic ratios and order parameters up to 0.7 (Figure 44). Perfluoroalkyl or cyano substituents on oligothiophenes are other approaches to produce n-type semiconducting materials exhibiting at best 0.08 cm²/V s; however, so far only crystalline materials have been used.^{293,294}

Apart from electron-withdrawing peripheral substituents, introduction of nitrogen in the core can also reduce the electron density of the aromatic system.

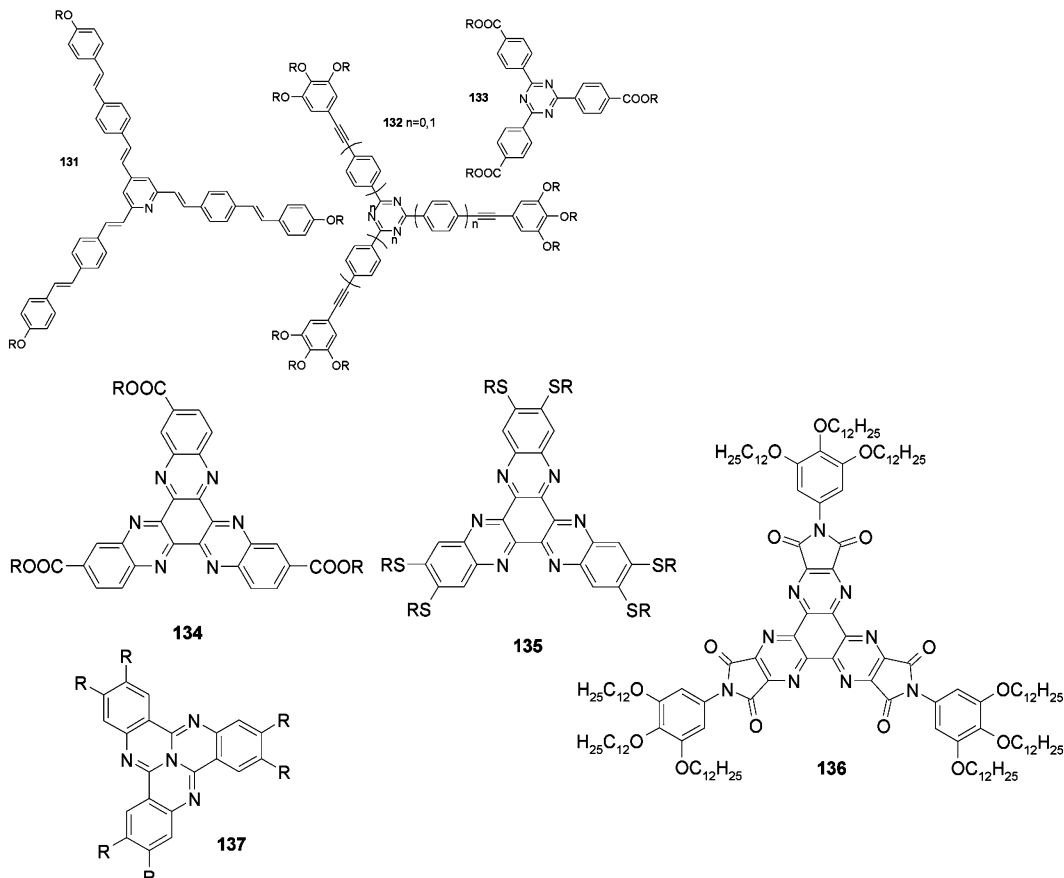


Figure 45. Several n-type liquid-crystalline materials with electron-deficient cores.

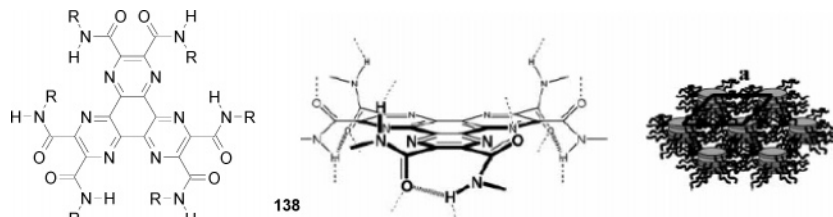


Figure 46. Hexaamide derivative **138** is able to form inter- and intramolecular hydrogen bonds allowing stacking with an interdisk distance of 0.32 nm. The columns further assemble into a hexagonal columnar phase as schematically drawn. (Reprinted with permission from ref 305. Copyright 2003 John Wiley & Sons, Inc.)

Different azaaromatic compounds that vary in size, the smallest being the pyridine (**131**) and triazine (**132**, **133**) units, can give rise to columnar mesophases of different degrees of order.^{295–298} Extended electron-deficient disks (**134**–**137**) are based on hexaaazatriphenylene^{299–301} and quinoxaline^{302–304} cores (Figure 45), having charge-carrier mobilities up to 10^{-3} cm²/V s.³⁰⁴ The potential application as electron-accepting materials in solar cell devices was demonstrated on liquid-crystalline films of **136** in the presence of a p-type polythiophene polymer by photoinduced absorption and fluorescence measurements.³⁰¹

Hydrogen bonding can be used to significantly enforce the intracolumnar stacking order. The smallest interdisk distance of 0.32 nm ever reported in a columnar stack was in a Col_{h0} mesophase of derivative **138** by Geerts et al. (Figure 46). The short distance was caused by amide hydrogen bonds between adjacent molecules in the stack resulting in a high charge-carrier mobility of 0.02 cm²/V s.³⁰⁵

Until recently, attempts to obtain liquid-crystalline C₆₀ derivatives were restricted to smectic phases.^{306–311a} The attachment of five phenylene groups equipped with long alkyl chains to one pentagon of a C₆₀ fullerene yielded a deeply conical molecule (**139**) that stacked into columnar assemblies.^{311b} The stacking is driven by attractive interactions between the spherical fullerene moiety and the hollow cone formed by the five aromatic side groups of a neighboring molecule in the same column.

7.1.3. Lyotropic Liquid Crystals

Discotics can also self-assemble in polar or apolar solvents by π – π interactions, forming rod- or worm-like polymers. Additional hydrogen-bonding and solvophobic forces can further strengthen attractive intermolecular stacking. Lateral interactions between the columns arise at higher concentrations resulting in formation of entangled three-dimensional networks, e.g., gel phases or lyotropic liquid-crystalline phases.^{312,313}

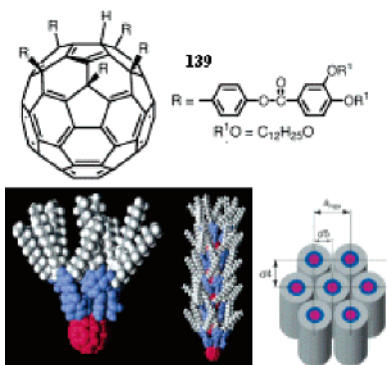


Figure 47. Chemical formula of fullerene derivative **139** with a modeled single conical structure. A stack of five of these structures is shown that exhibits a hexagonal columnar mesophase from 40 to 140 °C. (Reprinted with permission from *Nature* (<http://www.nature.com>), ref 311b. Copyright 2002 Nature Publishing Group.)

The synthesis of desymmetrized HBC derivatives^{314,315} allows one to create amphiphilic HBCs. Depending on the applied pressure, these amphiphiles can be organized in Langmuir layers resulting in two different packing arrangements at the air–water interface. Under low pressure a well-ordered, π -stacked lamellar arrangement of HBC derivative **140** was observed which was lost at high pressures.³¹⁶ The thickness of the first layer can be controlled by the ionic interactions between the carboxylate HBC derivative and polyethylene imine anchored on a silicon oxide wafer (Figure 48).^{317,318} Polarized absorption confirmed the orientation of the columns with their main axis parallel to the dipping direction. In another experiment complexation of the

carboxylate-functionalized HBC with an aminoethyl-proline-functionalized poly(dimethylsiloxane) results in a polymeric complex (**141**), which forms highly ordered discotic columnar structures. The polymeric nanostructures, which contain a hierarchy of three incompatible elements, i.e., aromatic cores embedded in a matrix of alkyl chains which itself is embedded in a matrix of polysiloxane, have lengths of at least 200 nm. The columns show two different degrees of internal order; low order was found when HBC cores were tilted with respect to the column axis and higher order when HBCs were perpendicularly oriented to the column axis. The extended columns could be visualized by TEM due to their electron conductivity (Figure 48).³¹⁹ Since polyelectrolytes can be deposited in a controlled way, this approach of ionic self-assembly can tremendously aid the orientation and positioning on a surface.³²⁰

Another approach is using organogelators as a director to control the morphology of the liquid-crystalline film. Oriented columns of triphenylene derivatives are formed when mixtures of **117** ($n = 6$) with a gelator (Figure 49) are cooled from the isotropic liquid states. The different phase sequence of the mixture determines the size of the domains. When gelator phase separation occurs after **117** enters the liquid-crystalline state on cooling, the aggregates of the gelator develop in the boundary of the liquid-crystalline domains because this mesophase and the isotropic liquid phase of **117** are immiscible. In this way, uniform domain sizes of approximately 30 μ m are obtained. If the phase sequence is reversed, the gelator forms aggregates

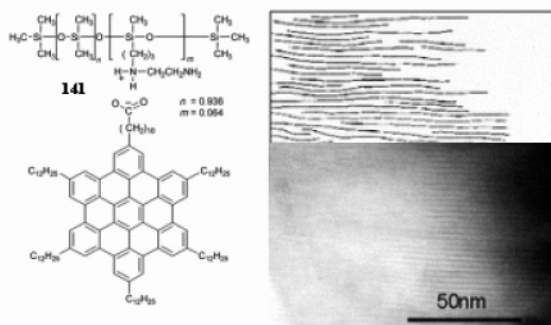
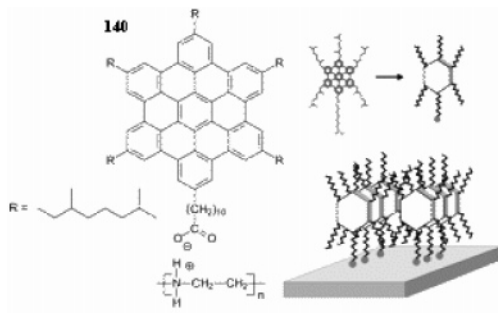


Figure 48. Chemical structure and schematic representation of the amphiphilic HBCs **140** (Reprinted with permission from ref 317. Copyright 2003 American Chemical Society.) and **141** complexed ionically to a silicon wafer surface. TEM image showing brighter lines corresponding to the HBC columns and dark ones to the surrounding siloxane matrix spaced by 2.3 nm. (For clarity, the copy of a transparent overlay is shown.) (Reprinted with permission from ref 319. Copyright 2000 Royal Chemical Society.)

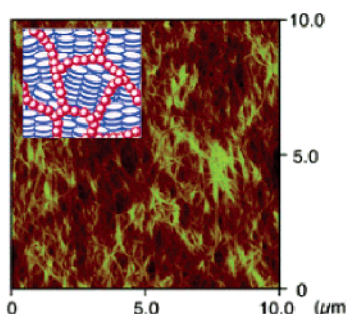
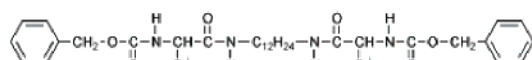


Figure 49. AFM image of the xerogel **117**/L-amino acid with a cartoon representing the LC domains in blue and the gel domains in red. (Reprinted with permission from ref 321. Copyright 2002 Royal Chemical Society.)

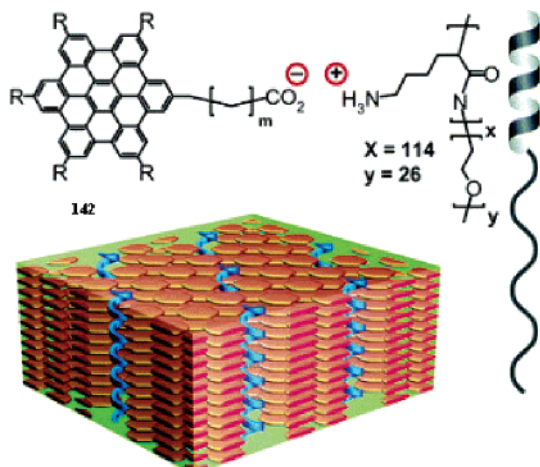


Figure 50. Molecular structure of an HBC (red) and poly(ethylene oxide)-block-poly(L-lysine) (blue) complex **142**, and a model showing the resulting morphology. (Reprinted with permission from ref 322. Copyright 2003 American Chemical Society.)

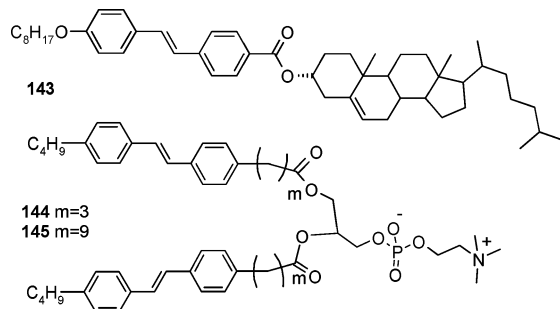


Figure 51. Stilbene derivatives capable of gelating various organic solvents.

in the isotropic state of the triphenylene, which is a miscible mixture. The fibers are able to form finer networks resulting in the formation of the liquid-crystalline domains at the submicrometer level (Figure 49).³²¹

Interestingly, vertical alignment of HBC stacks can be achieved using an amphiphilic poly(ethylene oxide)-poly(L-lysine) block copolymer. Poly(ethylene oxide)-poly(L-lysine) forms a vertical 2D hexagonal lattice on the air–water interface in which six discotic columns of HBC surround an α helix of poly(L-lysine) by acid–base interactions (**142**, Figure 50). The height of the columns could be tuned by changing the length of the L-lysine polymer.³²²

Organogelators based on π -conjugated systems are relatively rare in contrast to systems based on dyes (anthracene,^{323–330} porphyrine,^{331–342} phthalocyanine,^{353–362} pyrene,³⁶³ and squaraine^{364–366}). Cholesterol (**143**) and phospholipid (**144**, **145**) tethered *trans*-stilbenes are able to gelate different organic solvents in which the steroid or lipid unit serves as a template to form one-dimensional stacks, Figure 51.^{367,368}

Ajayaghosh et al. serendipitously extended this concept to OPV derivatives (**146–148**) and reported a completely thermoreversible self-assembly process in a series of hydrocarbon solvents from single OPV molecules to fibers and ultimately to an entangled network structure. The absorption and emission

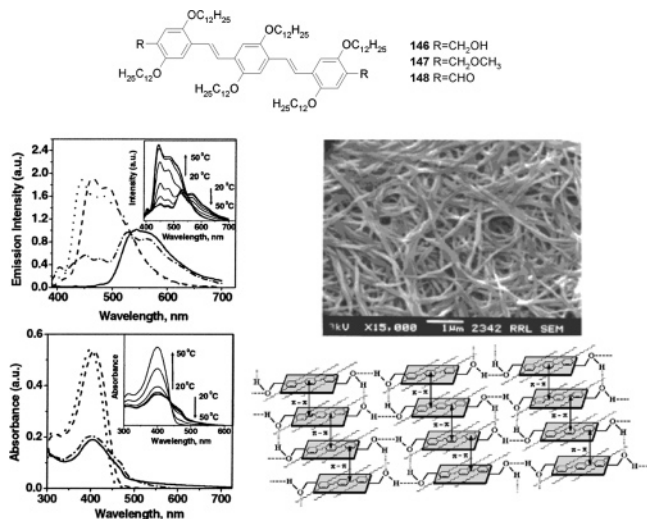


Figure 52. OPV derivatives **146**–**148** are able to gelate in hexane monitored by temperature-dependent absorption and emission spectra of **146**. For comparison, these spectra are also given in a good solvent like chloroform and as a film from hexane. The SEM picture of a dried gel of **146** shows an entangled fibrillar network. The self-assembly of the gel is proposed in the scheme. (Reprinted with permission from ref 369. Copyright 2001 American Chemical Society.)

properties showed dramatic changes during gelation, which is an indication of strong intermolecular π electronic coupling of the ordered OPV segments. In a comparative study it was shown that gelation was cooperative and strongly dependent on the choice of hydrogen-bonding motif, alkoxy side-chain length, and conjugation length. An alcohol OPV trimer (**146**) equipped with six lateral dodecyl chains easily forms a gel at moderate concentrations in hexane, whereas the aldehyde analogue (**148**) could not gelate the solvent nor a methyl ester analogue (**147**) under extreme conditions. SEM, X-ray diffraction, and IR on the gel from **146** revealed an entangled network of fibers up to micrometer lengths and 100–150 nm in width consisting of well-ordered lamellae of stacked molecules positioned by hydrogen bonds (Figure 52).³⁶⁹

Van Esch et al. have shown that high charge-carrier mobilities up to $5 \times 10^{-3} \text{ cm}^2/\text{V s}$ can be realized in gel networks built from thiophene derivatives **149**–**151** modified with bisurea units. The thiophene moieties formed closely packed arrays enforced by the urea hydrogen-bonding units, thereby creating an efficient pathway for charge transport.³⁷⁰ The nanostructures were studied on several substrates, like SiO_2 , mica, and highly oriented pyrolytic graphite (HOPG). Elongated twisted fibers were observed on SiO_2 with lengths of 20–100 μm and widths of 2–10 μm (Figure 53). These fibers are strongly birefringent, indicating a high degree of molecular ordering. After annealing extended monolayers are formed consisting of upright 1D arrays standing side-by-side.³⁷¹ On HOPG the 1D arrays lie flat on the surface with tilted thiophene rings allowing partially overlapping π systems.³⁷² Scanning tunneling spectroscopy indicates that an effective conjugation in the π stacks exists as the band gap of the thiophenes was decreased (Figure 53).³⁷³

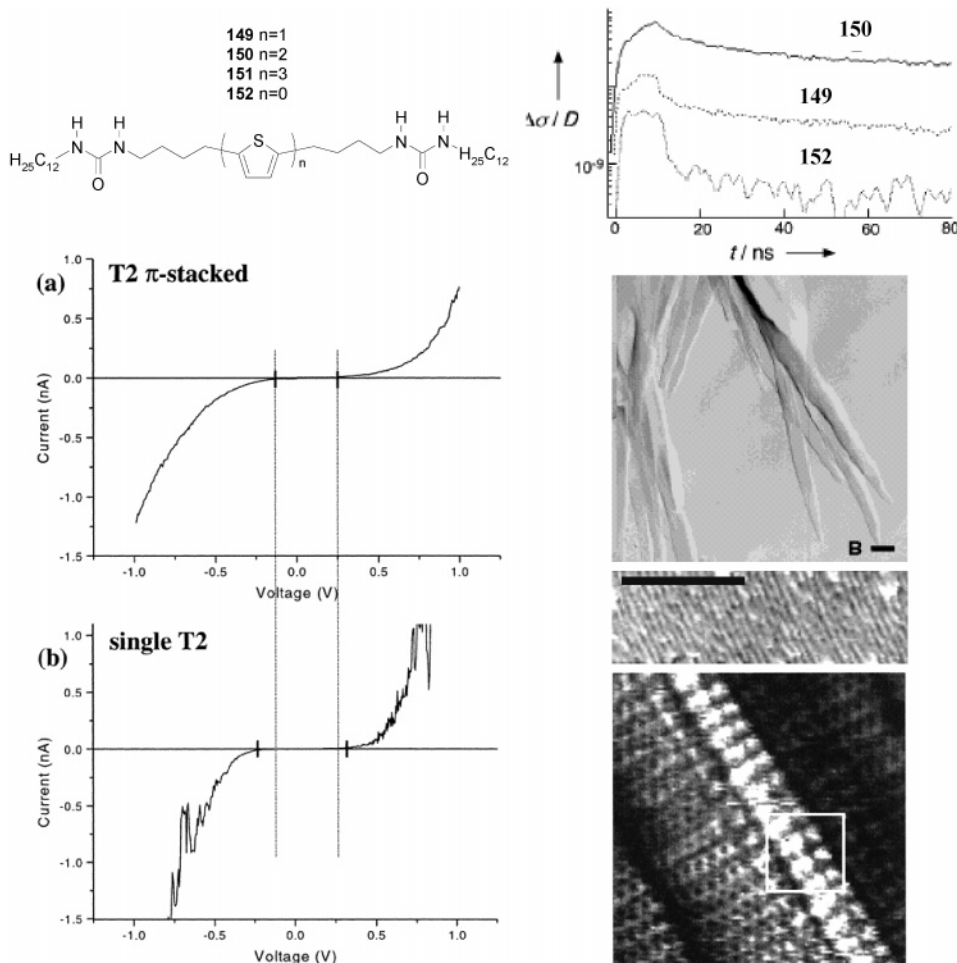


Figure 53. Urea-derivatized thiophenes (T_n) **149–151** form gel networks as visualized by SEM (top image). Single ribbons of **150** on HOPG are visualized by AFM (middle image) and analyzed by STM (bottom image). Bias-dependent STM yields evidence for π -overlapping stacked molecules as the band gap is decreased for stacked T2 (top graph, left) compared to single T2 (bottom graph, left). TRMC conductivity data (top graph, right) show a clear dependence on gelation or conjugation length. (Reprinted with permission from refs 370 and 371 and 372 and 373. Copyright 1999 and 2000 John Wiley & Sons, Inc. and 2001 American Chemical Society.)

7.2. Self-Assembly by Specific Interactions in Solution

Controlled self-assembly of oligomers in solution is of interest for obtaining objects of discrete size and shape. This process strongly depends on the nature of the interactions and the shape of the building blocks, and a large variety of architectures can be formed in solution. Structures ranging from random coil polymers to intertwined helices and discrete multimolecular objects have been obtained. A typical feature of these assemblies is the dynamic behavior of the molecules within the aggregates. The molecules located in the aggregates may still be mobile or have some positional disorder. Accordingly, understanding how self-assembly is controlled by the molecular architecture will enable the design of increasingly complex structures.

In the self-assembly of π -conjugated oligomers different specific interactions work simultaneously and the strength of the overall binding is the result of many cooperative processes. To create some order in this review we used in this section $\pi-\pi$, hydrophobic, or hydrogen-bonding interactions as the leading factor. Recently, ligand–metal interaction has

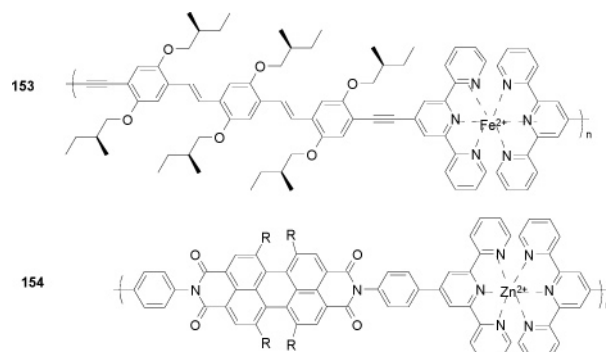


Figure 54. Supramolecular polymers by metal coordination to π -conjugated oligomers.

been used to link conjugated oligomers OPV (**153**) and perylene bisimide (**154**), both bearing terpyridine receptor groups (Figure 54). This is an interesting approach; however, it lacks the reversibility that is typical for noncovalent architectures.^{374,375}

7.2.1. Assembly by $\pi-\pi$ Interactions

Supramolecular organization in solution of well-defined oligomers has scarcely been taken into consideration.³⁷⁶ For example, the relation between

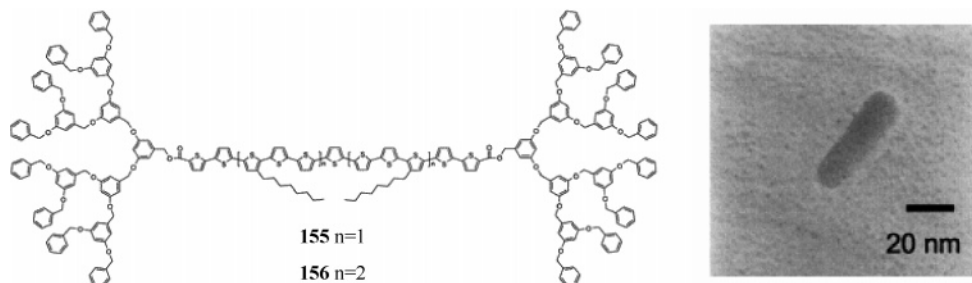


Figure 55. Dendritically substituted thiophenes that aggregate into nanorods as imaged by TEM. (Reprinted with permission from ref 386. Copyright 2001 American Chemical Society.)

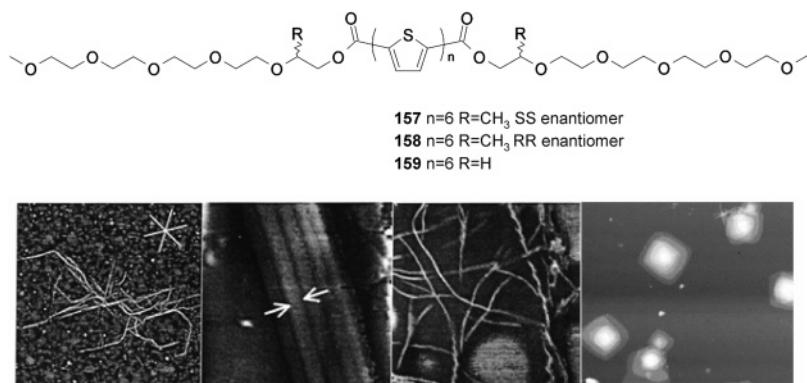


Figure 56. AFM images show (a) large ribbons on graphite, (c) left-handed helical aggregates on silicon oxide, and (d) pyrimidal assemblies on mica formed by the slow evaporation of a THF solution of **157**. (b) An $80 \times 80 \text{ nm}^2$ STM image shows the internal structure of a ribbon on graphite. The white arrows indicate the width of a single, thin ribbon. (Reprinted with permission from refs 393 and 394. Copyright 2004 Elsevier and 2002 American Chemical Society.)

intermolecular interactions and optical properties of substituted ter- and quarterthiophenes or tetra-thienylenevinylene has been studied by UV-vis and fluorescence spectroscopies in linear and branched alkane or PMMA matrixes.^{377,378} These results showed that aggregates of oligothiophenes display a blue-shifted absorption spectrum with respect to the molecularly dissolved state. This behavior was attributed to the formation of H aggregates, assemblies in which the conjugated segments have an orientation perpendicular to the packing axis.^{379,380}

Fréchet et al. synthesized triblock systems by symmetrically substituting undeca- and heptadecathiophene cores (**155**, **156**) with oligo(benzyl ether) dendrons. In such a way monodisperse macromolecular architectures³⁸¹ are obtained similar to dendritically substituted oligothienylenevinylene³⁸² and oligo-imides.^{383,384} Janssen et al. showed TEM images of the self-assembly of **156** into uniform nanoaggregates in size (20 nm) and shape (rodlike) in dichloromethane at low temperatures (Figure 55). Detailed analysis of the self-assembly in solution indicated a temperature-induced aggregation in which an intra-chain planarization preceded the intermolecular $\pi-\pi$ stacking. The favorable interactions led to an inter-chain delocalization of the photoexcited singlet, triplet, and charged states. Quantitative analysis of the aggregation process shows that the supramolecular aggregates are relatively small involving five to six molecules.³⁸⁵⁻³⁸⁷ The apparent size limitation of the aggregates is ascribed to steric constraints imparted by the dendritic wedges.³⁸⁸

7.2.2. Assembly by Amphiphilic Interactions

Advincula et al. designed a sexithiophene bearing cationic alkyl substituents at either end of the hydrophobic aromatic core. Ordered ultrathin films by layer-by-layer self-assembly from either a molecularly dissolved or an aggregated state was aimed for in this study.^{389,390} Cationic substituents were also used in a third-generation poly(propylene imine) dendrimer modified with oligo(*p*-phenylenevinylene)s to create a branched amphiphile. Spherical and rod-like aggregates form in protic solvents such as water and decanol. Interestingly, the spherical aggregates could be manipulated by optical tweezers.³⁹¹

Leclère et al. described the self-assembly process of amphiphilic sexithiophene derivatives substituted with chiral penta(ethyleneoxide) chains to control the interplay of hydrophobic and hydrophilic interactions, guiding the $\pi-\pi$ stacking of the oligomeric units and allowing this material to be used for fabrication of a thin film transistor.³⁹² On silicon wafers aggregation of **157** led to ropes with left-handed supramolecular helicity, which was not present in ropes from achiral analogue **159**.^{393,394} The oligomers adopt an edge-on orientation on oxidic surfaces by minimizing the contact area between hydrophobic parts of the molecule and surface (Figure 56). A face-on lamellar array of π -stacked oligomers, typically a 3–5 molecules in width, was observed on HOPG. Results reported for a series of oligo(*p*-phenyleneethynylene) derivatives revealed the importance of regular π -stacking interactions. Nano-ribbons are formed on HOPG from oligomers with seven repeat units and higher, whereas the shorter ones revealed globular aggregates.

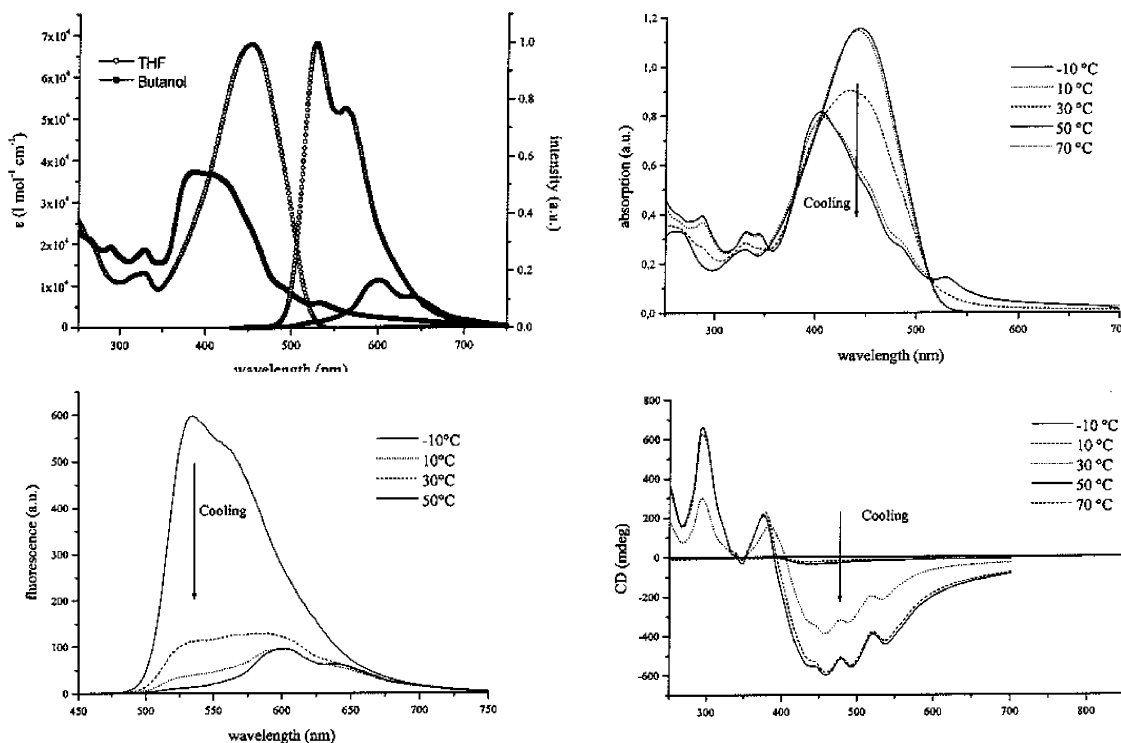


Figure 57. Absorption and fluorescence spectra of **159** in THF and butanol. Temperature-dependent absorption, CD, and fluorescence spectra of **157** in *n*-butanol. (Reprinted with permission from ref 394. Copyright 2002 American Chemical Society.)

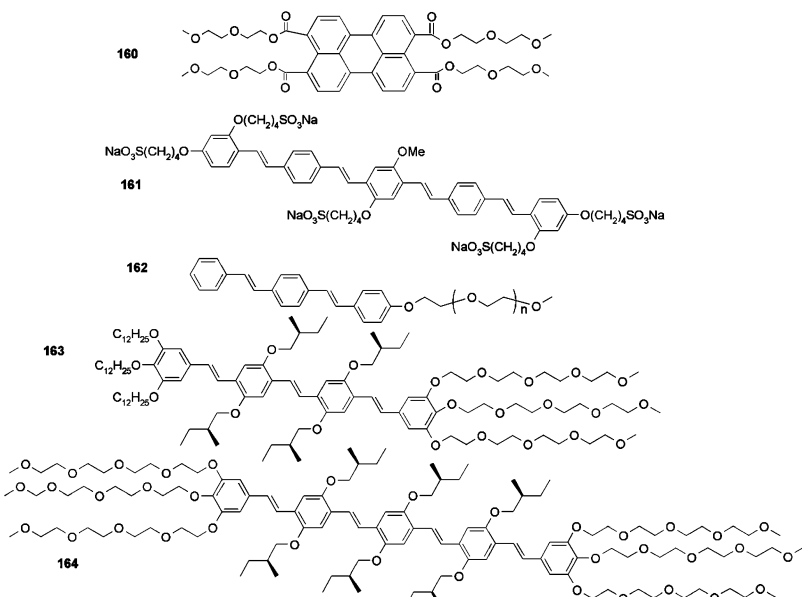


Figure 58. Amphiphilic oligomers designed to self-assemble in water.

Meijer and Feast et al. studied the aggregation of sexithiophenes **157** and **159** in protic media such as water and butanol (Figure 57).^{395,396} The self-assembly was accompanied by a blue shift of the UV-vis absorption, reduced fluorescence intensity, and, for **157**, observation of a bisignate CD effect indicating chiral superstructures. Thermochromic CD and UV-vis measurements showed a reversible transition at 30 °C, demonstrating that the chiral aggregates break up. The shape of these supramolecular assemblies was not elucidated by the authors; however, recent studies on analogous asymmetric quarterthiophene bearing only one oligo(ethylene

oxide) chain show the formation of multilamellar vesicles in water.³⁹⁷

Recently, Bouteiller et al. reported on amphiphilic perylene **160** that self-assembles into monomolecular flexible rods in water as demonstrated by UV-vis absorption and SANS measurements.³⁹⁸ Other molecules which have been reported to self-assemble through hydrophobic π – π interactions are OPVs bearing sulfonic acid side groups (**161**)³⁹⁹ or oligo(ethyleneoxide)s (**162**–**164**), Figure 58.⁴⁰⁰

The organization of OPV amphiphiles **163** and **164** in water revealed aggregation into chiral objects. Thermochromic CD measurements showed a transi-

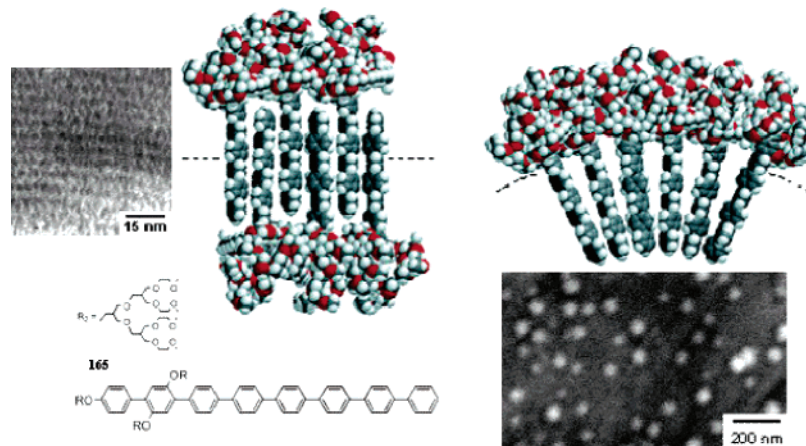


Figure 59. Schematic representation of the molecular arrangement of **165** either into an interdigitated parallel arrangement (TEM) of molecules or into an orientationally ordered radial arrangement of molecules resulting in nanocapsules (AFM). (Reprinted with permission from ref 403. Copyright 2004 American Chemical Society.)

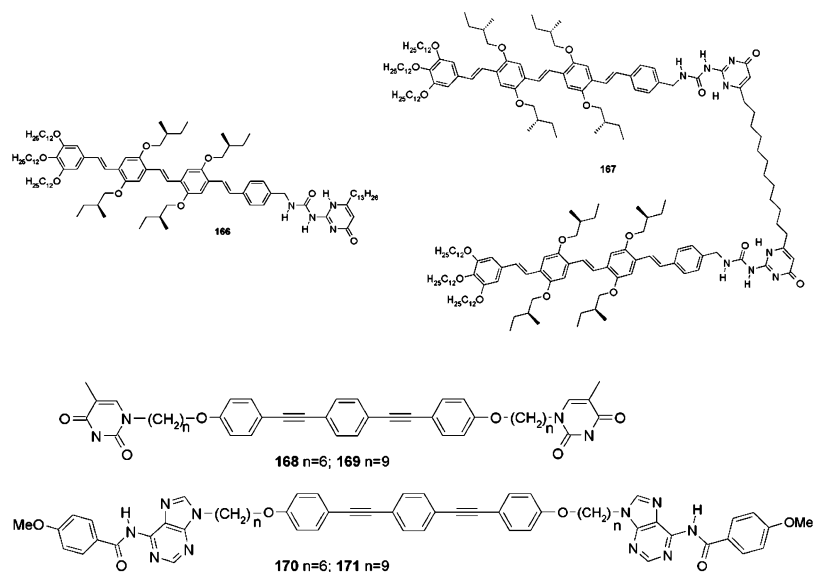


Figure 60. Conjugated oligomers provided with strong hydrogen-bonding interacting units.

tion at 50 °C from a chiral aggregated state to disordered aggregates in a moderately cooperative process.⁴⁰¹ A hexameric OPV analogue bearing methyl groups on either end of the OPV displayed a complicated aggregation behavior. The magnitude and sign of the Cotton effect varied in a range of solvents.⁴⁰²

The strong influence of solvophobic interactions on the change of the shape of the structures in water compared to bulk morphology was shown by Lee et al. In the bulk the octa-*p*-phenylenes equipped with oligo(ethyleneoxide) dendrons (**165**) formed an interdigitated parallel arrangement with a 2 nm periodicity, whereas in dilute solution an ordered radial arrangement was obtained resulting in nanocapsules 46 nm in diameter (Figure 59).⁴⁰³

7.2.3. Assembly by Hydrogen Bonding

Supramolecular polymers are constructed from monomeric units that are glued together by reversible noncovalent hydrogen-bond interactions and as such comprise a special class of self-assembled systems.⁴⁰⁴ Recently Meijer et al. reported on supramolecular

hydrogen-bonded OPV dimers (**166**) and polymers (**167**) in which the specific electronic and optical properties of conjugated OPV oligomers were combined with the material properties of polymers.^{405,406} These polymeric systems are based on the dimerization of strong quadruple hydrogen-bonding ureido-pyrimidinone units, resulting in a random coil polymer in solution lacking higher mesoscopic order. The supramolecular polymer could easily be processed, revealing smooth films, and photoinduced electron transfer was observed when blended with a C₆₀ derivative. This blend could be successfully incorporated in a photovoltaic device.

Hydrogen bonds have also been used to obtain liquid-crystalline phases. When nucleobases such as adenine and thymine are attached to known mesogens such as alkoxyphenylethylenes **168–171**, no liquid crystal phase could be observed. However, the 1:1 blends of the complementary nucleobase derivatives resulted in formation of fairly stable lyotropic liquid-crystalline phases, Figure 60.⁴⁰⁷

Hydrogen bonds have also been used to position π -conjugated molecules in self-assembled architectures. Multiple hydrogen-bonding interactions were

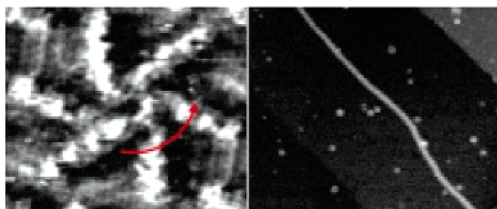
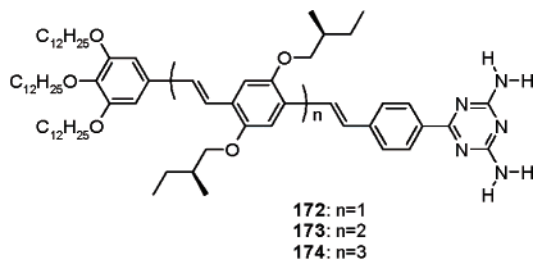


Figure 61. Representation of OPVs functionalized with a hydrogen-bonding triazine unit that form hexameric rosettes, which stack into helical wires in apolar solvents. (Reprinted with permission from ref 409. Copyright 2004 John Wiley & Sons, Inc.)

introduced in OPV systems to create organized structures, sheets, and wires. An OPV trimer, tetramer, and pentamer (**172–174**) were equipped with a diaminotriazine hydrogen-bonding motif and a tridodecyloxy wedge as end groups and substituted with enantiomerically pure (S)-2-methylbutoxy side chains on the OPV backbone. Stable monomolecular Langmuir films are constructed of the π -stacked tetramers with the triazine moieties pointing into the water phase.⁴⁰⁸ The possibility of recognizing complementary molecules present in the water subphase via multiple hydrogen-bonding interactions was considered to be an important application. On another ordered substrate, HOPG, monolayers were studied by STM. Chiral hexameric macrocycles at the solid–liquid interface were formed by hydrogen bonding between adjacent diaminotriazine moieties (Figure 61). These cycles further organize into tubes in apolar

solution, as demonstrated by UV–vis, fluorescence, and CD spectroscopy. The OPV molecules self-assemble hierarchically: first forming hexameric rosettes by hydrogen-bond formation, which subsequently develop into stacks aided by π – π interactions of the phenylenevinylenes. The chiral side chains induce supramolecular helicity. It was proposed that the cyclic hexameric rosettes were not fully planar, resulting in a propeller arrangement allowing interplanar hydrogen-bond interactions from rosette to rosette, thereby locking the rosettes within the tubules. Tubules 7 nm in diameter and 180 nm in length and with perfect space filling are still soluble due to the apolar shell that surrounds the stacks as revealed by SANS and AFM (Figure 61).⁴⁰⁹

Hydrogen-bond-mediated complexes of naphthalenebisimide and complementary dialkylated melamines can also result in mesoscopic tube-like nanostructures as shown by Kimizuka et al. (Figure 62). Molecular stacking of the hydrogen-bond-mediated aromatic sheets was proved by a red shift of the onset in absorption spectra of the naphthalenebisimide chromophore. The flexible alkyl chains that surround the aggregate probably stabilize the weak hydrogen bonds. Flexible rodlike aggregates with widths of 12–15 nm are found by electron microscopy, and a stacked cyclic dodecameric structure or a helically grown structure was proposed (Figure 62).^{410,411}

Würthner et al. extended the process of superstructure formation to perylene bisimide derivatives. The schematically outlined process in Figure 63 is hierarchical and involves multiple intermolecular interactions, appropriate solubilizing substituents, and a solvent of low polarity. NMR, optical spectroscopy, and DLS measurements revealed large-sized aggregates of 200 nm already in dilute methylcyclohexane solution. Complexation of perylene bisimide with chiral melamines exhibited exciton-coupled Cotton effects for the perylene bisimide absorption bands. SEM images of these mesoscopic superstructures showed a densely intertwined network with

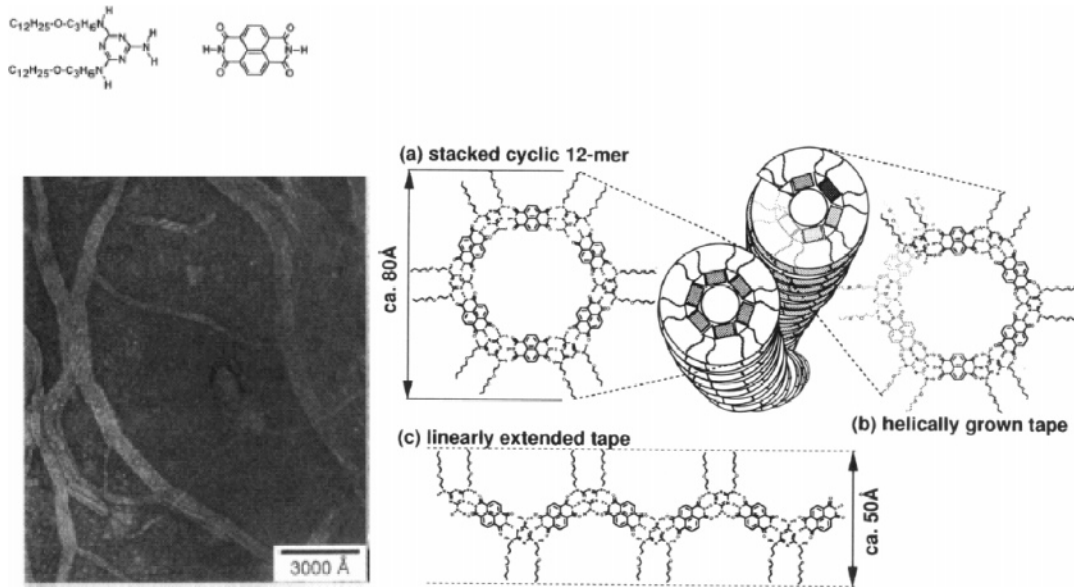


Figure 62. TEM image of self-assembled melamine-naphthalenebisimide complexes from apolar solvent. Three different modes of self-assembly are schematically depicted. (Reprinted with permission from ref 411. Copyright 1995 American Chemical Society.)

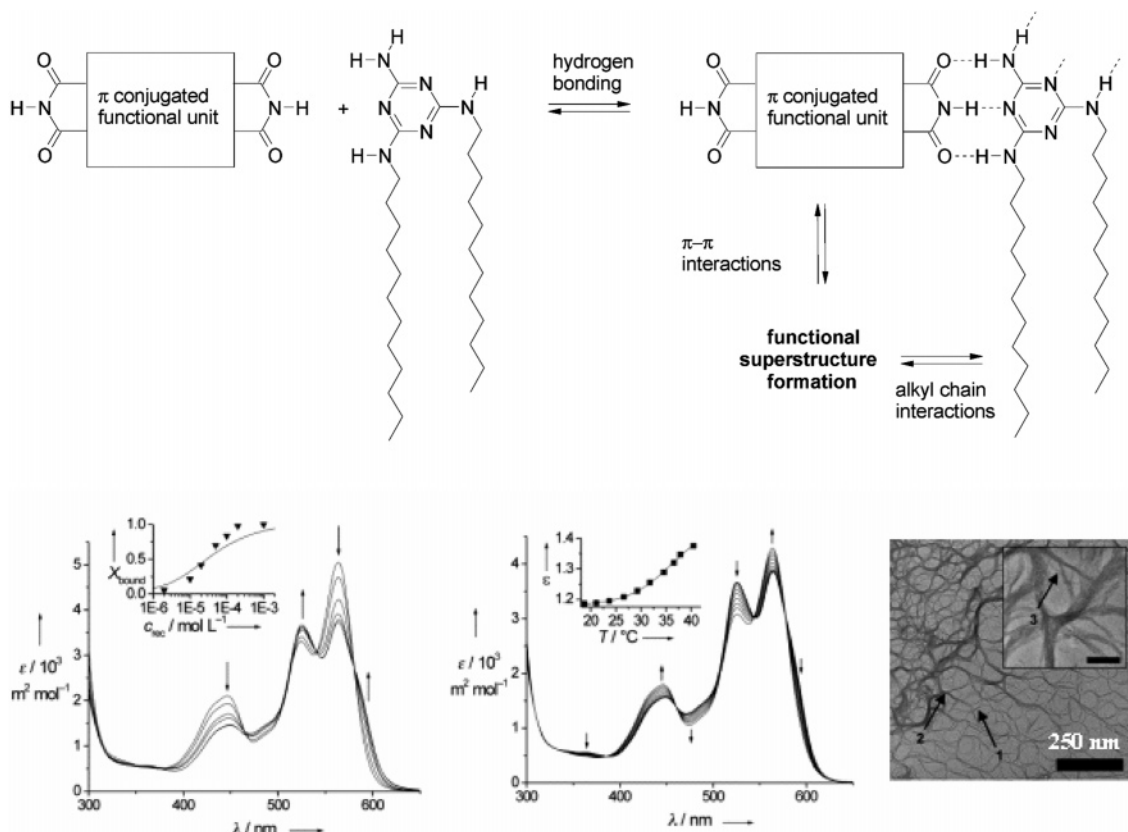


Figure 63. Concentration- and temperature-dependent self-assembly of a perylene-melamine complex in an apolar solvent. TEM imaging reveals an entangled network. (Reprinted with permission from ref 413. Copyright 2000 John Wiley & Sons, Inc.)

cylindrical strands having diameters in the range of 15–500 nm. These dimensions indicate that further self-assembly into tertiary structures takes place. Confocal fluorescence microscopy studies showed excellent photostability of these superstructures in the solid state.^{412–414}

The hydrogen-bonding strength in OPV systems could be augmented by increasing the number of hydrogen-bond interactions.^{404,415} OPVs that differ in conjugation length have been synthesized that contain chiral side chains, long aliphatic chains, and a ureido-s-triazine hydrogen-bonding unit (**175**–**177**).^{416,417} Quadruple hydrogen bonding plays a dominant role in the intermolecular interactions, and dimers are already formed in chloroform. ¹H NMR and photophysical measurements showed that the OPV oligomers grow hierarchically in an apolar solvent into chiral stacks by solvophobic and π – π interactions (Figure 64).

The melting temperature and the persistence length of the stacks increases with elongation of the π system of the OPV oligomers as shown by SANS and optical measurements. Rigid cylindrical objects are formed which, in the case of the tetramer **176a**, have a persistence length of 150 nm and a diameter of 6 nm, whereas trimer **175** shows rigid columnar domains 60 nm in length with a diameter of 5 nm (Figure 64). Melting of the stacks takes place in a relatively narrow temperature range, indicating that thermal denaturation of the stacks is a cooperative process. It is probable that the stability of the stacks is a consequence of many reinforcing bonds, each of

which is relatively weak. Formation of any of these stabilizing bonds is very dependent on whether adjacent bonds are also made. Melting of the stacks depends on the concentration, similar to what is found for denaturation of DNA in nature. Exciton quenching by either dissociation at charge-transfer traps or internal conversion in structural defects is fast, less than 50 ps for **176a** (Figure 65).⁴¹⁸ Exciton bimolecular annihilation is observed at high exciton densities. The electronic properties of the supramolecular OPV wires are intermediate between molecular crystals and disordered polymeric conductors, i.e., between collective excitation and hopping regimes.⁴¹⁹

When two hydrogen-bonding units are connected via a short spacer, a bifunctional OPV derivative was obtained, **176b**, which is capable of forming a random coil supramolecular polymer in chloroform. These supramolecular polymers form long columns in apolar solvents. However, no CD effect was observed, in contrast to their analogues that lack the OPV core.⁴²⁰ The presence of a covalent linkage between consecutive layers of the column conflicts with the favorable π – π interactions between OPVs; hence, so-called frustrated stacks are formed. AFM studies showed that transfer of single OPV cylinders of **176a** from solution to a solid support as isolated wires was only possible when specific concentrations and specific solid supports were used. On graphite, numerous single micrometer long fibers were found with a uniform height of 5.2 nm and a persistence length of 125 nm. At higher concentrations an intertwined

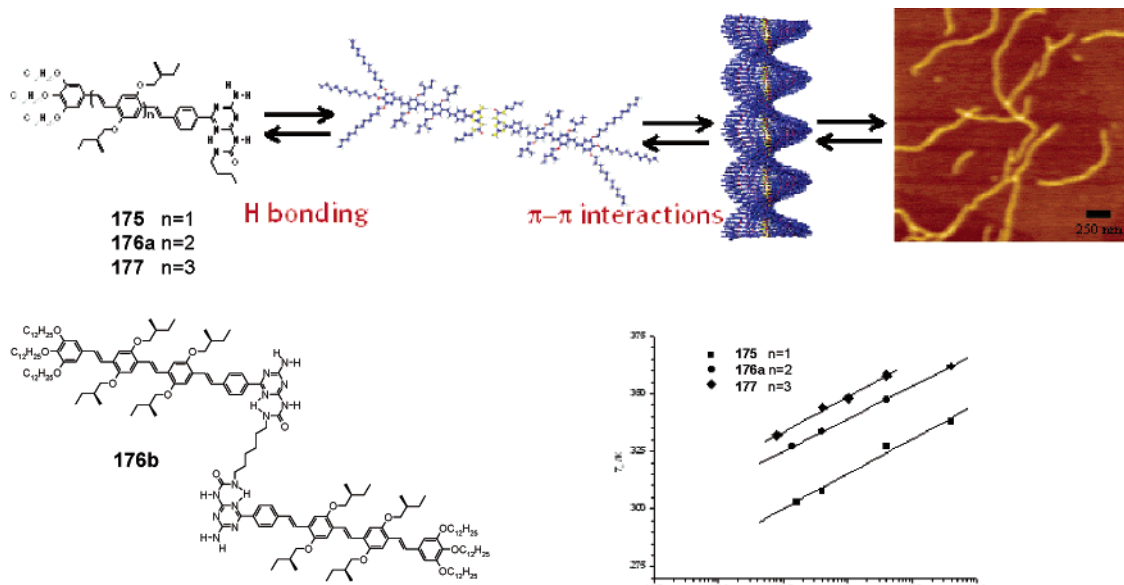


Figure 64. OPVs of different conjugation length functionalized with a hydrogen-bonding urideotriazine unit **175**–**177**, a representation of a helical assembly formed by stacked dimers of this molecule, and an AFM image showing single fibers. The variation of the melting transition temperature as a function of concentration is given for different conjugation lengths. (Reprinted with permission from ref 416. Copyright 2003 American Chemical Society.)

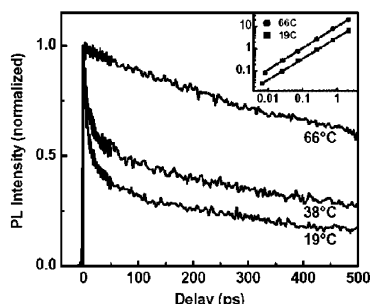


Figure 65. Time-resolved photoluminescence on stacks of **176a** at different temperatures. (Reprinted with permission from ref 418. Copyright 2003 American Physical Society.)

network was formed consisting of single wires, while at low concentration ill-defined globular objects were observed. On graphite and silicon oxide molecule–surface interactions were suppressed yielding a successful transfer of the supramolecular stack as single isolated entities on the substrate. On gold the molecule–molecule interactions in solution were perturbed by stronger molecule–surface interactions, so-called attractive surfaces. Repulsive surfaces (mica and glass) give rise to clustering of stacks due to minimization of the contact area between the stack and the support, resulting in lamellar arrays of stacks. Together with the fact that the concentration and temperature of the cast solution determines the equilibrium between individual molecules and the supramolecular stack it is obvious that many variables control the successful transfer of isolated single stacks from solution to surfaces. However, comprehensive knowledge of all intermolecular interactions gives rise to controlled transfer of π -conjugated assemblies to specific surfaces. Understanding the interactions in this transfer process will be crucial for applying these semiconducting stacks in the field of nanotechnology (Figure 66). The design of such nanodevices must be such that all components be-

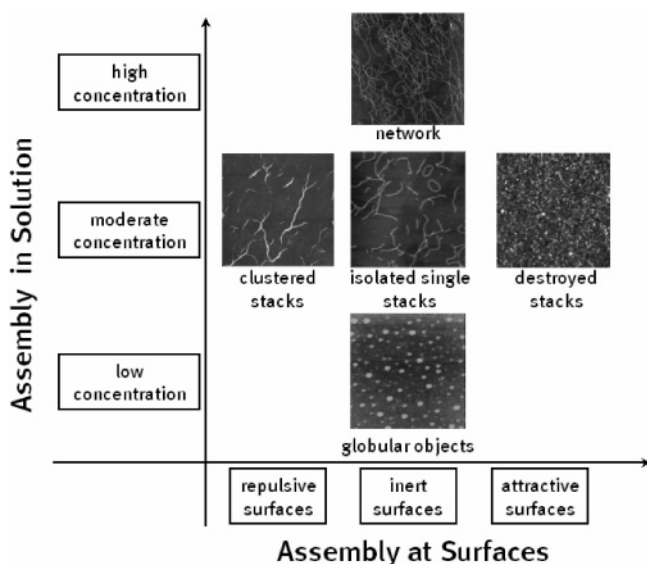


Figure 66. Plot showing the dependence of morphology of **176a** on both solution concentration and surface type. Depicted are tapping-mode AFM images on glass (repulsive surface), graphite (inert surface), and gold (attractive surface). (Reprinted with permission from ref 416. Copyright 2003 American Chemical Society.)

have as an inert surface toward self-assembled stacks.

8. Supramolecular Organization of Multicomponent Systems

Complexity resulting from self-assembly of individual building blocks and resulting long-distance, directional energy and electron transfer is appealing to scientists working in the field of organic electronics. Noncovalently assembling multiple components into large, well-defined architectures in which the different chromophores exhibit various functionalities remains a challenging task for chemists.

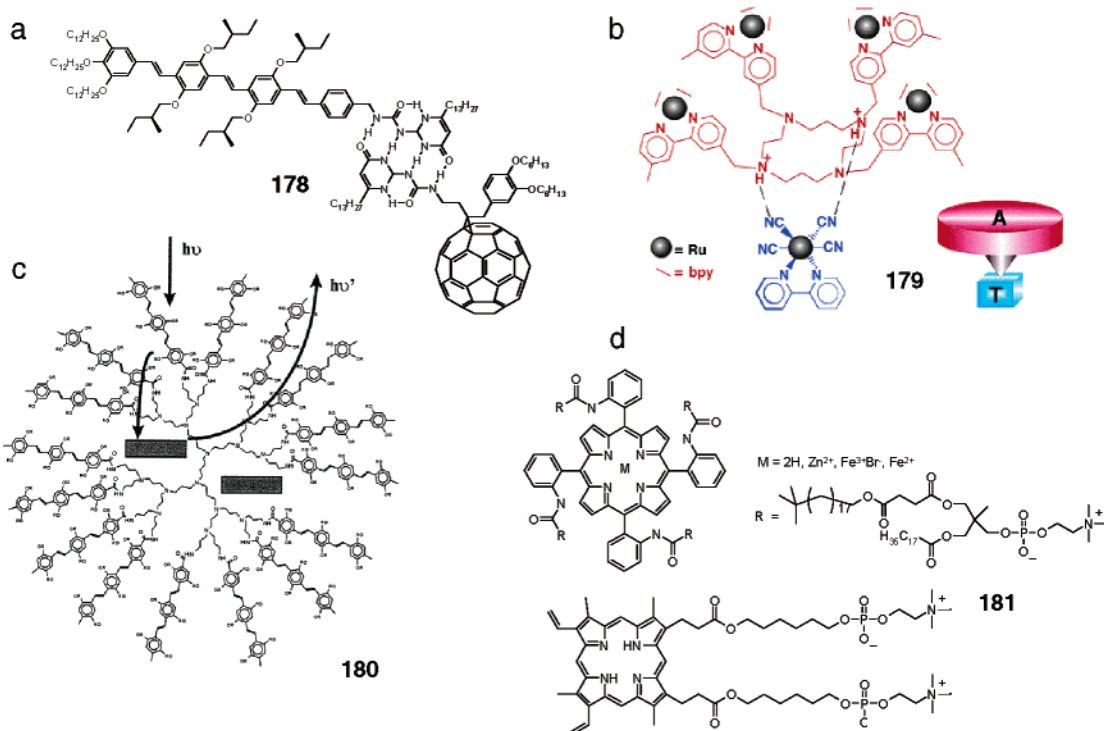


Figure 67. Various ways of electronically coupling one or more donors with energy acceptors in a supramolecular fashion: (a) quadruple hydrogen bonding between OPV and C_60 ,⁴²² (b) bipyridine coordination to Ru (Reprinted with permission from ref 429. Copyright 2003 The Royal Society of Chemistry.), (c) hydrophobic interactions between a dye and an OPV dendrimer (Reprinted with permission from ref 436. Copyright 2000 American Chemical Society.), and (d) mixed bilayer vesicles of amphiphilic porphyrins.⁴³⁵

Literature reports the use of noncovalent interactions to assemble donor and acceptor moieties by a.o. hydrogen bonding,^{421–424} metal coordination,^{425–429} and electrostatic interactions.^{430,431} This has led to a variety of functional structures in which the interplay between single acceptors and one or multiple donors could be studied in detail (Figure 67).

These supramolecular systems exhibit short-range order and lack designs for further self-assembly into three-dimensional architectures and are thus merely applicable to fundamental studies at the molecular level. Moreover, energy and electron transfer has been studied in Langmuir–Blodgett monolayers by either placing chromophores in a lipid monolayer matrix^{432,433} or direct formation from functionalized amphiphilic donors and acceptors.⁴¹⁰ In this way the dependence of energy transfer on monolayer compression, and thus donor–acceptor distance and molecular orientation, can be studied. Going to higher dimensions, preparation of bilayer vesicles from stacked π -electron arrays⁴³⁴ and mixed phospholipid-substituted porphyrins⁴³⁵ has been demonstrated in which energy and electron transfer occurs with high efficiencies. In some of these cases the number of donors that couple with a single acceptor chromophore can be very high. Other useful systems to couple a large, predetermined number of donor groups supramolecularly with a single acceptor are dendritic macromolecules, which enables directional energy transfer from the periphery to a dye in its hydrophobic core (Figure 67c).^{430,436} Other systems that have been studied are nanoparticles^{437,438} and inclusion compounds,^{439–441} which have been used as microenvironments for self-assembly of donors and

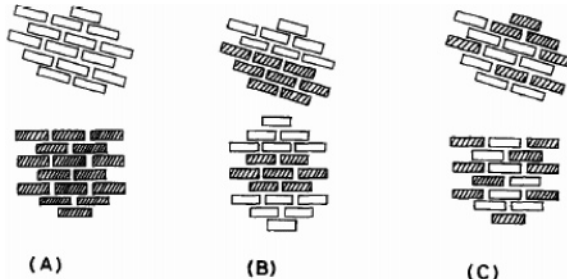


Figure 68. Schematic representation of different types of cyanine J-aggregates that have been observed in the literature: (a) separate donor and acceptor aggregates, (b) mixed mosaic aggregates, and (c) homogeneous donor–acceptor aggregates. (Reprinted with permission from ref 450. Copyright 1996 Elsevier.)

acceptors and subsequent photophysical excitation transfer. From these examples it becomes clear that a thorough design enables formation of a wide range of structures with the use of noncovalent interactions. This diversity illustrates but one of the strengths of a supramolecular approach. Using single molecules as building blocks enables a tight and well-defined positioning in space, though the challenge of this methodology will obviously lie in competing with devices based on their polymeric counterparts, for which high mobilities and especially ease of processing are generally obtained.

A classical example of the use of electrostatic interactions for ordering molecular donor–acceptor couples lies in the construction of mixed cyanine J-aggregates (Figure 68) on which comprehensive work has been performed by Yonezawa et al.⁴⁴² Within mixed cyanine assemblies high exciton delo-

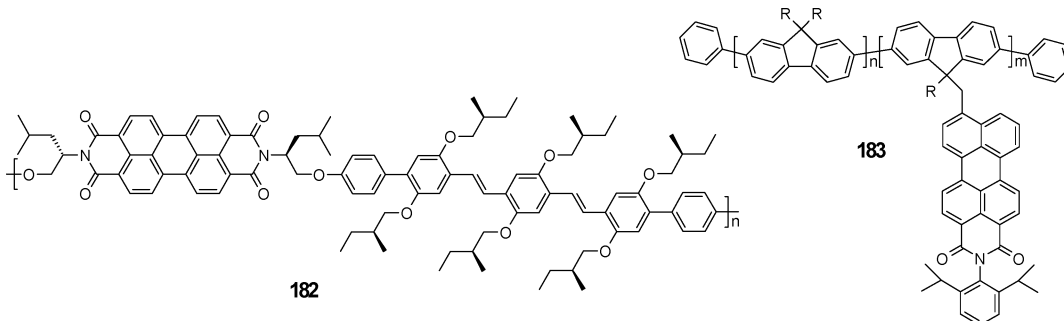


Figure 69. General structures of covalently linked donor–acceptor copolymers **182** and **183**. Both have been applied in photovoltaic devices and were characterized by highly efficient electron (left) and energy transfer (right) to the perylene moiety.

calization^{443,444} generally ensures efficient energy or electron transfer, enabled by tuning the electronic properties of the two different cyanine dyes. Sakomura et al. used this high excitonic coupling to efficiently harvest light and transfer energy to perylene doped into cyanine LB monolayers.⁴⁴⁵ It was shown that depending on the amount of perylene as much as 250 cyanines could electronically communicate with a single incorporated perylene, which mainly emits light. Originally used as spectral sensitizers in silver halide photography, experiments on mixed cyanine dyes have mostly been carried out in layer-by-layer alternate assemblies on surfaces^{446–448} and in (LB) films.^{449–456} Some examples focus on the use of silica or clay nanoparticles as hosts for self-assembly.^{457,458} A more recent paper by Pawlik et al.⁴⁵⁹ demonstrates the formation of supramolecular helices of novel cyanine assemblies in aqueous environment,⁴⁶⁰ displaying optical activity.⁴⁶¹

Supramolecular ordering of donor and acceptor molecules into defined architectures was also appreciated in the field of crystal engineering.⁴⁶² Growing single crystals from mixed equimolar donor/acceptor (DA) solutions yields infinite DA arrays in the solid state. However, in solution, only 1:1 charge-transfer dimers are present since the molecules lack the design for further assembly into well-defined higher structures.^{463–465} Nonetheless, crystal engineers were among the first to study charge transfer in ordered DA mixed structures.

This section will focus on construction of supramolecular DA architectures and their implementation as functional materials either for fundamental studies on energy and electron transfer or as active components in organic devices (see also section 4).

8.1. Assembly in Organic Devices

One of the major challenges in the field of electronics based on organic molecules is the design of functional, multicomponent architectures possessing long-range ordering. Having an electron-donating as well as an electron-accepting chromophore is a prerequisite to obtain organic photovoltaics. It has also been demonstrated that incorporation of energy- or electron-accepting chromophores into π -conjugated polymer backbones can rigorously alter the electro-optical properties of the resulting copolymers. For instance, block copolymers of perylene and fluorene⁴⁶⁶ have been prepared, and both porphyrin^{467,468} and

perylene bisimide (**182**)⁴⁶⁹ have been included into the PPV main chain (Figure 69). The resulting copolymers are characterized by either almost exclusive emission from the incorporated acceptor moiety or efficient charge transfer. Recently, an end was put to a long discussion about undesired green emission in polyfluorenes, which appeared to arise from efficient energy transfer to small amounts of oxidized monomer,⁴⁷⁰ indicating the necessity for high-purity polymers.

The viability of this functional approach has been shown by the successful tuning of electroluminescence in a light-emitting diode (LED) consisting of PPV with dangling porphyrins.⁴⁷¹ Also, a photovoltaic device based on a blend of PPV and polyfluorene with dangling perylene **183** proved to yield high external quantum efficiencies in both the perylene and the polyfluorene absorption regions, due to energy transfer from the polyfluorene to the perylene with near unit efficiency.⁴⁷² Some recent papers appeared on the functionalization of polyacetylene with either pyrene⁴⁷³ or carbazole.⁴⁷⁴

An elegant example which cleverly combined the advantages of microphase separation in rod–coil block copolymers (see also section 6.2) with donor–acceptor interactions was reported by Hadzioannou et al. Diblock copolymers were synthesized containing an OPV rod and a PS coil, the latter of which was functionalized with C₆₀ molecules (Figure 70).^{152,475,476} Apart from rich morphologies exhibited by **184**, photoinduced electron transfer from the excited PPV to C₆₀ occurs, as illustrated by the strong PPV lifetime decrease in time-resolved photoluminescence (Figure 70).

As an alternative to covalently incorporating acceptors, blending fluorescent or phosphorescent^{477–479} dyes into polymer films has received enormous attention over the years. Doping PPV-LEDs with small amounts of, e.g., porphyrin⁴⁸⁰ or boronic dyes⁴⁸¹ leads to sensitized emission from the guest molecules as a consequence of energy transfer, generally with very high efficiencies. This is desired for the purity of light emission as well as expected, since the process occurs in the solid phase and most dye molecules are within the Förster radius from the donor polymer, even at low dye incorporations. Welter et al.⁴⁸² elegantly applied this principle to an electroluminescent device containing PPV **185** doped with dinuclear ruthenium complex **186** in which switching between forward and

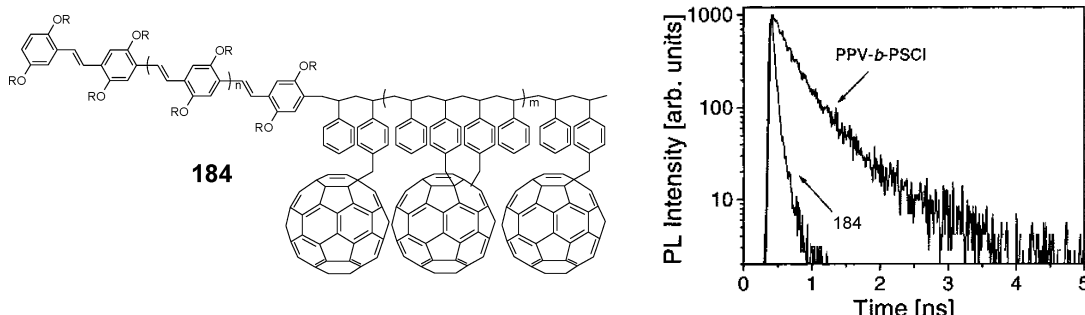


Figure 70. Structure of donor–acceptor diblock copolymer **184**. This is a general structure since cross-linking occurs. Time-resolved photoluminescence curves of spin-cast films of unfunctionalized PPV-*b*-PS and **184** indicated a strong decrease in PPV fluorescence lifetime as a consequence of electron transfer to C_60 . (Reprinted with permission from ref 475. Copyright 2000 American Chemical Society.)

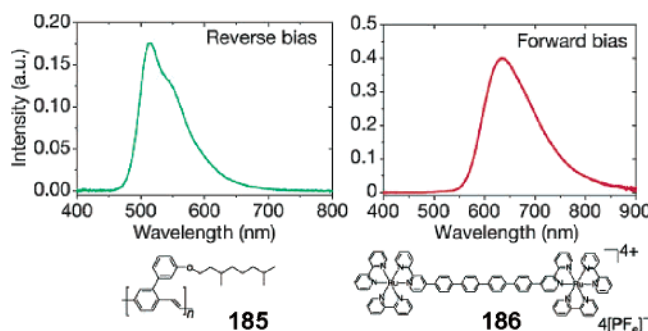


Figure 71. Device characteristics of PPV **185**, doped with bisruthenium dye **186**, enabling reversible emission switching as a consequence of the dual role of the dye as triplet emitter and electron-transfer mediator. (Reprinted with permission from *Nature* (<http://www.nature.com>), ref 482. Copyright 2003 Nature Publishing Group.)

backward bias enabled reversible switching between red and green emission (Figure 71).

In all polymer-based devices, however, due to their inherent polydisperse and defect containing nature, disordered samples are obtained which lack a uniform positioning of chromophores. This lack of higher order also stems from preparation methods such as spin coating, which is usually employed for polymeric systems but does not guarantee any structural organization at all. A uniform distribution will highly improve efficiencies that are reached in devices such as LEDs, solar cells, and FETs by creating regular pathways for charges between the two electrodes.

Phase separation between the polymer and incorporated dyes is also a possibility that is highly undesired, since this drastically reduces the energy- or charge-transfer efficiency and may lead to pollution of the emitted color.

One step closer to the self-assembly of well-defined, functional objects was reported by Stupp et al., who prepared oligomers consisting of pentameric OPV blocks and electroactive triphenylamine coils **187**.⁴⁸³ Although still polydisperse (PDI = 1.09), thin films of these oligomers showed a high degree of intermolecular order and efficient energy transfer from the coils to the blocks (Figure 72).

The beneficial outcome of attaining order at all hierarchical levels on device properties was illustrated by a beautiful example on the use of mono-disperse conjugated oligomers in organic LEDs, recently reported by Chen and Tang et al.⁴⁸⁴ They synthesized well-defined fluorene oligomers **189**–**193** containing central OPV, perylene, and benzothiadiazole chromophores,⁴⁸⁵ designed to act as efficient energy acceptors from the fluorene moieties (Figure 73). By using a uniaxially buffed PEDOT:PSS film, highly aligned thin films of the pure fluorene oligomer with varying amounts of acceptors were obtained. As a consequence, the electroluminescence of the resulting device was highly polarized and very efficient energy transfer to the incorporated acceptors lead to green, red, or white light emission. Moreover, the polarization ratio and luminance yield proved to

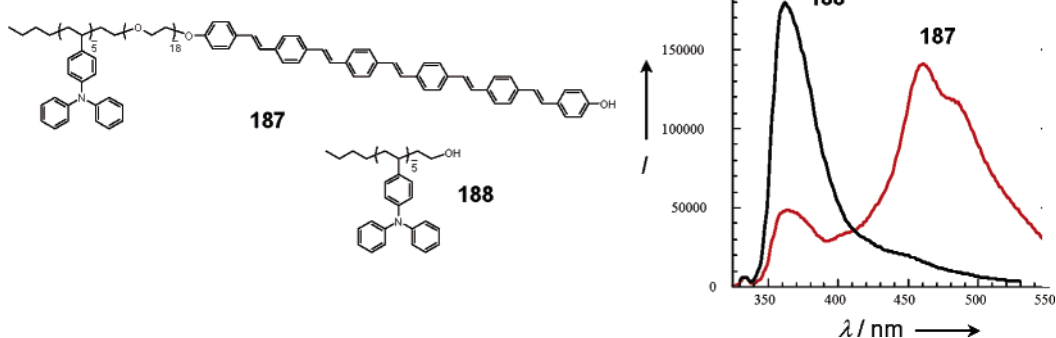


Figure 72. Rod–coil diblock oligomer **187** containing triphenylamine coils and pentameric OPV blocks and reference triphenylamine coil **188**. The spectrum compares the fluorescence of **187** and **188** upon almost exclusive excitation of triphenylamine. Quenched triphenylamine luminescence and sensitization of OPV fluorescence within self-assembled structures of **187** yields evidence for energy transfer. (Reprinted with permission from ref 483. Copyright 2000 John Wiley & Sons, Inc.)

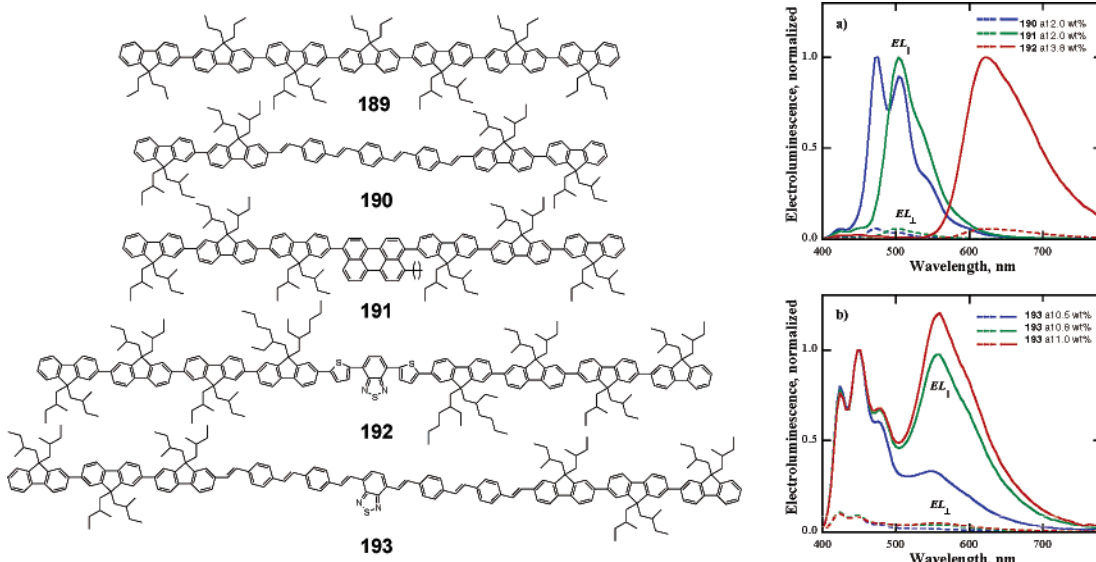


Figure 73. Fluorene donor oligomer **189** and analogues with incorporated acceptor chromophores **190–193**. (a) Polarized electroluminescence from devices with small amounts of acceptors **190–192** in donor **189** showing almost exclusive acceptor luminescence. (b) Electroluminescence from devices with varying amounts of acceptor **193** in donor **189** in order to obtain polarized white light emission. (Reprinted with permission from ref 484. Copyright 2004 John Wiley & Sons, Inc.)

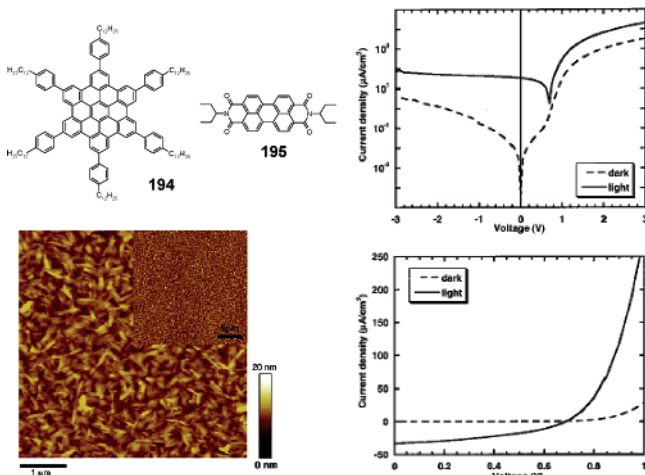


Figure 74. Thin films of hexabenzocoronene **194** and perylene bisimide **195** are self-organized into vertically segregated structures. AFM image of a thin film containing a **194:195** (40:60) blend. Current–voltage characteristics of a photodiode (having an identical composition) in the dark and under illumination at 490 nm. The fill factor is 40%, and the power efficiency maximum is 1.95% at 490 nm. (Reprinted with permission from ref 484. Copyright 2001 American Association for the Advancement of Science.)

be superior to the devices fabricated using merely the pure components.

This last example employs well-defined chemical structures and clearly indicates the strength of using monodisperse oligomers. Apart from implementation in LEDs, the concept of a well-defined supramolecular donor–acceptor assembly has also successfully been applied in a photovoltaic device by Müllen and Friend et al. (Figure 74).⁴⁸⁶ A discotic hexabenzocoronene and a perylene bisimide were organized into highly ordered, vertically segregated structures (see also section 7.1.2) in a single solution processing step. The resulting high interfacial area between donor and acceptor and favorable morphology gave rise to strong photoinduced charge separation, which in turn

lead to an external quantum efficiency (EQE) of $\sim 34\%$ and a power efficiency of $\sim 2\%$.

This last example describes liquid-crystalline hexabenzocoronene (HBC), the mesoscopic ordering of which leads to a one-dimensional charge transport, which is useful for optoelectronic applications. The next paragraph will further explore multicomponent liquid-crystalline materials.

8.2. Assembly by Liquid Crystallinity

High transport mobilities in liquid-crystalline columnar mesophases have prompted scientists to intensively investigate energy and charge transfer along the one-dimensional assemblies. Roughly, two distinct kinds of studies can be discerned, namely, the doping of pure liquid-crystalline phases with acceptor molecules and preparation of mesophases from covalent donor–acceptor complexes. The field of mixed liquid crystals is a major focus of this review since it comprises the bulk of research done on well-defined DA architectures that are promising materials for the actual implementation in high-efficiency devices.

8.2.1. Mixed Liquid Crystals

At the end of the 1980s numerous studies were performed on excitation transfer in columnar mesophases of pure triphenylene,⁴⁸⁷ phthalocyanine,^{488,489} triarylpypyrronium,⁴⁹⁰ and porphyrine.⁴⁹¹ General observations were high mobilities of both singlet and triplet exciton migration along the stacks and the detrimental effect of disorder on desired luminescence properties, i.e., efficient quenching at defect sites. The mechanism of charge transport within pure triphenylenes was investigated on the basis of transient photoconductivity spectroscopy and found to be highly anisotropic ($\mu_{||}/\mu_{\perp} \approx 10^3$).⁴⁹² The quasi-one-dimensional transport properties could be described using a hopping mechanism between neighboring triphenylene cores. Packing irregularities result in

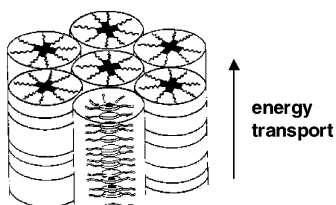


Figure 75. Energy transfer in a columnar mesophase formed by a random mixture of metal-free and copper phthalocyanine.³⁴⁸ Incorporation of 16% of the copper complex completely quenched the luminescence of the free-base derivative. (Reprinted with permission from ref 348. Copyright 1987 American Chemical Society.)

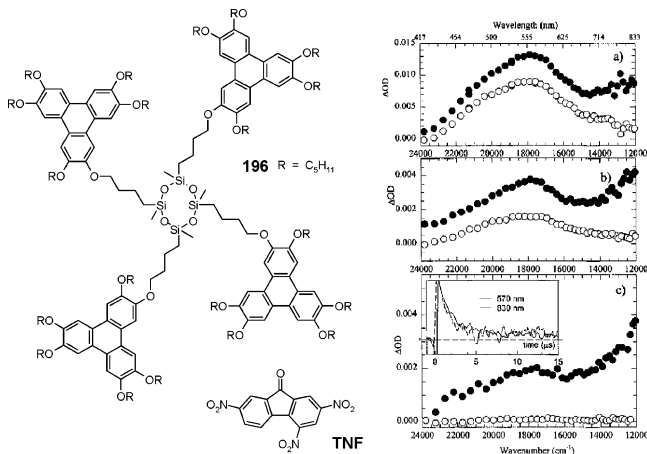


Figure 76. Triphenylene **196** fluorescence quenching as a function of mole fraction of **TNF** in the mesophase. The transient absorption spectra after 0.5 (solid circles) and 10 μ s (open circles) for mixed systems with (a) 10^{-3} , (b) 10^{-2} , and (c) 5×10^{-2} molar fractions **TNF** indicate triplet energy transfer to the incorporated trap. (Reprinted with permission from ref 499. Copyright 2001 American Chemical Society.)

local potential minima that act as traps in the crystalline state but much less in the liquid-crystalline state due to self-healing.

Various mixed liquid-crystalline systems have been studied as well, notably phthalocyanine^{348,449,493–495} (Figure 75) and triphenylene derivatives. Markovitsi et al. performed multiple detailed studies on doping discotic triphenylene mesophases with energy acceptors such as perylene,⁴⁹⁶ 2,4,7-trinitrofluorenone (TNF),^{263,497–499} and 1,2,4,5-tetracyanobenzene.⁵⁰⁰ Incorporation of dyes in various ratios into the columns results in a very efficient quenching of triphenylene fluorescence as a consequence of energy or charge transfer to the dyes (Figure 76).

Monte Carlo simulations show that the transport is initially one dimensional and becomes three dimensional at longer times, as excitonic hopping between columns becomes possible.⁵⁰¹

Other examples of compounds that have been mixed with triphenylene mesophases are electron-deficient perfluorotriphenylene,⁵⁰² aiming at a charge-transfer complex, and hexaalkylphenyltriphenylene,²⁵⁹ of which the enlarged π system leads to more ordered columnar structures. In both cases one-to-one complexes of donor and acceptor significantly enlarged the temperature range over which the mesophase is stable; for the latter case even higher mobilities were

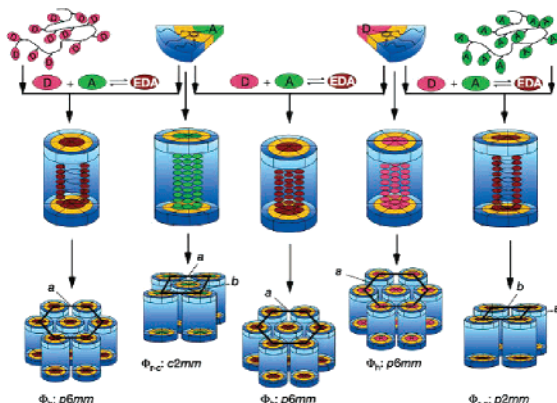


Figure 77. Schematic representation of the self-assembly of various donors and acceptors into highly ordered, complex structures. (Reprinted with permission from *Nature* (<http://www.nature.com>), ref 511. Copyright 2002 Nature Publishing Group.)

obtained in the binary mixture. In some cases the donor–acceptor interactions alter the liquid-crystalline packing, induce mesophases from non-liquid-crystalline materials,⁵⁰³ or induce supramolecular chirality in the mesophases when chiral dopants such as (−)-menthol-3,5-dinitrobenzoate are used.^{504,505} Another example is that of an electron-rich triaryl-amino-s-triazine mesophase doped with either TNF or 2,4,7-trinitrofluoren-9-yli-dene malodinitrile, of which the two-dimensional lattice symmetries can be controlled with hydrogen bonding to complementary alkoxy-substituted benzoic acids.^{506–508} The concept of doping liquid-crystalline triphenylene has been successfully applied in light-emitting diodes. Combined with incorporated pyrene and perylene acceptors it proved possible to tune electroluminescence over the entire visible spectral range.⁵⁰⁹ Very recently, mixed chromonic liquid crystals of a quater-rylene bisimide (an extended rylene dye with four aromatic repeating units) with a functionalized perylene bisimide were reported.⁵¹⁰ The high orientation after alignment by shearing may prove useful in the implementation of these materials in liquid-crystal displays, since the fact that both components absorb at different wavelengths significantly broadens the spectral range over which the polarization principle is applicable.

Supramolecular ordering of π -conjugated chromophores into efficient, electronic materials was reported by Percec et al.,^{511,512} who studied the self-assembly of various donor and acceptor dendrons into supramolecular columns (Figure 77).

The building blocks are composed of semifluorinated dendrons bearing electroactive carbazole, naphthalene, and pyrene as donors and trinitrofluorenone as acceptor. Moreover, co-assembly of donor and acceptor dendrons leads to columns incorporating a central donor–acceptor complex. The columns further self-organize between electrodes into highly ordered homeotropic liquid crystals of various symmetries. The beneficial effects of ordering the π -conjugated moieties on materials properties is clearly illustrated by the electron and hole mobilities, which are 2–5 orders of magnitude higher than those of the corresponding amorphous polymers. This dendritic ap-

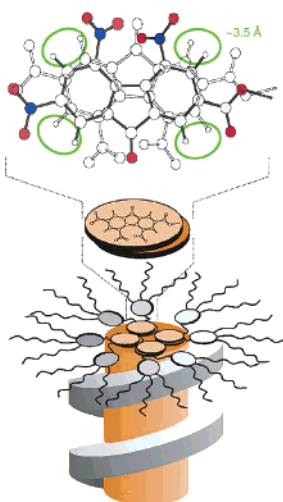


Figure 78. Proposed structure of a pure TNF column showing nitrofluorenone packing with an interdistance of 3.5 Å, jacketed by helical dendrons. (Reprinted with permission from *Nature* (<http://www.nature.com>), ref 511. Copyright 2002 Nature Publishing Group.)

proach is further enhanced by the possibility of ordering disordered polymer backbones, bearing donor or acceptor groups, into the interior of columns by complexation with dendrons, leading to much higher mobilities. Although details of the charge-transport process inside the ordered columns remain unclear, combination of X-ray diffraction and ^1H NMR yield valuable data on the supramolecular packing of its building blocks (Figure 78).

As shown in Figure 78, pure columns of the nitrofluorenone dendron are composed of highly ordered π stacks of sandwiched fluorenones surrounded by a helical packing of dendron phenyl rings. The electronically active inner column is subsequently shielded from water by the fluorenated, isolated jacket. However, lack of defects is only achieved upon slowly cooling the samples from the melt into the liquid-crystalline and glassy phases. In this way the system exhibits a ‘self-repairing’ mechanism, removing flaws in its internal organization.

8.2.2. Covalent Donor–Acceptor Liquid Crystals

Formation of columnar mesophases from covalently linked donor–acceptor mesogens has been studied, in particular, by Wendorff and Janietz⁵¹³ et al., who synthesized, e.g., complexes of electron-rich pentaalkynylbenzene attached directly to TNF.^{514,515} In these systems strong intermolecular donor–acceptor

interactions lead to the formation of highly ordered, columnar mesophases. In further studies elaborating on this work a calamitic azobenzene spacer was used to connect pentaalkynylbenzene⁵¹⁶ or triphenylene⁵¹⁷ (**197**, Figure 79) to TNF. Combination of a disklike donor, a rigid-rod bridge, and a strong electron acceptor within one molecular building block ensured preservation of a columnar mesophase, which is normally destroyed upon addition of a calamitic chromophore. As a drawback no clear intercolumnar order could be obtained. In the case of the pentaalkynylbenzene donor the columnar mesophase formed by intercalation of donor and acceptor is not destroyed upon isomerization of the azobenzene due to the favorable charge-transfer interactions with TNF.

These triple-compound systems exhibit interesting optical storage properties upon light-induced reorientation of the azobenzene, while the liquid-crystalline environment ensures a strong amplification of the optical response.⁵¹⁸

Combining covalent donor–acceptor synthesis with liquid-crystal mixing Manickam et al. synthesized central triphenylenes **198–204** bearing one to four and six covalently attached carbazole moieties (Figure 80). It was shown that the resulting molecules did not possess liquid-crystalline behavior but could form hexagonal columnar mesophases of various stability, induced by TNF doping.⁵¹⁹ However, this occurred only when the carbazole substitution did not exceed two, indicating that the higher substituted compounds do not display ordered stacking behavior.

Apart from a vast range of triphenylenes, much research has been done on discotic HBCs, which are excellent candidates for the use in optoelectronic devices due to high transport mobilities in its liquid-crystalline state. This self-assembly into highly ordered nanostructures provides an attractive scaffold for the study of multicomponent systems,⁵²⁰ the success of which relies on a high degree of inter- or intramolecular order. Müllen and Rabe et al. performed considerable work in this field by tethering additional functional π systems to the HBC core, like pyrene (**205**)⁵²¹ or anthraquinone (**206** and **207**, Figure 81).^{522a}

If successfully applied, both systems would form an attractive, supramolecular alternative to doubleable polymers from the possibility of obtaining homeotropically aligned donor and acceptor stacks. In the latter case one or six strongly electron-deficient anthraquinones are covalently attached to the elec-

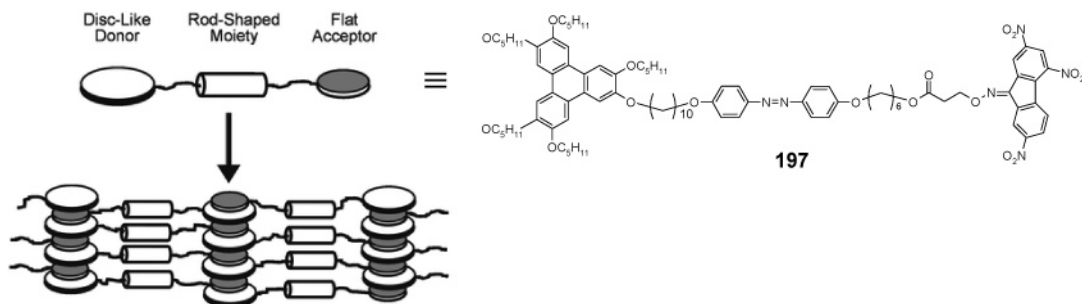


Figure 79. The formation of a columnar mesophase from covalently linked donor–acceptor molecule **197** containing a switchable azobenzene bridge. The rigid-rod azobenzene does not destroy the columnar packing due to its covalent incorporation. (Reprinted with permission from ref 517. Copyright 2000 The Royal Society of Chemistry.)

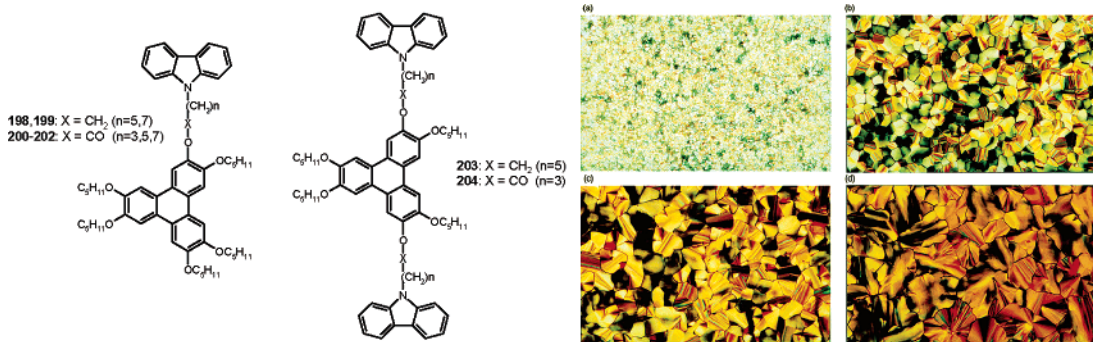


Figure 80. Structures of triphenylene derivatives **198–204** with one and two carbazole units attached. Columnar mesophases of **198** doped with various amounts of TNF: (a) 2.3, (b) 9.5, (c) 32.9, and (d) 41.1 mol %. (Reprinted with permission from ref 519. Copyright 2001 The Royal Society of Chemistry.)

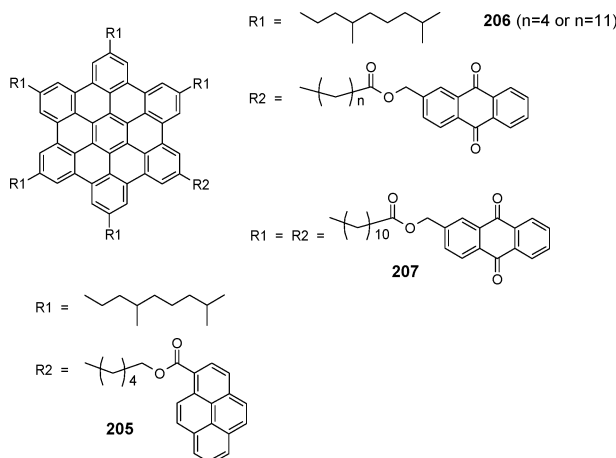


Figure 81. Donor–acceptor systems **205–207** consisting of hexabenzocoronene with covalently tethered pyrene and anthraquinone moieties, as studied by Müllen and Rabe.

tron-rich HBC, leading to photoinduced charge-transfer efficiencies up to 96%. By comparing the STM data on both systems with a reference HBC system bearing only alkyl tails it can be concluded that separate stacks of donors and acceptors are formed on HOPG. However, due to the cross-section mismatch between donor and acceptor and dimorphism (multiple packing arrangements) for the anthraquinone moiety, rather loose packing is observed for **206**. Even though the size mismatch also exists for the HBC–pyrene dyad **205**, pyrene probably has a greater affinity for HOPG than anthraquinone. The fact that monolayers of **207** form much more ordered 2D crystals (Figure 82) is explained by satisfying space-filling requirements better.

Cooling of **206** from its isotropic phase leads to a highly mobile, discotic hexagonal mesophase, in clear contrast with **207**, which directly passes into a polycrystalline state as a consequence of the entropic disruption that the six tethered anthraquinones provide. Very recently, Langmuir and Langmuir–Blodgett studies were performed on **206** with which well-defined thin films could be obtained containing cofacially packed columns aligned along the dipping direction.⁵²³ Very recently, Müllen et al. synthesized HBC that was peripherally substituted with six triarylamines, aiming for coaxial ‘double-cable’ hole transporting materials.^{522b} Interestingly, a combination of wide-angle X-ray diffraction and mobility measurements on these systems showed that a

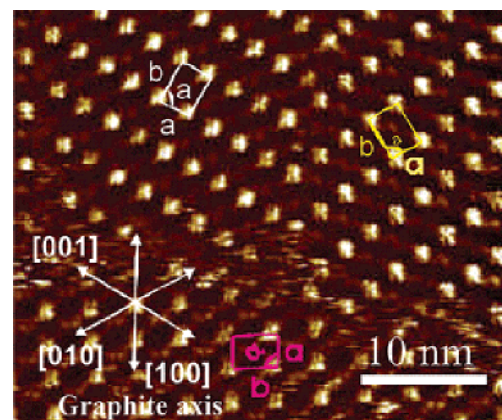
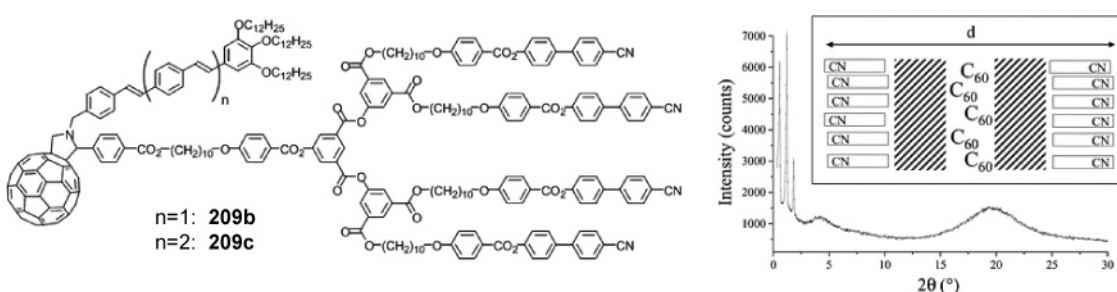
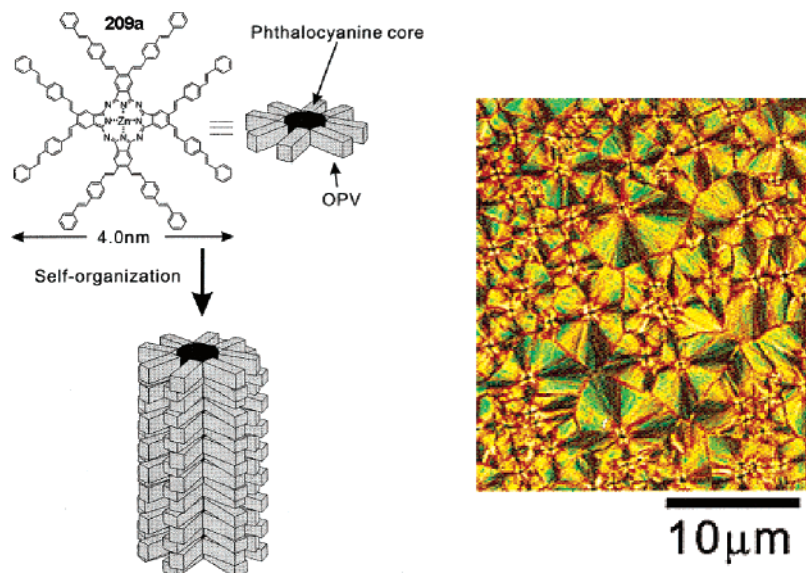
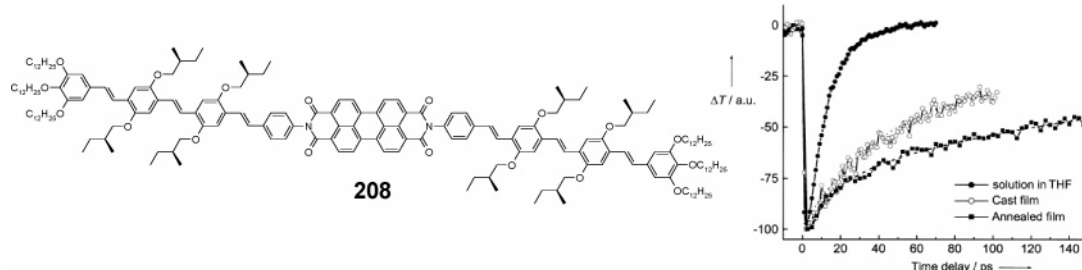


Figure 82. STM image showing very regular patterning of **207** on an HOPG surface. Its high symmetry leads to three rectangular, energetically equivalent orientations of the unit cell, which follow the crystallographic axes of the surface. (Reprinted with permission from ref 522. Copyright 2004 American Chemical Society.)

higher degree of columnar order resulted in better charge-transport properties.

Electron transfer in supramolecular donor–acceptor assemblies has also been the focus of attention for Meijer and Janssen et al., who synthesized covalent triad **208** consisting of a central perylene bisimide directly linked to two OPV4 units (Figure 83).⁵²⁴ The resulting compound showed liquid-crystalline behavior and was characterized by subpicosecond electron transfer from the OPVs to the perylene bisimide. Upon going from THF solution to thin films, the lifetime of the charges significantly increased, since migration and spatial separation of charges in the film decreased geminate recombination. This process could be monitored by probing the transient absorption of the $\text{OPV}^{\bullet+}$ radical cation. Triad **208** seems to be an ideal system for obtaining vertical segregation of donor and acceptor, which is necessary for obtaining efficient charge-transport pathways in devices. Attempts to incorporate system **208** in a photovoltaic device, however, were not successful since the devices exhibited little or no photovoltaic effect. This may be a consequence of too small domain sizes or wrong alignment with respect to the electrodes.

Apart from electron transfer in supramolecular DA aggregates, energy transfer has also been studied in literature. The use of phthalocyanines in liquid-crystalline donor–acceptor aggregates was explored



by Kimura et al.,⁵²⁵ who functionalized a Zn(II)–phthalocyanine core with four or eight OPV side chains (**209a**, Figure 84). It was possible to obtain fully conjugated, star-shaped stilbenoid phthalocyanines in which very efficient photoinduced intramolecular energy transfer occurred from the donating OPVs to the accepting phthalocyanine.

Moreover, when OPVs with flexible hexyl tails were used as building blocks the system displayed liquid crystallinity in the bulk. Slow cooling from the isotropic phase yielded a hexagonal columnar mesophase driven by π – π and van der Waals interactions. UV-vis on a thin film at 130 °C revealed strong hypsochromic shifts of both donor and acceptor

chromophores, whereas X-ray diffraction revealed a stacking interdistance of 3.5 Å. These results confirm that **209a** self-assembles into one-dimensional columns, which may be applied as electron-conducting wires in devices. However, due to the lack of control over the ordering of the OPVs with respect to one another the question remains whether a high excitonic coupling might be obtained within these aggregates.

With the aim of constructing high-performance thin films, Nierengarten et al. studied energy transfer in donor–acceptor liquid crystals using OPV as an energy donor and covalently attached C_{60} as an energy acceptor (Figure 85).^{526a,b} It was shown using

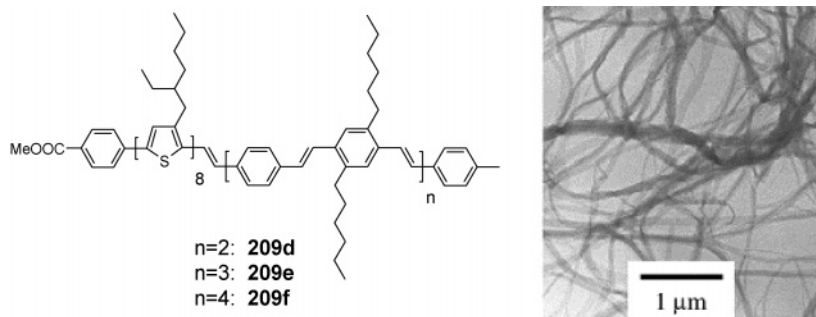


Figure 86. Covalently bound thiophene and OPV blocks construct co-oligomers **209d–f**, which exhibit complete, intramolecular energy transfer from OPV to thiophene. These molecules display interesting self-assembly properties, as shown in the TEM image for **209e**. (Reprinted with permission from ref 526d. Copyright 2002 John Wiley & Sons, Inc.)

X-ray diffraction indicated that molecules **209b** and **209c** formed smectic mesophases due to the appended cyanobiphenyl dendrons.^{526c} Within these phases the strong dipolar interactions between the cyano groups ensured a bilayered organization in which C₆₀ was confined to an inner sublayer of high electron density. The presence of donor and acceptor groups and the degree of ordering may be promising for photovoltaic applications.

A last example of well-defined, multicomponent assembly stems from the group of Yu et al., who synthesized monodisperse, liquid-crystalline rod–rod co-oligomers **209d–f** consisting of thiophene and phenylene–vinylene blocks (Figure 86).^{526d} A thorough analysis using X-ray diffraction indicated that these molecules form various interesting self-assemblies, which could be visualized using TEM. For instance, **209e** forms highly ordered, layered stripes when drop cast on a carbon-coated copper or SiN grid. The occurrence of complete, intramolecular energy transfer from OPV to thiophene renders these systems interesting for molecular electronic applications.

8.3. Assembly in Mixed Gels

Among a variety of tools to arrange molecules into ordered arrays with functional properties, gelation of either water⁵²⁷ or organic solvents^{312,313} is a widely implemented phenomenon. Gels based on low molecular weight organic dyes such as anthra-

cene,^{324,325,328–330} azobenzene,^{528–530} porphyrine,^{332,335,337} phthalocyanine,^{341,347} and squaraine³⁶⁴ have been intensively investigated for potential use as, e.g., molecular wires or sensors. Some of these examples show the feasibility of obtaining gels that contain highly ordered, chirally twisted stacks due to the use of enantiomerically pure building blocks.^{335,341} However, despite the potential possibilities for supramolecular electronics, relatively few examples exist in the literature of organogels based on π-conjugated molecules.^{84,370,371,531,532}

An interesting contribution to this field was made by Ajayaghosh et al., who prepared organogels based on oligo(*p*-phenylenevinylene)s³⁶⁹ and used these assemblies for light-harvesting applications and energy transfer to an incorporated dye (Figure 87).⁵³³ The gels emerge as a combination of hydrogen bonding between the benzylic alcohols of OPVs **146** and π–π stacking of the conjugated backbones in cyclohexane. Upon doping with excess Rhodamine B, using selective excitation of the OPV chromophores, fluorescence of the self-assembled OPVs is quenched in favor of Rhodamine luminescence, indicating energy transfer to the dye. The increased luminescence at $\lambda_{\text{em}} = 620$ nm as compared to direct Rhodamine excitation points to a significant light-harvesting effect. Energy transfer occurs merely from assembled OPVs but not from molecularly dissolved

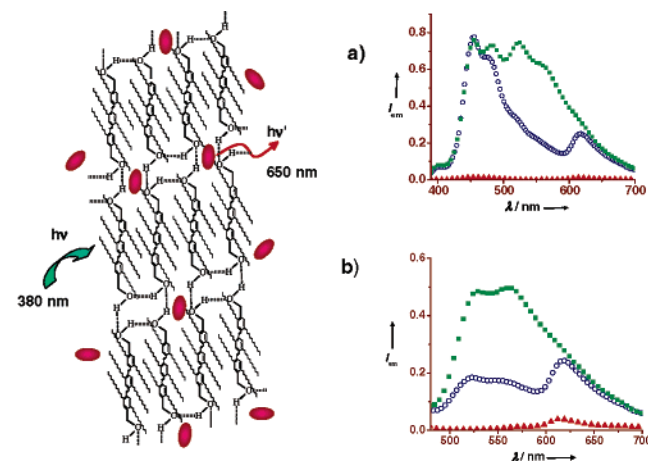
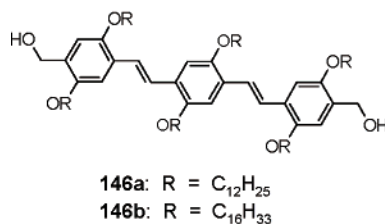


Figure 87. Supramolecular π-conjugated framework of **146** with incorporated Rhodamine B depicted as ellipsoids. Quenching of OPV fluorescence at (a) $\lambda_{\text{exc}} = 380$ and (b) 470 nm and concomitant sensitized Rhodamine B luminescence at 620 nm. Squares show the fluorescence of **146**, circles the fluorescence of **146** with Rhodamine B, and triangles the fluorescence of Rhodamine B after selective dye excitation. (Reprinted with permission from ref 533. Copyright 2003 John Wiley & Sons, Inc.)

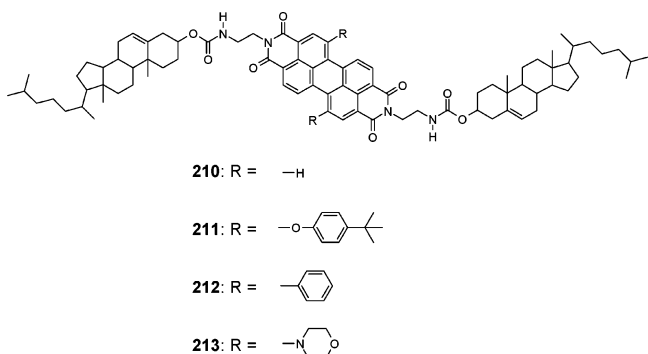


Figure 88. Cholesterol-based perylene gelators **210**–**213** with increasing electron-accepting character.

oligomers, as indicated by the unaffected OPV luminescence around $\lambda_{\text{em}} = 450$ nm. Efficient energy transfer was also observed in a xerogel film, doped with a 2:1 ratio of dye molecules, in which OPV fluorescence was almost completely quenched. The crucial role of the supramolecular OPV organization on energy transfer was illustrated with a temperature-dependent study on a mixed xerogel in which the reversible gel formation with temperature was used to switch the energy-transfer process on and off. Finally, a scanning electron microscopy (SEM) study on this mixed system revealed that the dye molecules are partly trapped inside the gel structure, in this way bringing donor and acceptor within the Förster radius from each other.

This clearly demonstrates the power of organogels as regular host networks, the properties of which can be altered by the supramolecular incorporation of guest molecules. This concept was demonstrated before for pyrene organogels that were doped with *N,N*-dimethylaniline⁵³⁴ or TNF,^{363,535} resulting in charge transfer to the intercalated acceptor and expressing the requirement of both π – π stacking and hydrogen-bonding interactions for gel formation. Another elegant example stems from Kimizuka et al., who prepared light-harvesting hydrogels by electrostatically incorporating naphthalene and anthracene chromophores into a framework of cationic L-glutamate gelators.⁵³⁶ The regular packing of the glutamate chains into bilayers ensures highly ordered dye self-assembly and, consequently, efficient energy transfer from the naphthalene donors to the anthracene acceptors. Bundles of bilayer membranes further assemble into fibers of micrometer length, which could be visualized using AFM.

Shinkai et al. studied energy transfer in mixed organogels.⁵³⁷ Using perylene bisimide functionalized cholesterol-based gelators **210**–**213** (Figure 88) they were able to create a light-harvesting energy-transfer cascade.

For this purpose the absorption spectra of four perylene bisimides were tuned across the visible spectrum by attaching different substituents at the bay position of the chromophores. Gels of the parent perylene were prepared in a mixture of *p*-xylene and 1-propanol and shown to yield fibrous, chiral networks of 1D-stacked molecules. Various binary, ternary, and quaternary perylene gels were studied with fluorescence spectroscopy in order to observe excita-

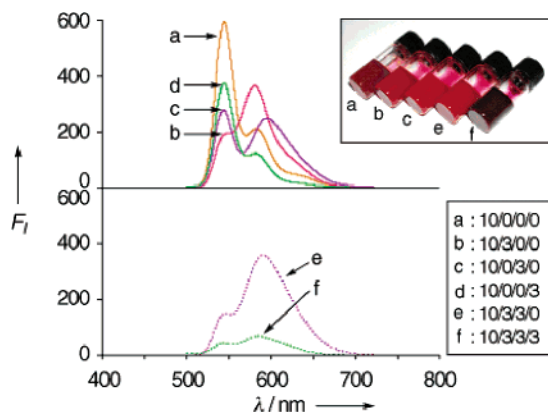


Figure 89. Fluorescence curves indicating energy and ultimate electron transfer inside mixed perylene gels. The molar ratio **210/211/212/213** is given for the various mixtures a–f. (Reprinted with permission from ref 537. Copyright 2004 John Wiley & Sons, Inc.)

tion energy transfer from **210** to **213** using **211** and **212** as stepping stones. Excitation at $\lambda_{\text{exc}} = 457$ nm, i.e., almost selective **210** excitation, resulted in quenching efficiencies at $\lambda_{\text{em}} = 544$ nm of 68% for **211**, 53% for **212**, and 34% for **213**, consistent with decreasing donor–acceptor spectral overlap.

In the quaternary system perylene bisimide **213** effectively acts as an energy sink as a consequence of its twisted intramolecular charge-transfer character (Figure 89). This is reminiscent of natural photosynthetic systems in which red-shifted absorption of pigment molecules triggers an energy-transfer cascade and eventually leads to a charge-separated state in a reaction center. Here, it is the supramolecular organization in the gel state that guarantees the success of this cascade transfer process, since in solution the mentioned effects are not observed.

9. Supramolecular Organization of Nanoscopic Multicomponent Systems in Solution

Although tremendous amounts of work have been performed on both covalent and hydrogen-bonded diads, triads, and higher order donor–acceptor systems in solution, reports on further self-assembly of these complexes are relatively scarce. This is quite unfortunate since this self-assembly process may have enormous potential for scientists working in organic electronics by providing a pathway to order donor and acceptor moieties into higher architectures. In solution these systems would be ideal for either studying (long-range) energy or electron transfer on a more fundamental basis or simply probing the feasibility of the simultaneous use of multiple supramolecular interactions. It is known, for example, that multiple noncovalent interactions such as π – π stacking and hydrogen bonding do not always have a synergistic effect on the regular stacking of chromophores. Eventually, the transfer of these shape-persistent structures from solution to the active layer of organic devices will prove to be crucial as well. However, for the successful implementation of supramolecular electronics in practice the molecular building blocks should be programmed in such a way that the design enables the organization of

functional chromophores into ordered, nanosized aggregates. This was illustrated by a recent report on a triple hydrogen-bonded triad consisting of a central perylene that was connected to two C₆₀ chromophores.⁵³⁸ In solution the hydrogen bonding enables electron transfer between the components, but since the system lacks the design for specific further self-assembly, random ball-like superstructures are observed on a copper surface.

To achieve control over the architecture of complex molecular aggregates in solution it is required to make use of all available secondary interactions simultaneously. To create some order in this section we subdivided the different topics by its leading supramolecular interaction. However, note that the self-assembling behavior is always a combined effect of all active ingredients.

9.1. Assembly by π - π Interactions

Torres and Nolte et al. reported monodisperse nanoaggregates of mixed phthalocyanines.⁵³⁹ These aggregates were comprised of stacked donor–acceptor couples **214**, each consisting of a donor Zn(II)–phthalocyanine and an acceptor Ni(II)–phthalocyanine covalently joined together by a para-cyclophane bridge (Figure 90).

Both pure donor and acceptor phthalocyanines were designed not to form aggregates by using very short solubilizing chains, thereby minimizing columnar stacking due to favorable van der Waals interactions. Mixtures of these two components, however, did show the formation of a heterodimer with a dimerization constant of $K_{\text{dimer}} = 2 \times 10^7 \text{ M}^{-1}$. In addition to these results a charge-transfer band in the UV–vis spectrum for **214** indicates that the donor–acceptor interaction is the main driving force for aggregation in chloroform, a unique feature for phthalocyanines. From UV–vis studies a dimerization constant of $K_{\text{dimer}} = 1.1 \times 10^6 \text{ M}^{-1}$ was determined. The lower value for the bifunctional molecule represents the fact that cofacial stacking for this molecule is hampered by the steplike cyclophane unit. Nevertheless, large one-dimensional aggregates were observed using transmission electron microscopy (Figure 91).

Another example of a covalently bound donor–acceptor complex that self-assembles into elongated stacks stems from Wasielewski et al.³⁴² A detailed study was performed on large, ordered photoactive aggregates composed of stacked porphyrins with four

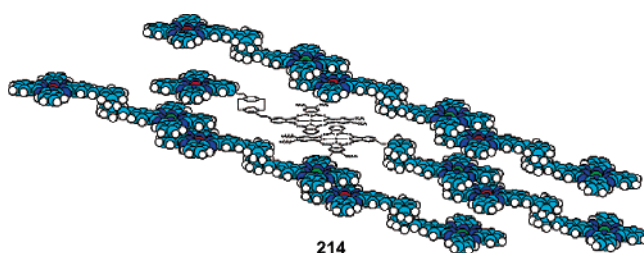


Figure 90. Highly ordered assemblies of bifunctional phthalocyanine **214** in chloroform solution. The building blocks comprise covalently linked donor Zn(II)– and acceptor Ni(II)–phthalocyanine. (Reprinted with permission from ref 539. Copyright 2003 American Chemical Society.)

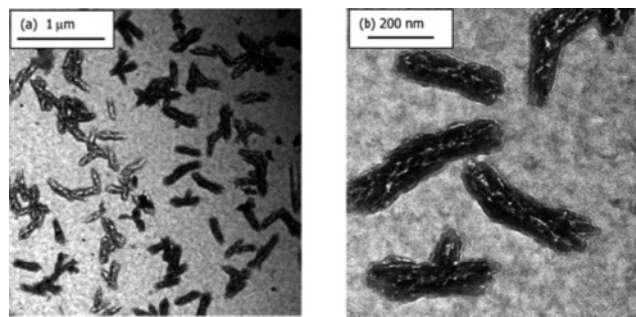


Figure 91. TEM images showing rodlike aggregates of mixed phthalocyanine **214**. (Reprinted with permission from ref 539. Copyright 2003 American Chemical Society.)

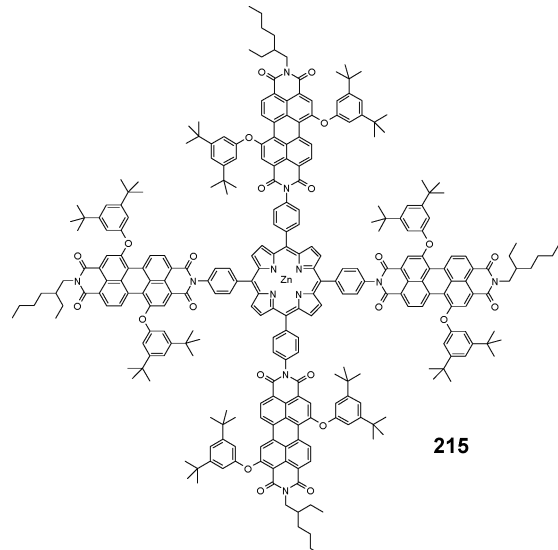


Figure 92. Four perylene bisimides attached to a central Zn–porphyrin core represents **215**, which is used as a building block for supramolecular nanoparticles. The Zn–porphyrin acts as an electron donor for the perylene bisimides.

perylene bisimides attached to it (**215**, Figure 92). Since the bridging phenyl rings are almost perpendicular to the plane of both the porphyrin and the imide, stacking becomes possible between the large, extended π surfaces.

Inside these assemblies the perlyenes act as antenna chromophores for a large absorption cross-section, preceding charge separation where the Zn(II)–porphyrin acts as an electron donor to the perylene moieties. The strong tendency of **215** to aggregate was illustrated by the matrix-assisted laser desorption time-of-flight (MALDI-TOF) spectrum, indicating the presence of up to 20-mers in the gas phase. In toluene solution a bathochromic shift of the perylene absorption suggests that the perlyenes are aggregated in a stacked, parallel fashion. On the basis of the observed excitonic coupling between the ZnTPP moieties, a stacking model is proposed in which the porphyrins are separated by 7 Å and the perlyenes by 3.5 Å (Figure 93). In thin films of the compound on a quartz substrate this stacking geometry is believed to persist and photoinduced charge separation in the nanoparticles is established with almost unit efficiency by selective excitation of either the porphyrin or the perylene moiety.

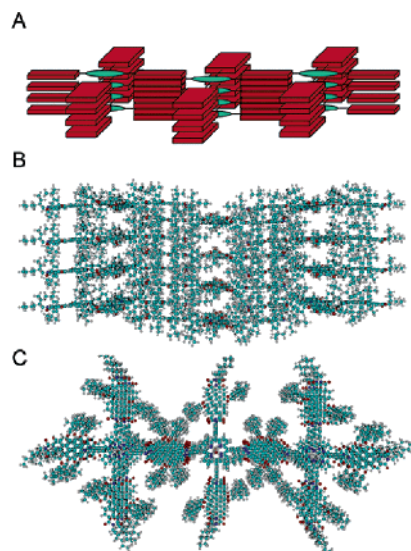


Figure 93. (a) Proposed and (b,c) calculated aggregate structure consisting of 12 molecules of **215** in which both porphyrin and perylene are packed into highly ordered sheets. After photoexcitation the electron is shown to delocalize over multiple perylene bisimide layers. (Reprinted with permission from ref 342. Copyright 2002 American Chemical Society.)

The observed line broadening of the PDI_4^- radical anion at $\lambda = 720 \text{ nm}$ suggests that after formation the charges are able to delocalize among the perylenes. The mean electron–hole distance is calculated to be 21 \AA , placing the electron on a PDI unit which is five layers removed from the ZnTPP radical cation. The formation of superstructures of **215**, with perylene bisimide and porphyrin stacked in a parallel fashion, resembles an ideal LED or solar cell morphology. Donors and acceptors are co-aggregated into an intimate network, yielding fast charge separation, with one-dimensional transport pathways for both holes and electrons that are formed after excitation. Recently, the authors extended this work to supramolecular aggregates of multichromophoric perylene bisimides antennae, which formed dimers in solution and self-assembled into $\sim 130 \text{ nm}$ long fibers on a hydrophobic surface. The high electronic coupling among chromophores resulted in fast singlet exciton–exciton annihilation among excimer-like states.^{540a} Elaborating on this, self-assembled light-harvesting arrays of covalently linked central zinc phthalocyanine and four perylene bisimide derivatives were synthesized.^{540b} These molecules stacked into fibers of micrometer length which displayed ultrafast energy transfer from the aggregated peripheral perylene bisimides to the central zinc phthalocyanine. Further energetic delocalization among zinc phthalocyanines was observed before excited-state decay occurred.

9.2. Aided-Assembly Using DNA, RNA, or PNA

Nature has evolved functional assemblies over millions of years; hence, scientists often gather inspiration from the beautiful structures that are encountered. One of the fundamental, supramolecular building blocks of life itself, the DNA double helix, may be a promising electronic material. Over the years much interest has arisen in the use of DNA as

a charge-transport material⁵⁴¹ due to the possibilities of electron^{542,543} and hole^{544,545} transport along stacked base pairs. Originally engaged in genetic coding, these findings offer potential for new applications, such as the use of DNA as one-dimensional molecular wires in electronic systems. As a result of its negative charge, DNA can be used as a template for the binding of cationic organic molecules. Dye molecules such as porphyrins^{546–551} and cyanines^{552–556} were designed to target the major and minor groove of double-stranded DNA, resulting in helical chromophore assemblies. Moreover, by synthetically modifying oligonucleotides by attaching chromophores, electron transfer in the duplex could be investigated⁵⁵⁷ and energy transfer was observed between various chromophores, often for the sake of DNA detection.^{558–560} It has also been shown that duplex, triplex, and quadruplex hairpins can be stabilized to a large extent by noncovalent stacking interactions with, e.g., stilbenes⁵⁶¹ or perylenes.^{562,563} These conjugates can subsequently be used in studying electron transfer through the DNA strands^{564,565} by charge-transfer interactions with the nucleobases or appended acceptor molecules.⁵⁶⁶ Recently, Wang and co-workers reported the synthesis of alternated DNA and π -conjugated perylene bisimide sequences,⁵⁶⁷ which folded into nanostructures by $\pi-\pi$ stacking and hydrophobic interactions. The folding could be controlled with temperature and was disrupted upon complexation with complementary DNA, leading to a color change.

Considerable work on the interplay between DNA and π -conjugated polymers has been performed by Bazan et al., who used polycationic oligo- and polyfluorenes to create interpolyelectrolyte complexes based on electrostatic interactions.^{568–570} By using dye-labeled DNA, RNA, or PNA, energy transfer from the conjugated polymer to the dye is observed upon complexation to the complementary oligonucleotide, providing the means for implementation of these systems as sensors. By synthesizing a copolymer of fluorene-*co*-phenylene incorporating 5% benzothiadiazole traps (**216**, Figure 94), luminescence could be tuned from blue to green upon random DNA binding and from green to red upon binding to a dye-labeled complementary DNA strand.⁵⁷¹

In another work an energy-transfer cascade was constructed by complexing a positively charged phenylene–fluorene polymer with fluorescein-end-capped ds-DNA, which was intercalated with ethidium bromide.⁵⁷² Exciting the conjugated polymer lead to energy transfer to the fluorescein, which in turn transferred its excitation energy to the ethidium bromide, having the most red-shifted absorption. It was nicely shown that the luminescence intensity of the ethidium bromide increased almost eight times, as compared to direct excitation, and that this concept only worked when a complementary strand of DNA was added to the fluorescein-end-capped ss-DNA.

9.3. Assembly of Mixed Porphyrins

In the beginning of this review we encountered the ring-like photosystems of green plants and purple

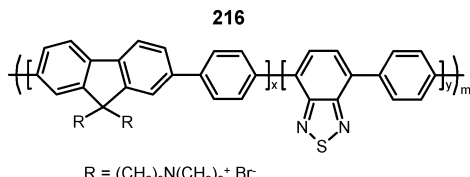
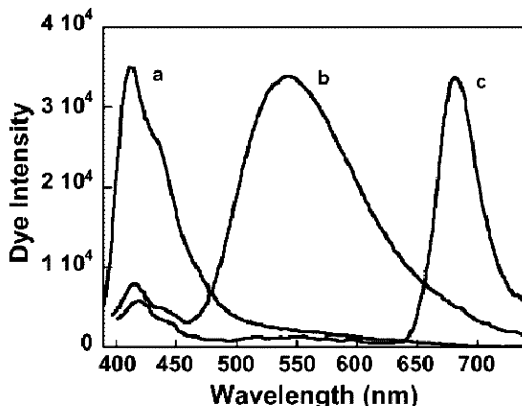


Figure 94. Polycationic copolymer **216** containing fluorene donors and 5 wt % benzothiadiazole acceptors and normalized fluorescence spectra in water (a) **216**/dye-labeled PNA leads to blue fluorene emission due to the absence of *intramolecular* energy transfer. (b) **216**/dye-labeled PNA with noncomplementary DNA yields green benzothiadiazole luminescence by polymer aggregation and subsequent efficient energy transfer from fluorene parts. (c) **216**/dye-labeled PNA with complementary DNA results in red emission as a consequence of essentially complete energy transfer to the dye. (Reprinted with permission from ref 571. Copyright 2004 American Chemical Society.)

bacteria and the unique antennae system of green bacteria.^{74–76} In the latter system instead of employing chlorophyll molecules that are embedded in a protein matrix, the positioning of light-harvesting chromophores occurs primarily by means of supramolecular interactions between the individual porphyrin rings with little use of protein support. In this way huge chlorosomes arise, comprised of stacked pigments, which incorporate up to tens of thousands of chlorophyll moieties. Recently, accessibility to the characterization of these complex systems was greatly enhanced by implementation of powerful NMR techniques.⁷⁷ Combined with molecular modeling, elucidation of the structural assembly of a modified bacteriochlorophyll *d* yielded a valuable model for extended chromophore aggregation in green bacteria. The chlorosome superstructure is especially appealing to supramolecular chemists working in electronics since it cleverly combines cooperative supramolecular interactions into a functional object, approaching directional, one-dimensional energy transport. The preparation of supramolecular imidazolylporphyrin assemblies through hydrogen-bonding and stacking interactions was demonstrated by Nagata et al.⁵⁷³ Fluorescence quenching using chloranil and Mn(III)-porphyrin as acceptors was studied in toluene, indicating efficient energy transport in the aggregates to the incorporated guests.

A collaboration between the groups of Tamiaki and Holzwarth has yielded valuable data on energy transfer within self-assembled porphyrin aggregates.^{574–576} They employed synthetic analogues of natural porphyrins (Figure 95) to mimic the light-harvesting system of green photosynthetic bacteria in a thorough, time-resolved fluorescence study.⁵⁷⁷ By co-aggregation of zinc chlorins and bacteriochlorophylls with various energy traps an artificial supramolecular antenna system could be designed, strongly reminiscent of its natural analogue. The strong red shift of the absorption maxima of **217**, **218**, and **219** in an aqueous environment as compared to the monomers points to aggregation of the compounds. Upon adding ~4% energy traps **220** or **221** to aggregates of **217** or **221** to aggregates of **219** the



characteristic trap absorption around $\lambda = 800$ nm becomes visible as a small shoulder. However, the steady-state fluorescence spectra have undergone much more rigorous changes (Figure 95). The luminescence of **217** is quenched to a large extent in favor of that of the trap molecules, indicating efficient energy transfer to the incorporated energy trap (59% and 68% efficiency for **220** and **221**, respectively). The system **219** + **221** shows much less efficient energy transfer.

The experiments were performed in the presence of sodium dithionite, i.e., under reducing conditions, to rule out effective quenching by small amounts of chlorin cations. From decay-associated fluorescence spectroscopy (DAS) and kinetic modeling it was shown that the excitation in the chlorin aggregates must be effectively delocalized over at least 10–15 pigment molecules. The high efficiency for the collection of energy at the trap position yields interesting perspectives for further use in artificial photosynthetic systems for the creation of a charge-separated state.

Co-aggregation of donor and acceptor occurs in dilute solution as a consequence of strong intermolecular interactions and solvophobicity. However, in this last example the possibility presents itself to dope the donor aggregates with arbitrary amounts of acceptor, as opposed to the co-aggregation that was observed in section 9.1. For the latter systems aggregates composed of either covalent or supramolecular complexes are formed but the ratio between donor and acceptor is fixed. In gelated and liquid-crystalline systems we observed that it is, in principle, always possible to randomly vary the amount of acceptor, although in the latter case mesophases are often most stable when a 1:1 donor–acceptor ratio is used. However, reports on the incorporation of variable amounts of acceptor into one-dimensional supramolecular stacks in solution are scarce, probably because of the stringent requirements for the design of such mixed systems and the difficulty of avoiding phase separation.

Another system that allows for variation in donor–acceptor ratio was studied by Ihara et al.,⁵⁷⁸ who

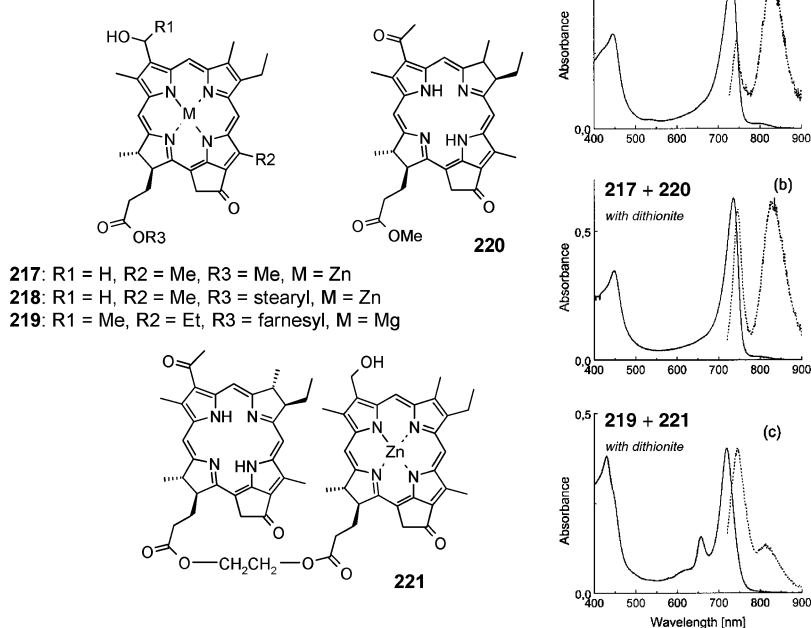


Figure 95. Structures of porphyrins **217–219** and energy traps **220** and **221**. Absorption (solid) and fluorescence (dashed) curves of (a) co-aggregates of **217** and **220** without dithionite, (b) co-aggregates of **217** and **220** with dithionite, and (c) co-aggregates of **219** and **221** with dithionite. The mixed systems in a and b indicate efficient energy transfer to the acceptors, while that in c shows less efficient energy transfer. (Reprinted with permission from ref 577. Copyright 2002 American Chemical Society.)

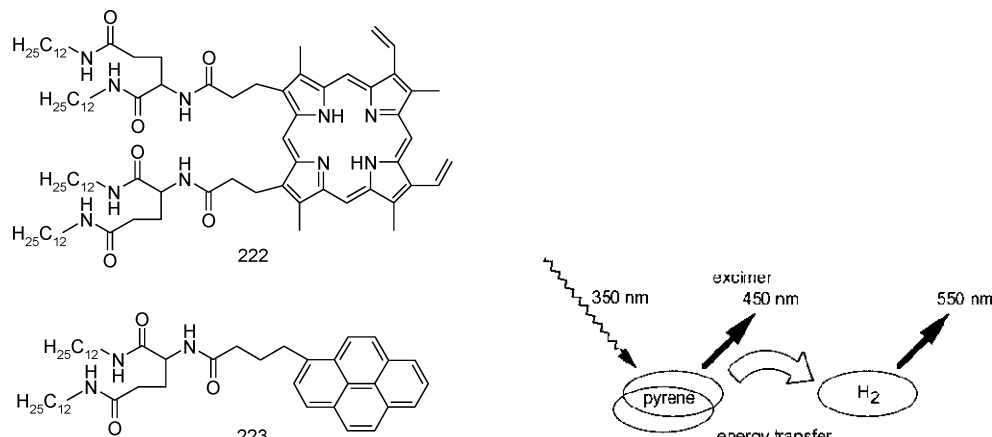


Figure 96. Didodecyl L-glutamic acid-substituted porphyrin **222** and pyrene **223** form mixed assemblies in benzene. Energy transfer from pyrene excimers to porphyrin acceptors in the assemblies is schematically depicted. (Reprinted with permission from ref 578. Copyright 2002 American Chemical Society.)

prepared fibrous assemblies of porphyrin- (**222**) and pyrene-substituted (**223**) L-glutamic acid (Figure 96).

By amide hydrogen bonding both chromophores self-assemble cofacially into chiral fibers as long as hundreds of micrometers, and the assembly process can be controlled with temperature. The porphyrin forms a physical gel, and optical studies confirm the presence of highly ordered aggregates even below the critical gel-forming concentration. Although the pyrene did not produce a gel state at room temperature, it does form ordered aggregates in solution. Preliminary results indicate energy transfer within mixed assemblies in solution from pyrene excimers to porphyrin traps. Moreover, the L-glutamic acid induces helicity into the fibers, as concluded from the observed Cotton effects for both the porphyrin and the pyrene systems.

9.4. Assembly by Hydrogen Bonding

As encountered in section 8.2.2, Meijer et al. synthesized a covalent triad that formed an ordered liquid crystal in the bulk. In an extension of this work, donor–acceptor–donor triad **224** was synthesized in which the two OPVs and the central perylene bisimide are connected by a chiral linker incorporating amide bonds (Figure 97).⁵⁷⁹

Molecule **224** was designed to self-assemble in toluene solution into chiral aggregates. Photoinduced electron transfer from the OPVs to the perylene occurred with high efficiency, creating a nanoscopic p–n-heterojunction in solution. From IR studies on a model compound it was observed that the presence of the amide bonds leads to strong intermolecular hydrogen bonding in toluene solution.

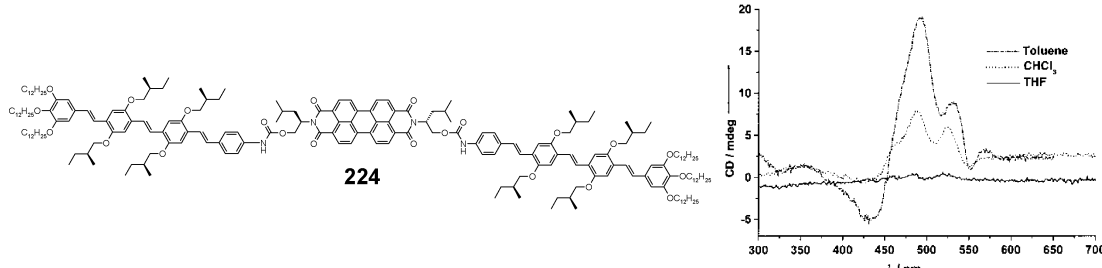


Figure 97. Donor–acceptor–donor triad **224** consists of two chiral OPVs that are covalently attached to a central perylene bisimide via a chiral amide linker. CD spectra of **224** in various solvents indicating supramolecular chirality in chloroform and toluene. (Reprinted with permission from ref 579. Copyright 2002 The Royal Society of Chemistry.)

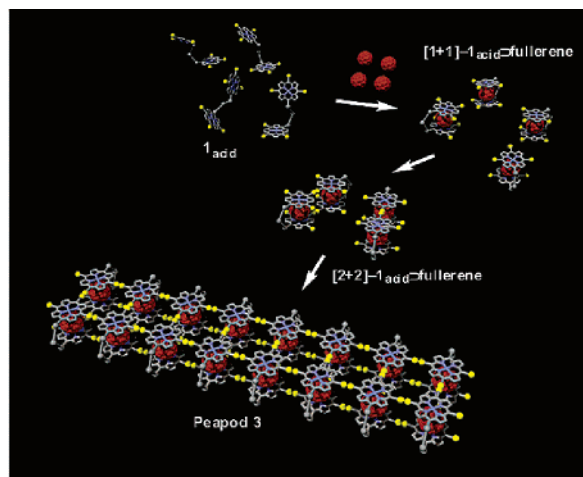


Figure 98. Schematic representation of the self-assembly of porphyrin-sandwiched-C₆₀ complexes into highly ordered structures resembling peapods. After the sandwiched complex has been formed, intermolecular hydrogen bonding ensures supramolecular polymerization. (Reprinted with permission from ref 580. Copyright 2003 American Chemical Society.)

In a recent paper by Aida et al. the authors report an elegant design for one-dimensional ordering of Zn(II)porphyrin and C₆₀, thereby creating electronic structures that resemble peapods (Figure 98).⁵⁸⁰ An acyclic zinc porphyrin dimer, bearing large dendritic wedges for solubility, can incorporate fullerenes such as C₆₀ and C₇₀,⁵⁸¹ after which the free porphyrin carboxylic acid groups ensure supramolecular polymerization by hydrogen bonding. As opposed to pure porphyrin assembly, the fullerene-triggered self-assembly occurs in a highly ordered fashion as a consequence of conformational changes of the porphyrin dimer upon sandwiching of C₆₀.

It is shown that these carboxylic acid groups are essential for the self-assembly since methyl-ester-

functionalized building blocks do not show any signs of the formation of superstructures. With TEM fibers of uniform width and very high aspect ratios are observed, making these assemblies promising electroactive components in the field of supramolecular electronics.

Meijer, Schenning and Würther et al. extended the concept presented in Figure 97 to chiral aggregates of triple-hydrogen-bonded 1:2 complexes of perylene bisimide and OPVs **225–227** in methylcyclohexane (MCH) (Figure 99).⁵⁸² These superstructures are formed in a hierarchical process in which the hydrogen-bonded triad further self-assembles in one dimension by π – π interactions. The resulting J-type aggregates are characterized by bathochromic shifts for both chromophores, as high as 40 nm for the perylene moiety. The chirality of the OPV side chains imparts chirality to the aggregates as well and is transferred to the perylene bisimide as observed with CD spectroscopy. From fluorescence and photoinduced absorption (PIA) measurements it can be concluded that within the aggregates photoinduced electron transfer occurs from the OPVs to the perylene bisimide. Moreover, the optical techniques prove the existence of two phases for the hydrogen-bonded complex in solution, namely, a molecularly dissolved one at high temperatures and an aggregated state at low temperatures. A sharp transition between the two states is observed at ~ 55 °C (10⁻⁵ M in MCH). AFM measurements using **226** on glass clearly show rodlike aggregates consisting of left-handed helical π – π co-aggregates of the two dyes that are further assembled to right-handed nanometer-scale supercoils (Figure 100).

Recently, using a modular approach,⁴¹⁶ it was possible to extend this concept to a series of OPVs of different length.⁵⁸³ Temperature- and concentration-dependent results clearly indicate that the stability

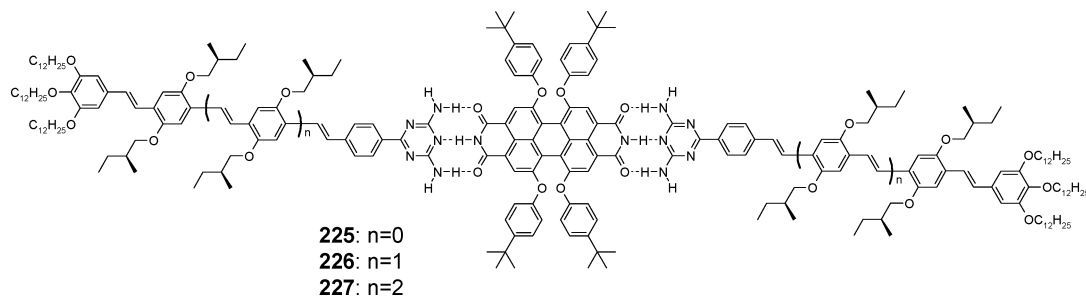


Figure 99. Two chiral OPVs, of which the conjugation length can be varied, are joined with a central perylene bisimide by triple hydrogen bonding. These supramolecular donor–acceptor–donor triads **225–227** self-assemble in apolar solvent and are characterized by efficient intermolecular electron transfer to the perylene bisimide.

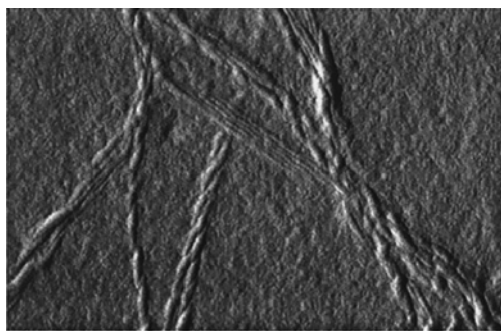


Figure 100. Tapping-mode AFM image ($715 \text{ nm} \times 475 \text{ nm}$) showing right-handed supercoils, consisting of left-handed helices of **226** on a glass slide. (Reprinted with permission from ref 582. Copyright 2002 American Chemical Society.)

of the donor–acceptor aggregates increases with OPV conjugation length due to the possibility of having more $\pi-\pi$ stacking interactions between the building blocks. These co-aggregates can be regarded as nanoscopic p–n-heterojunctions, which may serve as valuable models for photoinduced electron-transfer processes in solid-state devices.

Meijer and Schenning et al. also focused on the preparation of mixed aggregates of pure hydrogen-bonded OPVs **175** and **176a** (Figure 101) in solution.⁵⁸⁴ These helical assemblies are formed in a hierarchical process in which hydrogen-bonded dimers further self-assemble into extended columnar aggregates by $\pi-\pi$ stacking interactions. The oligomers of different length possess an identical ureido-striazine hydrogen-bonding motif, enabling the formation of heterodimers and thus mixed stacks in an apolar environment.

It was shown that by doping small amounts of **176a** into donor **175** aggregates, with intermediate heating, fast and efficient energy transfer occurs from the short to the longer oligomers inside the mixed assemblies (Figure 101b,c). The stacks ensure an effective pathway for the transfer of excitation energy, as illustrated by the loss of acceptor signal at temperatures above the melting temperatures of the stacks. Up to about 2 mol %, **176a** exists as isolated

energy traps inside **175** aggregates. Above this content, clustering of the acceptor molecule occurs as can be concluded from its quenched and red-shifted fluorescence, probably due to the possibility of having more favorable $\pi-\pi$ interactions. When the addition of the longer oligomer is performed below the melting temperature of the aggregates, no exchange is possible between the two oligomeric stacks and the energy-transfer process is consequently blocked.

One of the main drawbacks of the system in Figure 101 is that there is no possibility of controlling the length of the stacks. Though the persistence length of the donor columns is around 60 nm, the system appears to be a quite dynamic. Moreover, the same hydrogen-bonding motif which enables the formation of mixed stacks in the first place prevents the exact control of the trap position due to its self-complementarity. This eventually leads to the observed phase separation between donor and acceptor and thus the undesired clustering of guest molecules.

The energy-transfer process is characterized by a very fast component in the rise of the acceptor luminescence, which is absent when the stacks are dissociated at high temperatures. This component is directly correlated with the high degree of order inside the OPV assemblies, which enables fast excitonic diffusion⁴¹⁸ along the stacks before excitations are trapped inside local potential minima. At longer time scales coupling between the chromophores is weaker and a direct Förster-type of energy transfer to the guest molecules starts to dominate. Here, an analogy can be drawn between natural and synthetic systems. It is known from the literature that electron transfer merely occurs through DNA when the base pairs are aligned in a certain, well-coupled fashion and is characterized by an ultrafast decay component.⁵⁸⁵ This means that when there is disorder in a DNA duplex, electron transfer is only possible upon rearrangement into an ordered stack within the lifetime of the excited donor base. In this way, both systems indicate that a high degree of order is a prerequisite for fundamental issues such as energy and electron transfer to occur with high efficiency.

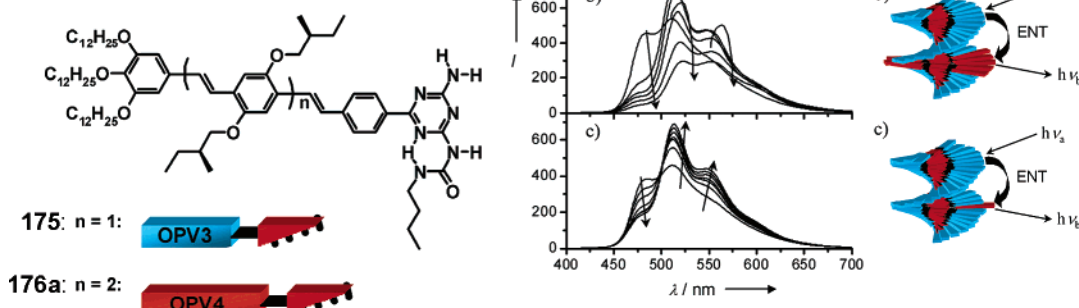


Figure 101. The self-complementary hydrogen-bonding motif of OPVs **175** and **176a** enables the formation of mixed dimers and mixed aggregates. Photoluminescence spectra for mixtures in dodecane solution: (a) 0–30 mol % **176a** at 80 °C, (b) 0–30 mol % **176a** at 10 °C, and (c) 0–1.2 mol % **176a** at 10 °C. Inside the mixed stacks efficient energy transfer is observed from **175** to **176a**. (Reprinted with permission from ref 584. Copyright 2004 John Wiley & Sons, Inc.)

10. Conclusions and Prospects

Self-assembly offers an attractive tool to construct well-organized π -conjugated materials. As can be deduced from this review, it is possible not only to study material properties at the supramolecular level, but also to tune the macroscopic properties of π -conjugated systems. These tailor-made supramolecular assemblies will enormously influence the macroscopic properties. The combination of supramolecular architecture with functionality in macromolecules will not only give rise to emerging opportunities in materials science, but also significantly contribute to bridge the gap between natural and artificial systems in an effort to fully understand the guidelines used to assemble natural units in the different hierarchies of organization. On the other hand, progress in synthetic methodologies has also been used to prepare completely new structures with unique properties. However, there are still a number of very appealing targets that should be reached before these very promising organic and polymeric materials with tailored supramolecular architectures will be used in active devices. The inability to exactly position chromophores with nanometer precision and difficulty in controlling the dimensions of supramolecular nanostructures will be challenges to tackle to improve this relatively new discipline. The use of templates could be one attractive approach to solve these problems. Another issue is the robustness of noncovalent interactions, which are often temperature and solvent sensitive. Recently, several new approaches have been reported to fixate self-organized π -conjugated systems. Thermotropic and lyotropic liquid-crystalline phases of π -conjugated systems^{586,587} and specific conformations of polymers⁵⁸⁸ have been polymerized in order to create shape-persistent objects. Another elegant method in this respect is to remove the solubilizing groups in an additional processing step after self-assembly.⁵⁸⁹ For fabricating plastic electronic devices, extra manipulation steps such as alignment layers are often required to obtain long-range order. Moreover, vertical or homeotropic alignment of self-assembled objects is extremely difficult and is still a great challenge.⁵⁹⁰ This review also shows that successful implementation of self-assembled π -conjugated systems in electronics largely depends on the other layers and electrodes present in the devices. To increase the compatibility and simplify processability it would be a dream to self-assemble all these components at once like nature does. Recently, the first step in this direction was reported in the orthogonal self-assembly of p- and n-type fibers. In one step separate stacks of electron donor and acceptor were constructed in which photoinduced electron transfer is still possible.⁵⁹¹

From a chemical point of view it is a prerequisite to join the disciplines of organic, polymer, and materials chemistry. Only then can the specificity and selectivity in molecular synthesis, recognition, and function be combined with synthetic polymers and materials, leading to artificial polymers with natural efficiency. Taking into account the recent progress in obtaining full control over large three-

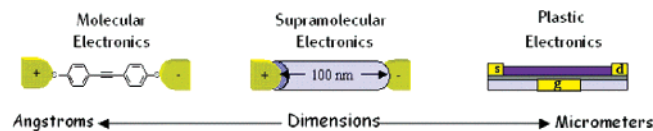


Figure 102. Schematic representation illustrating the gap, with respect to length scales, between molecular electronics, where single molecules are studied, and plastic electronics, which relies on bulk properties of π -conjugated polymers. Supramolecular electronics is an intermediate field with the aim to construct and investigate self-assembled architectures on the 5–100 nm length scale that can be connected to electrodes.¹

dimensional polymeric architectures, it is safe to conclude that soon a next generation of functional conjugated polymers, which by molecular design will possess a unique polymeric architecture, will be used in devices. This review, however, clearly shows that the persistence length of the supramolecular architectures is often in the nanometer range.

Since many supramolecular architectures have a persistence length in the 100 nm range, it seems attractive to use them as independent objects in supramolecular electronics as alternatives for single-wall carbon nanotubes or inorganic wires. Supramolecular electronics¹ could bridge the gap between molecular electronics,⁵⁹² having Ångstrom dimensions, and plastic electronics, having dimensions in the micrometer range. Recently, Aida et al. showed that such objects can be constructed.⁵⁹³ An amphiphilic hexa-peri-hexabenzocoronene was self-assembled into nanotubes that upon oxidation showed a 2.5 M Ω resistivity when placed between 180 nm gap electrodes. This behavior shows that self-assembled π -conjugated systems can serve as a beautiful starting point for the search of supramolecular electronics, Figure 102.

11. Acknowledgment

The authors acknowledge the many discussions with and contributions of all our former and current colleagues. Their names are given in the references cited. A special word of thanks is expressed to our colleague Professor René Janssen, without his continuous support of our activities the writing of this review would have been impossible. The research in Eindhoven has been supported by the Eindhoven University of Technology and The Netherlands Organization for Chemical Research (CW) with financial aid from The Netherlands Organization for Scientific Research (NWO).

12. Note Added after ASAP Publication

This paper was published on the Web on March 10, 2005, with some figures represented in black and white instead of color. The article including color figures was reposted on March 16, 2005.

13. References

- (1) Meijer, E. W.; Schenning, A. P. H. J. *Nature* **2002**, *419*, 353–354.
- (2) Dimitrakopoulous, C. D.; Malenfant, P. R. L. *Adv. Mater.* **2002**, *14*, 99–117.
- (3) Braun, D. *Mater. Today* **2002**, *5*, 32–36.

- (4) Friend, R. H.; Gymer, R. W.; Holmes, A. B.; Burroughes, J. H.; Marks, R. N.; Taliani, C.; Bradley, D. D. C.; dos Santos, D. A.; Brédas, J.-L.; Lögglund, M.; Salaneck, W. R. *Nature* **1999**, *397*, 121–128.
- (5) Brabec, C. J.; Dyakonov, V.; Parisi, J.; Sariciftci, N. S. *Organic Photovoltaics Concepts and Realization*; Springer-Verlag: London, 2003.
- (6) Patil, A. O.; Heeger, A. J.; Wudl, F. *Chem. Rev.* **1988**, *88*, 183–200.
- (7) Kraft, A.; Grimsdale, A. C.; Holmes, A. B. *Angew. Chem., Int. Ed.* **1998**, *37*, 402–428.
- (8) Becker, H.; Spreitzer, H.; Kreuder, W.; Kluge, E.; Schenk, H.; Parker, I.; Cao, Y. *Adv. Mater.* **2000**, *12*, 42–46.
- (9) Roex, H.; Adriaensens, P.; Vanderzande, D.; Gelan, J. *Macromolecules* **2003**, *36*, 5613–5621.
- (10) Xing, K. Z.; Johansson, N.; Beaman, G.; Clark, T. D.; Brédas, J.-L.; Salaneck, W. R. *Adv. Mater.* **1997**, *9*, 1027–1031.
- (11) Sutherland, D. G. J.; Carlisle, J. A.; Elliker, P.; Fox, G.; Hagler, T. W.; Jimenez, I.; Lee, H. W.; Pakbaz, K.; Terminello, L. J.; Williams, S. C.; Himpel, F. J.; Shuh, D. K.; Tong, W. M.; Jia, J. J.; Callcott, T. A.; Ederer, D. L. *Appl. Phys. Lett.* **1996**, *68*, 2046–2049.
- (12) Ma, L.; Wang, X.; Wang, B.; Wang, J.; Chen, J.; Huang, K.; Zhang, B.; Cao, Y.; Han, Z.; Qian, S.; Yao, S. *Chem. Phys.* **2002**, *285*, 85–92.
- (13) Kumar, P.; Mehta, A.; Dadmun, M. D.; Zheng, J.; Peyser, L.; Bartko, A. P.; Dickson, R. M.; Thundat, T.; Sumpter, B. G.; Noid, D. W.; Barnes, M. D. *J. Phys. Chem. B* **2003**, *107*, 6252–6256.
- (14) Hu, D.; Yu, J.; Wong, K.; Bagchi, B.; Rossky, P. J.; Barbara, P. F. *Nature* **2000**, *405*, 1030–1032.
- (15) McCullough, R. D. *Adv. Mater.* **1998**, *10*, 93–116.
- (16) Fischou, D. *Handbook of oligo- and polythiophene*; Wiley-VCH: Weinheim, 1999.
- (17) Martens, H. C. F.; Blom, P. W. M.; Schoo, H. F. M. *Phys. Rev. B* **2000**, *61*, 7489–7493.
- (18) Ruseckas, A.; Namdas, E. B.; Theander, M.; Svensson, M.; Yartsev, A.; Zigmantas, D.; Andersson, M. R.; Inganas, O.; Sundstrom, V. *JPPA* **2001**, *144*, 3–12.
- (19) Jakubiak, R.; Collison, C. J.; Wan, W. C.; Rothberg, L. J.; Hsieh, B. R. *J. Phys. Chem. A* **1999**, *103*, 2394–2398.
- (20) Kemerink, M.; van Duren, J. K. J.; Jonkheijm, P.; Pasveer, W. F.; Koenraad, P. M.; Janssen, R. A. J.; Salemink, H. W. M.; Wolter, J. H. *Nano Lett.* **2003**, *3*, 1191–1196.
- (21) DiCésare, N.; Belletête, M.; Raymond, F.; Leclerc, M.; Durocher, G. *J. Phys. Chem. A* **1998**, *102*, 2700–2707.
- (22) Raymond, F.; Di Cesare, N.; Belletête, M.; Durocher, G.; Leclerc, M. *Adv. Mater.* **1998**, *10*, 599–602.
- (23) Krebs, F. C.; Jorgensen, M. *Macromolecules* **2003**, *36*, 4374–4384.
- (24) Krebs, F. C.; Jorgensen, M. *Polym. Bull.* **2003**, *51*, 127–134.
- (25) Grimsdale, A. C.; Leclère, Ph.; Lazzaroni, R.; MacKenzie, J. D.; Murphy, C.; Setayesh, S.; Silva, C.; Friend, R. H.; Mullen, K. *Adv. Funct. Mater.* **2002**, *12*, 729–733.
- (26) Winokur, M. J.; Chunwachirasiri, W. *J. Polym. Sci., Part B: Polym. Phys.* **2003**, *41*, 2630–2648.
- (27) McCullough, R. D.; Lowe, R. D.; Jayaraman, M.; Anderson, D. L. *J. Org. Chem.* **1993**, *58*, 904–912.
- (28) McCullough, R. D.; Tristram-Nagle, S.; Williams, S. P.; Lowe, R. D.; Jayaraman, M. *J. Am. Chem. Soc.* **1993**, *115*, 4910–4911.
- (29) McCullough, R. D.; Lowe, R. D.; Jayaraman, M.; Ebwank, P. C.; Anderson, D. L.; Tristram-Nagle, S. *Synth. Met.* **1993**, *55*, 1198–1203.
- (30) Faid, K.; Cloutier, R.; Leclerc, M. *Macromolecules* **1993**, *26*, 2501–2507.
- (31) Sirringhaus, H.; Tessler, N.; Friend, R. H. *Science* **1998**, *280*, 1741–1744.
- (32) Sirringhaus, H.; Brown, P. J.; Friend, R. H.; Nielsen, M. M.; Beechgaard, K.; Langeveld-Voss, B. M. W.; Spiering, A. J. H.; Janssen, R. A. J.; Meijer, E. W.; Herwig, P.; De Leeuw, D. M. *Nature* **1999**, *401*, 685–688.
- (33) Kline, R. J.; McGehee, M. D.; Kadnikova, E. N.; Liu, J.; Fréchet, J. M. J. *Adv. Mater.* **2003**, *15*, 1519–1522.
- (34) Shaked, S.; Tal, S.; Roichman, Y.; Razin, A.; Xiao, S.; Eichen, Y.; Tessler, N. *Adv. Mater.* **2003**, *15*, 913–916.
- (35) Banach, M. J.; Friend, R. H.; Sirringhaus, H. *Macromolecules* **2003**, *36*, 2838–2844.
- (36) Schwartz, B. J. *Annu. Rev. of Phys. Chem.* **2003**, *54*, 141–172.
- (37) Sirringhaus, H.; Wilson, R. J.; Friend, R. H.; Inbasekaran, M.; Wu, W.; Woo, E. P.; Grell, M.; Bradley, D. D. C. *Appl. Phys. Lett.* **2000**, *77*, 406–408.
- (38) Redecker, M.; Bradley, D. D. C.; Inbasekaran, M.; Woo, E. P. *Appl. Phys. Lett.* **1999**, *74*, 1400–1403.
- (39) Brabec, C. J.; Winder, C.; Scharber, M. C.; Sariciftci, N. S.; Hummelen, J. C.; Svensson, M.; Andersson, M. R. *J. Chem. Phys.* **2001**, *115*, 7235–7244.
- (40) Camaiora, N.; Ridolfi, G.; Casalbore-Miceli, G.; Possamai, G.; Maggini, M. *Adv. Mater.* **2002**, *14*, 1735–1739.
- (41) Padinger, F.; Rittberger, R. S.; Sariciftci, N. S. *Adv. Funct. Mater.* **2003**, *13*, 85–88.
- (42) Liu, J.; Guo, T.-F.; Yang, Y. *J. Appl. Phys.* **2002**, *91*, 1595–1600.
- (43) Heil, H.; Finnberg, T.; von Malm, N.; Schmechel, R.; von Seggern, H. *J. Appl. Phys.* **2003**, *93*, 1636–1641.
- (44) Teetsov, J.; Vanden Bout, D. A. *Langmuir* **2002**, *18*, 897–903.
- (45) Blatchford, J. W.; Gustafson, T. L.; Epstein, A. J.; Vanden Bout, D. A.; Kerimo, J.; Higgins, D. A.; Barbara, P. F.; Fu, D. K.; Swager, T. M.; MacDiarmid, A. G. *Phys. Rev. B* **1996**, *54*, R3683–R3686.
- (46) Hassenkam, T.; Greve, D. R.; Bjørnholm, T. *Adv. Mater.* **2001**, *13*, 631–634.
- (47) Wei, P.-K.; Lin, Y.-F.; Fann, W.; Lee, Y.-Z.; Chen, S.-A. *Phys. Rev. B* **2001**, *63*, 045417/1–045417/5.
- (48) Lehn, J.-M. *Science* **2002**, *295*, 2400–2403.
- (49) Steed, J. W.; Atwood, J. L. *Supramolecular Chemistry*; Wiley & Sons: Chichester, 2000.
- (50) Sinnokrot, M. O.; Cherrill, C. D. *J. Am. Chem. Soc.* **2004**, *126*, 7690–7697.
- (51) Hunter, C. A.; Sanders, J. K. M. *J. Am. Chem. Soc.* **1990**, *112*, 5525–34.
- (52) Prins, L. J.; Reinhoudt, D. N.; Timmerman, P. *Angew. Chem., Int. Ed.* **2001**, *40*, 2383–2426.
- (53) Klok, H.-A.; Lecommandoux, S. *Adv. Mater.* **2001**, *13*, 1217–1229.
- (54) Kühlbrandt, W.; Wang, D. N. *Nature* **1991**, *350*, 130–134.
- (55) Kühlbrandt, W.; Wang, D. N.; Fujiyoshi, Y. *Nature* **1994**, *367*, 614–621.
- (56) Kühlbrandt, W. *Nature* **1995**, *374*, 497–498.
- (57) McDermott, G.; Prince, S. M.; Freer, A. A.; Hawthornthwaite-Lawless, A. M.; Papiz, M. Z.; Cogdell, R. J.; Isaacs, N. W. *Nature* **1995**, *374*, 517–521.
- (58) Hu, X.; Schultheis, K. *Phys. Today* **1997**, *50*, 28–34.
- (59) Hofmann, C.; Francia, F.; Venturoli, G.; Oesterhelt, D.; Kohler, J. *FEBS Lett.* **2003**, *546*, 345–348.
- (60) Steensgaard, D. B.; Wackerbarth, H.; Hildebrandt, P.; Holzwarth, A. R. *J. Phys. Chem. B* **2000**, *104*, 10379–10386.
- (61) van Rossum, B. J.; Steensgaard, D. B.; Mulder, F. M.; Boender, G. J.; Schaffner, K.; Holzwarth, A. R.; de Groot, H. J. M. *Biochemistry* **2001**, *40*, 1587–1595.
- (62) Haycock, R. A.; Hunter, C. A.; James, D. A.; Michelsen, U.; Sutton, L. R. *Org. Lett.* **2000**, *2*, 2435–2438.
- (63) Takahashi, R.; Kobuke, Y. *J. Am. Chem. Soc.* **2003**, *125*, 2372–2373.
- (64) Peng, X.; Aratani, N.; Takagi, A.; Matsumoto, T.; Kawai, T.; Hwang, I.-W.; Ahn, T. K.; Kim, D.; Osuka, A. *J. Am. Chem. Soc.* **2004**, *126*, 4468–4469.
- (65) Choi, M.-S.; Yamazaki, T.; Yamazaki, I.; Aida, T. *Angew. Chem., Int. Ed.* **2003**, *43*, 150–158.
- (66) Haycock, R. A.; Yartsev, A.; Michelsen, U.; Sundstrom, V.; Hunter, C. A. *Angew. Chem., Int. Ed.* **2000**, *39*, 3616–3619.
- (67) Kuroda, Y.; Sugou, K.; Sasaki, K. *J. Am. Chem. Soc.* **2000**, *122*, 7833–7834.
- (68) Sugou, K.; Sasaki, K.; Kitajima, K.; Iwaki, T.; Kuroda, Y. *J. Am. Chem. Soc.* **2002**, *124*, 1182–1183.
- (69) Wasielewski, M. R. *Chem. Rev.* **1992**, *92*, 435–61.
- (70) Gust, D.; Moore, T. A.; Moore, A. L. *Acc. Chem. Res.* **2001**, *34*, 40–48.
- (71) Choi, M.-S.; Aida, T.; Yamazaki, T.; Yamazaki, I. *Angew. Chem., Int. Ed.* **2001**, *40*, 3194–3198.
- (72) Weil, T.; Reuther, E.; Mullen, K. *Angew. Chem., Int. Ed.* **2002**, *41*, 1900–1904.
- (73) Serin, J. M.; Brousseau, D. W.; Fréchet, J. M. J. *Chem. Commun.* **2002**, 2605–2607.
- (74) Tamiaki, H.; Takeuchi, S.; Tsudzuki, S.; Miyatake, T.; Tanikaga, R. *Tetrahedron* **1998**, *54*, 6699–6718.
- (75) Balaban, T. S.; Eichhofer, A.; Lehn, J.-M. *Eur. J. Org. Chem.* **2000**, 4047–4057.
- (76) Balaban, T. S.; Bhise, A. D.; Fischer, M.; Linke-Schaetzl, M.; Roussel, C.; Vanthuyne, N. *Angew. Chem., Int. Ed.* **2003**, *42*, 2140–2144.
- (77) de Boer, B.; Stalmach, U.; Nijland, H.; Hadzioannou, G. *Adv. Mater.* **2000**, *12*, 1581–1583.
- (78) Holdcroft, S. *Adv. Mater.* **2001**, *13*, 1753–1765.
- (79) Martin, R. E.; Diederich, F. *Angew. Chem., Int. Ed. Engl.* **1999**, *38*, 1351–1377.
- (80) Tour, J. M. *Chem. Rev.* **1996**, *96*, 537–53.
- (81) Gelinck, G. H.; Huitema, H. E. A.; van Veenendaal, E.; Cantatore, E.; Schrijnemakers, L.; van der Putten, J. B. P. H.; Geuns, T. C. T.; Beenakkers, M.; Giesbers, J. B.; Huisman, B.-H.; Meijer, E. J.; Benito, E. M.; Touwslager, F. J.; Marsman, A. W.; van Rens, B. J. E.; de Leeuw, D. M. *Nature Mater.* **2004**, *3*, 106–110.
- (82) Yu, L.; Bao, Z.; Cai, R. *Angew. Chem., Int. Ed. Engl.* **1993**, *32*, 1345–1347.
- (83) Kloppenburg, L.; Jones, D.; Claridge, J. B.; Zur Loye, H.-C.; Bunz, U. H. F. *Macromolecules* **1999**, *32*, 4460–4463.
- (84) Grell, M.; Bradley, D. D. C.; Long, X.; Chamberlain, T.; Inbasekaran, M.; Woo, E. P.; Soliman, M. *Acta Polym.* **1998**, *49*, 439–444.

- (85) Steiger, D.; Smith, P.; Weder, C. *Macromol. Rapid Commun.* **1997**, *18*, 643–649.
- (86) Bao, Z.; Amundson, K. R.; Lovinger, A. J. *Macromolecules* **1998**, *31*, 8647–8649.
- (87) Surin, M.; Hennebicq, E.; Ego, C.; Marsitzky, D.; Grimsdale, A. C.; Müllen, K.; Brédas, J.-L.; Lazzaroni, R.; Leclerc, Ph. *Chem. Mater.* **2004**, *16*, 994–1001.
- (88) ten Hoeve, W.; Wynberg, H.; Havinga, E. E.; Meijer, E. W. *J. Am. Chem. Soc.* **1991**, *113*, 5887–5888.
- (89) Rughooputh, S. D. D. V.; Hotta, S.; Heeger, A. J.; Wudl, F. J. *Polym. Sci., Part B: Polym. Phys.* **1987**, *25*, 1071–1074.
- (90) Chen, S. A.; Ni, J. M. *Macromolecules* **1992**, *25*, 6081–6089.
- (91) Daoust, G.; Leclerc, M. *Macromolecules* **1991**, *24*, 455–459.
- (92) Heffner, G. W.; Pearson, D. S. *Macromolecules* **1991**, *24*, 6295–6299.
- (93) Roux, C.; Leclerc, M. *Macromolecules* **1992**, *25*, 2141–2144.
- (94) Drake, A. F.; Udvarhelyi, P.; Ando, D. J.; Bloor, D.; Obhi, J. S.; Mann, S. *Polymer* **1989**, *30*, 1063–1067.
- (95) Xu, R.; Chu, B. *Macromolecules* **1989**, *22*, 3153–3161.
- (96) Wenz, G.; Müller, M. A.; Schmidt, M.; Wegner, G. *Macromolecules* **1991**, *24*, 5606–5610.
- (97) Taylor, M. A.; Odell, J. A.; Bachelder, D. N.; Campbell, A. J. *Polymer* **1990**, *31*, 1116–1120.
- (98) Patel, G. N.; Chance, R. R.; Witt, J. D. *J. Chem. Phys.* **1979**, *70*, 4387–4392.
- (99) Lim, K. C.; Fincher, C. R.; Heeger, A. J. *Phys. Rev. Lett.* **1983**, *50*, 1934–1937.
- (100) Chu, B.; Xu, R. *Acc. Chem. Res.* **1991**, *24*, 384–389.
- (101) Yamamoto, T.; Komarudin, D.; Arai, M.; Lee, B.-L.; Suganuma, H.; Asakawa, N.; Inoue, Y.; Kubota, K.; Sasaki, S.; Fukuda, T.; Matsuda, H. *J. Am. Chem. Soc.* **1998**, *120*, 2047–2048.
- (102) Faïd, K.; Fréchette, M.; Ranger, M.; Mazerolle, L.; Lévesque, I.; Leclerc, M.; Chen, T.-A.; Rieke, R. D. *Chem. Mater.* **1995**, *7*, 1390–1396.
- (103) Lévesque, I.; Leclerc, M. *Chem. Mater.* **1996**, *8*, 2843–2849.
- (104) Bunz, U. H. F. *Chem. Rev.* **2000**, *100*, 1605–1644.
- (105) Pu, L. *Acta Polym.* **1997**, *48*, 116–141.
- (106) Bouman, M. M.; Havinga, E. E.; Janssen, R. A. J.; Meijer, E. W. *Mol. Cryst. Liq. Cryst. Technol., Sect A* **1994**, *256*, 439–448.
- (107) Langeveld-Voss, B. M. W.; Janssen, R. A. J.; Christiaans, M. P. T.; Meskers, S. C. J.; Dekkers, H. P. J. M.; Meijer, E. W. *J. Am. Chem. Soc.* **1996**, *118*, 4908–4909.
- (108) Lermo, E. R.; Langeveld-Voss, B. M. W.; Janssen, R. A. J.; Meijer, E. W. *Chem. Commun.* **1999**, 791–792.
- (109) Ramos Lermo, M. E.; Langeveld-Voss, B. M. W.; Meijer, E. W. *Polym. Prepr.* **1998**, *39*, 1087–1088.
- (110) Bouman, M. M.; Meijer, E. W. *Adv. Mater.* **1995**, *7*, 385–387.
- (111) Bidan, G.; Guillerez, S.; Sorokin, V. *Adv. Mater.* **1996**, *8*, 157–160.
- (112) Langeveld-Voss, B. M. W.; Christiaans, M. P. T.; Janssen, R. A. J.; Meijer, E. W. *Macromolecules* **1998**, *31*, 6702–6704.
- (113) Langeveld-Voss, B. M. W.; Waterval, R. J. M.; Janssen, R. A. J.; Meijer, E. W. *Macromolecules* **1999**, *32*, 227–230.
- (114) Fiesel, R.; Scherf, U. *Acta Polym.* **1998**, *49*, 445–449.
- (115) Fiesel, R.; Neher, D.; Scherf, U. *Synth. Met.* **1999**, *102*, 1457–1458.
- (116) Li, Y.; Chu, B. *Macromolecules* **1991**, *24*, 4115–4122.
- (117) Xu, R.; Chu, B. *Macromolecules* **1989**, *22*, 4523–4528.
- (118) Harlev, E.; Wudl, F. *Conjugated polymers and related materials. The interconnections of chemical and electronic structure*; Oxford University Press: Oxford, 1993.
- (119) Langeveld-Voss, B. M. W.; Peeters, E.; Janssen, R. A. J.; Meijer, E. W. *Synth. Met.* **1997**, *84*, 611–614.
- (120) (a) Fiesel, R.; Scherf, U. *Macromol. Rapid Commun.* **1998**, *19*, 427–431. (b) Fiesel, R.; Halkyard, C. E.; Rampey, M. E.; Kloppenburg, L.; Studer-Martinez, S. L.; Scherf, U.; Bunz, U. H. F. *Macromol. Rapid Commun.* **1999**, *20*, 107–111.
- (121) Zahn, S.; Swager, T. M. *Angew. Chem., Int. Ed.* **2002**, *41*, 4225–4230.
- (122) Andreani, F.; Angiolini, L.; Caretta, D.; Salatelli, E. *J. Mater. Chem.* **1998**, *8*, 1109–1111.
- (123) Cornelissen, J. J. L. M.; Peeters, E.; Janssen, R. A. J.; Meijer, E. W. *Acta Polym.* **1998**, *49*, 471–476.
- (124) Goldoni, F.; Janssen, R. A. J.; Meijer, E. W. *Polym. Prepr.* **1998**, *39*, 1049–1050.
- (125) Goldoni, F.; Janssen, R. A. J.; Meijer, E. W. *J. Polym. Sci., Part A: Polym. Chem.* **1999**, *37*, 4629–4639.
- (126) Langeveld-Voss, B. M. W.; Beljon, D.; Shuai, Z.; Janssen, R. A. J.; Meskers, S. C. J.; Meijer, E. W.; Brédas, J.-L. *Adv. Mater.* **1998**, *10*, 1343–1348.
- (127) Peeters, E.; Christiaans, M. P. T.; Janssen, R. A. J.; Schoo, H. F. M.; Dekkers, H. P. J. M.; Meijer, E. W. *J. Am. Chem. Soc.* **1997**, *119*, 9909–9910.
- (128) Peeters, E.; Janssen, R. A. J.; Meijer, E. W. *Synth. Met.* **1999**, *102*, 1105–1106.
- (129) Meskers, S. C. J.; Peeters, E.; Langeveld-Voss, B. M. W.; Janssen, R. A. J. *Adv. Mater.* **2000**, *12*, 589–594.
- (130) Fiesel, R.; Huber, J.; Scherf, U. *Angew. Chem., Int. Ed. Engl.* **1996**, *35*, 2111–2113.
- (131) Oda, M.; Nothofer, H.-G.; Lieser, G.; Scherf, U.; Meskers, S. C. J.; Neher, D. *Adv. Mater.* **2000**, *12*, 362–365.
- (132) Craig, M. R.; Jonkheijm, P.; Meskers, S. C. J.; Schenning, A. P. H. J.; Meijer, E. W. *Adv. Mater.* **2003**, *15*, 1435–1438.
- (133) Wilson, J. N.; Steffen, W.; McKenzie, T. G.; Lieser, G.; Oda, M.; Neher, D.; Bunz, U. H. F. *J. Am. Chem. Soc.* **2002**, *124*, 6830–6831.
- (134) McQuade, D. T.; Pullen, A. E.; Swager, T. M. *Chem. Rev.* **2000**, *100*, 2537–2574.
- (135) Marsella, M. J.; Swager, T. M. *J. Am. Chem. Soc.* **1993**, *115*, 12214–1215.
- (136) Crawford, K. B.; Goldfinger, M. B.; Swager, T. M. *J. Am. Chem. Soc.* **1998**, *120*, 5187–5192.
- (137) Kim, J.; McQuade, D. T.; McHugh, S. K.; Swager, T. M. *Angew. Chem., Int. Ed.* **2000**, *39*, 3868–3872.
- (138) Boldea, A.; Lévesque, I.; Leclerc, M. *J. Mater. Chem.* **1999**, *9*, 2133–2138.
- (139) Lévesque, I.; Leclerc, M. *J. Chem. Soc., Chem. Commun.* **1995**, 2293–2294.
- (140) Morgado, J.; Cacialli, F.; Friend, R. H.; Chuah, B. S.; Moratti, S. C.; Holmes, A. B. *Synth. Met.* **2000**, *111*–*112*, 449–452.
- (141) Luo, Y.-H.; Liu, H.-W.; Xi, F.; Li, L.; Jin, X.-G.; Han, C. C.; Chan, C.-M. *J. Am. Chem. Soc.* **2003**, *125*, 6447–6451.
- (142) Angelopoulos, M.; Dipietro, R.; Zheng, W. G.; MacDiarmid, A. G.; Epstein, A. J. *Synth. Met.* **1997**, *84*.
- (143) Zheng, W. G.; Angelopoulos, M.; Epstein, A. J.; MacDiarmid, A. G. *Macromolecules* **1997**, *30*, 7634–7640.
- (144) McCullough, R. D.; Ebwank, P. C.; Lowe, R. D. *J. Am. Chem. Soc.* **1997**, *119*, 633–640.
- (145) Stokes, K. K.; Heuze, K.; McCullough, R. D. *Macromolecules* **2003**, *36*, 7114–7118.
- (146) Faïd, K.; Leclerc, M. *J. Am. Chem. Soc.* **1998**, *120*, 5274–5278.
- (147) Nguyen, T.-Q.; Schwartz, B. J. *J. Chem. Phys.* **2002**, *116*, 8198–8208.
- (148) Lee, M.; Cho, B.-K.; Zin, W.-C. *Chem. Rev.* **2001**, *101*, 3869–3892.
- (149) Widawski, G.; Rawiso, M.; François, B. *Nature* **1994**, *369*, 387–389.
- (150) Zhong, X. F.; François, B. *Makromol. Chem.* **1991**, *192*, 2277–2291.
- (151) François, B.; Zhong, X. F. *Synth. Met.* **1991**, *1991*, 955–958.
- (152) de Boer, B.; Stalmach, U.; van Hutten, P. F.; Melzer, C.; Krasnikov, V. V.; Hadzioannou, G. *Polymer* **2001**, *42*, 9097–9109.
- (153) François, B.; Pitois, O.; Francois, J. *Adv. Mater.* **1995**, *7*, 1041–1044.
- (154) François, B.; Widawski, G.; Rawiso, M.; Cesar, B. *Synth. Met.* **1995**, *69*, 463–466.
- (155) Olinga, T.; François, B. *Makromol. Chem., Rapid Comm.* **1991**, *12*, 575–582.
- (156) Liu, J.; Sheina, E.; Kowalewski, T.; McCullough, R. D. *Angew. Chem., Int. Ed.* **2002**, *41*, 329–332.
- (157) Ng, S.-C.; Chan, H. S. O.; Xia, J.-F.; Yu, W. *J. Mater. Chem.* **1998**, *8*, 2347–2352.
- (158) Francke, V.; Räder, H. J.; Geerts, Y.; Müllen, K. *Macromol. Chem., Rapid Commun.* **1998**, *19*, 275–281.
- (159) Marsitzky, D.; Brand, T.; Geerts, Y.; Klapper, M.; Müllen, K. *Macromol. Chem., Rapid Commun.* **1998**, *19*, 385–389.
- (160) Bianchi, C.; Cecchetto, E.; François, B. *Synth. Met.* **1999**, *102*, 916–917.
- (161) Marsitzky, D.; Klapper, M.; Müllen, K. *Macromolecules* **1999**, *32*, 8685–8688.
- (162) Leclerc, Ph.; Calderone, A.; Marsitzky, D.; Francke, V.; Geerts, Y.; Müllen, K.; Brédas, J.-L.; Lazzaroni, R. *Adv. Mater.* **2000**, *12*, 1042–1046.
- (163) Leclerc, Ph.; Parente, V.; Brédas, J.-L.; François, B.; Lazzaroni, R. *Chem. Mater.* **1998**, *10*, 4010–4014.
- (164) Leclerc, Ph.; Hennebicq, E.; Calderone, A.; Brocorens, P.; Grimsdale, A. C.; Müllen, K.; Brédas, J.-L.; Lazzaroni, R. *Prog. Polym. Sci.* **2003**, *28*, 55–81.
- (165) Jenekhe, S. A.; Zhang, X.; Chen, X. L.; Choong, V.-E.; Gao, Y.; Hsieh, B. R. *Chem. Mater.* **1997**, *9*, 409–412.
- (166) Zhang, X.; Shetty, A. S.; Jenekhe, S. A. *Acta Polym.* **1998**, *49*, 52–55.
- (167) Jenekhe, S. A.; Chen, X. L. *Science* **1998**, *279*, 1903–1907.
- (168) Jenekhe, S. A.; Chen, X. L. *J. Phys. Chem. B* **2000**, *104*, 6332–6335.
- (169) Chen, X. L.; Jenekhe, S. A. *Macromolecules* **2000**, *33*, 4610–4612.
- (170) Ikkala, O.; ten Brinke, G. *Science* **2002**, *295*, 2407–2409.
- (171) Ruokolainen, J.; Makinen, R.; Torkkeli, M.; Makela, T.; Serimaa, R.; Ten Brinke, G.; Ikkala, O. *Science* **1998**, *280*, 557–560.
- (172) Ruokolainen, J.; Ten Brinke, G.; Ikkala, O. *Adv. Mater.* **1999**, *11*, 777–780.
- (173) Ruotsalainen, T.; Torkkeli, M.; Serimaa, R.; Maekelae, T.; Maeki-Ontto, R.; Ruokolainen, J.; Ten Brinke, G.; Ikkala, O. *Macromolecules* **2003**, *36*, 9437–9442.

- (174) van Ekenstein, G. A.; Polushkin, E.; Nijland, H.; Ikkala, O.; ten Brinke, G. *Macromolecules* **2003**, *36*, 3684–3688.
- (175) de Moel, K.; Alberda van Ekenstein, G. O. R.; Nijland, H.; Polushkin, E.; ten Brinke, G.; Maeki-Ontto, R.; Ikkala, O. *Chem. Mater.* **2001**, *13*, 4580–4583.
- (176) Knaapila, M.; Ikkala, O.; Torkkeli, M.; Jokela, K.; Serimaa, R.; Dolbnya, I. P.; Bras, W.; ten Brinke, G.; Horsburgh, L. E.; Palsson, L. O.; Monkman, A. P. *Appl. Phys. Lett.* **2002**, *81*, 1489–1491.
- (177) Hong, Y.; Miller, L. L. *Chem. Mater.* **1995**, *7*, 1999–2000.
- (178) Kunugi, Y.; Miller, L. L.; Maki, T.; Canavesi, A. *Chem. Mater.* **1997**, *9*, 1061–1062.
- (179) Jenekhe, S. A. *Macromolecules* **1990**, *23*, 2848–2854.
- (180) Donat-Bouillud, A.; Mazerolle, L.; Gagnon, P.; Goldenberg, L.; Petty, M. C.; Leclerc, M. *Chem. Mater.* **1997**, *9*, 2815–2821.
- (181) Henze, O.; Feast, W. J. *J. Mater. Chem.* **2003**, *13*, 1274–1278.
- (182) Kilbinger, A. F. M.; Feast, W. J. *J. Mater. Chem.* **2000**, *10*, 1777–1784.
- (183) Henze, O.; Fransen, M.; Jonkheijm, P.; Meijer, E. W.; Feast, W. J.; Schenning, A. P. H. J. *J. Polym. Sci., Part A: Polym. Chem.* **2003**, *41*, 1737–1743.
- (184) Cacialli, F.; Feast, W. J.; Friend, R. H.; de Jong, M.; Lovenich, P. W.; Salaneck, W. R. *Polymer* **2002**, *43*, 3555–3561.
- (185) Cacialli, F.; Friend, R. H.; Feast, W. J.; Lovenich, P. W. *Chem. Commun.* **2001**, 1778–1779.
- (186) Neuteboom, E. E.; Meskers, S. C. J.; Meijer, E. W.; Janssen, R. A. J. *Macromol. Chem. Phys.* **2004**, *205*, 217–222.
- (187) Neuteboom, E. E.; Janssen, R. A. J.; Meijer, E. W. *Synth. Met.* **2001**, *121*, 1283–1284.
- (188) Li, W.; Maddux, T.; Yu, L. *Macromolecules* **1996**, *29*, 7329–7334.
- (189) Hempenius, M. A.; Langeveld-Voss, B. M. W.; van Haare, J. A. E. H.; Janssen, R. A. J.; Sheiko, S. S.; Spatz, J. P.; Möller, M.; Meijer, E. W. *J. Am. Chem. Soc.* **1998**, *120*, 2798–2804.
- (190) Li, K.; Wang, Q. *Macromolecules* **2004**, *37*, 1172–1174.
- (191) Kukula, H.; Ziener, U.; Schöps, M.; Godt, A. *Macromolecules* **1998**, *31*, 5160–5163.
- (192) Chochos, C. L.; Tsolakis, P. K.; Gregoriou, V. G.; Kallitsis, J. K. *Macromolecules* **2004**, *37*, 2502–2510.
- (193) Tew, G. N.; Li, L.; Stupp, S. I. *J. Am. Chem. Soc.* **1998**, *120*, 5601–5602.
- (194) (a) Tew, G. N.; Pralle, M. U.; Stupp, S. I. *J. Am. Chem. Soc.* **1999**, *121*, 9852–9866. (b) Messmore, B. W.; Hulvat, J. F.; Sone, E. D.; Stupp, S. I. *J. Am. Chem. Soc.* **2004**, *126*, 14452–14458.
- (195) Pralle, M. U.; Urayama, K.; Tew, G. N.; Neher, D.; Wegner, G.; Stupp, S. I. *Angew. Chem., Int. Ed.* **2000**, *39*, 1486–1489.
- (196) Maddux, T.; Li, W.; Yu, L. *J. Am. Chem. Soc.* **1997**, *119*, 844–845.
- (197) Wang, H.; You, W.; Jiang, P.; Yu, L.; Wang, H. H. *Chem. Eur. J.* **2004**, *10*, 986–93.
- (198) Wang, H. H.; Wang, H.; Yu, L.; Thiagarajan, P. *J. Am. Chem. Soc.* **2000**, *122*, 6855–6861.
- (199) Urban, V.; Wang, H. H.; Thiagarajan, P.; Littrell, K. C.; Wang, H. B.; Yu, L. *J. Appl. Crystallogr.* **2000**, *33*, 645–649.
- (200) Li, W.; Wang, H.; Yu, L.; Morkved, T. L.; Jaeger, H. M. *Macromolecules* **1999**, *32*, 3034–3044.
- (201) Nawa, K.; Imae, I.; Noma, N.; Shiota, Y. *Macromolecules* **1995**, *28*, 723–729.
- (202) Imae, I.; Nawa, K.; Ohnsed, Y.; Noma, N.; Shiota, Y. *Macromolecules* **1997**, *30*, 380–386.
- (203) Ohnsed, Y.; Imae, I.; Shiota, Y. *J. Polym. Sci., Part B: Polym. Phys.* **2003**, *41*, 2471–2484.
- (204) Shiota, Y.; Jeon, I.-R.; Noma, N. *Synth. Met.* **1993**, *55–57*, 803–806.
- (205) Mastrorilli, P.; Nobile, C. F.; Grisorio, R.; Rizzutti, A.; Suranna, G. P.; Acienro, D.; Amendola, E.; Iannelli, P. *Macromolecules* **2004**, *37*, 4488–4495.
- (206) Schenning, A. P. H. J.; Fransen, M.; van Duren, J. K. J.; van Hal, P. A.; Janssen, R. A. J.; Meijer, E. W. *Macromol. Rapid Commun.* **2002**, *23*, 271–275.
- (207) Hayakawa, T.; Horiuchi, S. *Angew. Chem., Int. Ed.* **2003**, *42*, 2285–2289.
- (208) Hatano, T.; Bae, A.-H.; Takeuchi, M.; Fujita, N.; Kaneko, K.; Ihara, H.; Takafuji, M.; Shinkai, S. *Angew. Chem., Int. Ed.* **2004**, *43*, 465–469.
- (209) Smith, R. C.; Fisher, W. M.; Gin, D. L. *J. Am. Chem. Soc.* **1997**, *119*, 4092–4093.
- (210) Carswell, A. D. W.; O'Rear, E. A.; Grady, B. P. *J. Am. Chem. Soc.* **2003**, *125*, 14793–14800.
- (211) Wilson, J. N.; Bangcuyo, C. G.; Erdogan, B.; Myrick, M. L.; Bunz, U. H. F. *Macromolecules* **2003**, *36*, 1426–1428.
- (212) Merlo, J. A.; Frisbie, C. D. *J. Polym. Sci., Part B: Polym. Phys.* **2003**, *41*, 2674–2680.
- (213) Mas-Torrent, M.; Boer, D. d.; Durkut, M.; Hadley, P.; Schenning, A. P. H. J. *Nanotechnology* **2004**, *15*, S265–S269.
- (214) Kiriy, N.; Jähne, E.; Adler, H.-J.; Schneider, M.; Kiriy, A.; Gorodyska, G.; Minko, S.; Jehnichen, D.; Simon, P.; Fokin, A. A.; Stamm, M. *Nano Lett.* **2003**, *3*, 707–712.
- (215) (215) Kameoka, J.; Czaplewski, D.; Liu, H.; Craighead, H. G. *Nano Lett.* **2004**, *14*, 1503–1505.
- (216) Rikukawa, M.; Nakagawa, M.; Ishida, K.; Abe, H.; Sanui, K.; Ogata, N. *Thin Solid Films* **1996**, *285*, 636–635.
- (217) Rikukawa, M.; Nakagawa, M.; Abe, H.; Ishida, K.; Sanui, K.; Ogata, N. *Thin Solid Films* **1996**, *273*, 240–243.
- (218) Sluch, M. I.; Pearson, C.; Petty, M. C.; Halim, M.; Samuel, I. D. W. *Synth. Met.* **1998**, *94*, 285–289.
- (219) Breitenkamp, R. B.; Tew, G. N. *Macromolecules* **2004**, *37*, 1163–1165.
- (220) Kim, J.; Swager, T. M. *Nature* **2001**, *411*, 1030–1034.
- (221) Kim, J.; McHugh, S. K.; Swager, T. M. *Macromolecules* **1999**, *32*, 1500–1507.
- (222) Bjørnholm, T.; Greve, D. R.; Reitzel, N.; Hassenkam, T.; Kjaer, K.; Howes, P. B.; Larsen, N. B.; Bogelund, J.; Jayaraman, M.; Ebwank, P. C.; McCullough, R. D. *J. Am. Chem. Soc.* **1998**, *120*, 7643–7644.
- (223) Bjørnholm, T.; Hassenkam, T.; Greve, D. R.; McCullough, R. D.; Jayaraman, M.; Savoy, S. M.; Jones, C. E.; McDevitt, J. T. *Adv. Mater.* **1999**, *11*, 1218–1221.
- (224) Reitzel, N.; Greve, D. R.; Kjaer, K.; Howes, P. B.; Jayaraman, M.; Savoy, S.; McCullough, R. D.; McDevitt, J. T.; Bjørnholm, T. *J. Am. Chem. Soc.* **2000**, *122*, 5788–5800.
- (225) Boggild, P.; Grey, F.; Hassenkam, T.; Greve, D. R.; Bjørnholm, T. *Adv. Mater.* **2000**, *12*, 947–950.
- (226) Martin, R. E.; Diederich, F. *Adv. Mater.* **1999**, *38*, 1350–1377.
- (227) Tour, J. M. *Chem. Rev.* **1996**, *96*, 537–553.
- (228) Katz, H. E.; Bao, Z.; Gilat, S. L. *Acc. Chem. Res.* **2001**, *34*, 359–369.
- (229) Azumi, R.; Gotz, G.; Debaerdemaeker, T.; Bäuerle, P. *Chem. Eur. J.* **2000**, *6*, 735–744.
- (230) Samori, P.; Francke, V.; Müllen, K.; Rabe, J. P. *Chem. Eur. J.* **1999**, *5*, 2312–2317.
- (231) Gesquiere, A.; Jonkheijm, P.; Schenning, A. P. H. J.; Mena-Osteritz, E.; Bäuerle, P.; de Feyter, S.; de Schryver, F. C.; Meijer, E. W. *J. Mater. Chem.* **2003**, *13*, 2164–2167.
- (232) Wöhrl, D.; Kreinhoop, L.; Schnurpeil, G.; Elbe, J.; Tennigkeit, B.; Hiller, S.; Schlettwein, D. *J. Mater. Chem.* **1995**, *5*, 1819–1829.
- (233) Garnier, F.; Yasser, A.; Hajlaoui, R.; Horowitz, G.; Deloffre, F.; Servet, B.; Ries, S.; Alnot, P. *J. Am. Chem. Soc.* **1993**, *115*, 8716–8721.
- (234) Mushrush, M.; Facchetti, A.; Lefenfeld, M.; Katz, H. E.; Marks, T. J. *J. Am. Chem. Soc.* **2003**, *125*, 9414–9423.
- (235) Geens, W.; Tsamouras, D.; Poortmans, J.; Hadzioannou, G. *Synth. Met.* **2001**, *122*, 191–192.
- (236) Melucci, M.; Gazzano, M.; Barbarella, G.; Cavallini, M.; Biscarini, F.; Maccagnani, P.; Ostojá, P. *J. Am. Chem. Soc.* **2003**, *125*, 10266–10274.
- (237) van Hutton, P. F.; Wildeman, J.; Meetsma, A.; Hadzioannou, G. *J. Am. Chem. Soc.* **1999**, *121*, 5910–5918.
- (238) Funahashi, M.; Hanna, J. *Appl. Phys. Lett.* **2000**, *76*, 2574–2576.
- (239) Katz, H. E.; Laquindanum, J. G.; Lovinger, A. J. *Chem. Mater.* **1998**, *10*, 633–638.
- (240) Ponomarenko, S.; Kirchmeyer, S. *J. Mater. Chem.* **2003**, *13*, 197–202.
- (241) Azumi, R.; Gotz, G.; Bäuerle, P. *Synth. Met.* **1999**, *101*, 544–545.
- (242) Lovinger, A. J.; Katz, H. E.; Dodabalapur, A. *Chem. Mater.* **1998**, *10*, 3275–3277.
- (243) Garnier, F.; Hajlaoui, R.; El Kassami, A.; Horowitz, G.; Laigre, L.; Porzio, W.; Armanini, M.; Provasoli, F. *Chem. Mater.* **1998**, *10*, 3334–3339.
- (244) Gray, G. W.; Jones, B. *J. Chem. Soc., Abstract* **1955**, 236–44.
- (245) Hildebrandt, F.; Schröter, J. A.; Tschierske, C.; Festag, R.; Kleppinger, R.; Wendorff, J. H. *Angew. Chem., Int. Ed. Engl.* **1995**, *34*, 1631–1633.
- (246) Hildebrandt, F.; Schröter, J. A.; Tschierske, C.; Festag, R.; Wittenberg, M.; Wendorff, J. H. *Adv. Mater.* **1997**, *9*, 564–567.
- (247) Liu, P.; Nakano, H.; Shiota, Y. *Liq. Cryst.* **2001**, *28*, 581–589.
- (248) Schenning, A. P. H. J.; El-Ghazouri, A.; Peeters, E.; Meijer, E. W. *Synth. Met.* **2001**, *121*, 1253–1256.
- (249) Gill, R. E.; Meetsma, A.; Hadzioannou, G. *Adv. Mater.* **1996**, *8*, 212–214.
- (250) Eckert, J. F.; Nicoud, J. F.; Guillon, D.; Nierengarten, J. F. *Tetrahedron Lett.* **2000**, *41*, 6411–6414.
- (251) Eckert, J.-F.; Maciejczuk, U.; Guillon, D.; Nierengarten, J.-F. *Chem. Commun.* **2001**, 1278–1279.
- (252) Chandrasekhar, S.; Sadashiva, B. K.; Suresh, K. A. *Pramana* **1977**, *9*, 471–480.
- (253) Malthete, J.; Debraide, C.; Tinh, N. H.; Jacques, J. *Mol. Crystallogr. Liq. Crystallogr. Lett.* **1981**, *64*, 233–238.
- (254) Debraide, C.; Nguyen, H. T.; Gasparoux, H.; Malhtete, J.; Levelut, A. M. *Mol. Cryst. Liq. Cryst.* **1981**, *71*, 111–114.
- (255) Malthete, J.; Jacques, J.; Tinh, N. H.; Debraide, C. *Nature* **1982**, *298*, 46–48.
- (256) Adam, D.; Schuhmacher, P.; Simmerer, J.; Häussling, L.; Siemensemeyer, K.; Etzbach, K. H.; Ringsdorf, H.; Haarer, D. *Nature* **1994**, *371*, 141–143.

- (257) Van de Craats, A. M.; Warman, J. M.; De Haas, M. P.; Adam, D.; Simmerer, J.; Haarer, D.; Schuhmacher, P. *Adv. Mater.* **1996**, *8*, 823–826.
- (258) Boden, N.; Bushby, R. J.; Cooke, G.; Lozman, O. R.; Lu, Z. *J. Am. Chem. Soc.* **2001**, *123*, 7915–7916.
- (259) Pecchia, A.; Lozman, O. R.; Movaghbar, B.; Boden, N.; Bushby, R. J.; Donovan, K. J.; Kreouzis, T. *Phys. Rev. B* **2002**, *65*, 104204/1–104204/10.
- (260) Wegewijs, B. R.; Siebbeles, L. D. A.; Boden, N.; Bushby, R. J.; Movaghbar, B.; Lozman, O. R.; Liu, Q.; Pecchia, A.; Mason, L. A. *Phys. Rev. B* **2002**, *65*, 245112/1–245112/8.
- (261) Arikainen, E. O.; Boden, N.; Bushby, R. J.; Clements, J.; Movaghbar, B.; Wood, A. *J. Mater. Chem.* **1995**, *5*, 2161–2165.
- (262) Tang, B. Y.; Ge, J. J.; Zhang, A.; Calhoun, B.; Chu, P.; Wang, H.; Shen, Z.; Harris, F. W.; Cheng, S. Z. *D. Chem. Mater.* **2001**, *13*, 78–86.
- (263) Markovitsi, D.; Germain, A.; Millié, P.; Lécuyer, P.; Gallos, L.; Argyrakis, P.; Bengs, H.; Ringsdorf, H. *J. Phys. Chem.* **1995**, *99*, 1005–1017.
- (264) Senthilkumar, K.; Grozema, F. C.; Bickelhaupt, F. M.; Siebbeles, L. D. A. *J. Chem. Phys.* **2003**, *119*, 9809–9817.
- (265) Bengs, H.; Closs, F.; Frey, T.; Funhoff, D.; Ringsdorf, H.; Siemsmeyer, K. *Liq. Cryst.* **1993**, *15*, 565–574.
- (266) Van de Craats, A. M.; Warman, J. M.; Müllen, K.; Geerts, Y.; Brand, J. D. *Adv. Mater.* **1998**, *10*, 36–38.
- (267) van de Craats, A. M.; Warman, J. M. *Adv. Mater.* **2001**, *13*, 130–133.
- (268) Van De Craats, A. M.; Warman, J. M.; Fechtenkötter, A.; Brand, J. D.; Harbison, M. A.; Müllen, K. *Adv. Mater.* **1999**, *11*, 1469–1472.
- (269) Lemaire, V.; da Silva Filho, D. A.; Coropceanu, V.; Lehmann, M.; Geerts, Y.; Piris, J.; Debije, M. G.; van de Craats, A. M.; Senthilkumar, K.; Siebbeles, L. D. A.; Warman, J. M.; Brédas, J.-L.; Cornil, J. *J. Am. Chem. Soc.* **2004**, *126*, 3271–3279.
- (270) Berresheim, A. J.; Müller, M.; Müllen, K. *Chem. Rev.* **1999**, *99*, 1747–1785.
- (271) Herwig, P.; Kayser, C. W.; Müllen, K.; Spiess, H. W. *Adv. Mater.* **1996**, *8*, 510–513.
- (272) Fechtenkötter, A.; Tchebotareva, N.; Watson, M.; Müllen, K. *Tetrahedron* **2001**, *57*, 3769–3783.
- (273) Fechtenkötter, A.; Saalwächter, K.; Harbison, M. A.; Müllen, K.; Spiess, H. W. *Angew. Chem., Int. Ed. Engl.* **1999**, *38*, 3039–3042.
- (274) Liu, C.-y.; Bard, A. J. *Chem. Mater.* **2000**, *12*, 2353–2363.
- (275) van de Craats, A. M.; Stutzmann, N.; Bunk, O.; Nielsen, M. M.; Watson, M.; Müllen, K.; Chanzy, H. D.; Sirringhaus, H.; Friend, R. H. *Adv. Mater.* **2003**, *15*, 495–499.
- (276) Piris, J.; Debije, M. G.; Stutzmann, N.; van de Craats, A. M.; Watson, M. D.; Müllen, K.; Warman, J. M. *Adv. Mater.* **2003**, *15*, 1736–1740.
- (277) Tracz, A.; Jeszka, J. K.; Watson, M. D.; Pisula, W.; Müllen, K.; Pakula, T. *J. Am. Chem. Soc.* **2003**, *125*, 1682–1683.
- (278) Fleming, A. J.; Coleman, J. N.; Dalton, A. B.; Fechtenkoetter, A.; Watson, M. D.; Müllen, K.; Byrne, H. J.; Blau, W. J. *J. Phys. Chem. B* **2003**, *107*, 37–43.
- (279) Wu, J.; Watson, M. D.; Zhang, L.; Wang, Z.; Müllen, K. *J. Am. Chem. Soc.* **2004**, *126*, 177–186.
- (280) Schlichting, P.; Rohr, U.; Müllen, K. *J. Mater. Chem.* **1998**, *8*, 2651–2655.
- (281) Rohr, U.; Schlichting, P.; Bohm, A.; Gross, M.; Meerholz, K.; Brauchle, C.; Müllen, K. *Angew. Chem., Int. Ed. Engl.* **1998**, *37*, 1434–1437.
- (282) Göltner, C.; Pressner, D.; Müllen, K.; Spiess, H. W. *Angew. Chem., Int. Ed. Engl.* **1993**, *32*, 1660–1662.
- (283) Pressner, D.; Göltner, C.; Spiess, H. W.; Müllen, K. *Acta Polym.* **1994**, *45*, 188–95.
- (284) Müller, G. R. J.; Meiners, C.; Enkelmann, V.; Geerts, Y.; Müllen, K. *J. Mater. Chem.* **1998**, *8*, 61–64.
- (285) Rohr, U.; Kohl, C.; Müllen, K.; van de Craats, A.; Warman, J. J. *Mater. Chem.* **2001**, *11*, 1789–1799.
- (286) Liu, S.-G.; Sui, G.; Cormier, R. A.; Leblanc, R. M.; Gregg, B. A. *J. Phys. Chem. B* **2002**, *106*, 1307–1315.
- (287) Cormier, R. A.; Gregg, B. A. *Chem. Mater.* **1998**, *10*, 1309–1319.
- (288) Würthner, F.; Thalacker, C.; Diele, S.; Tschiesske, C. *Chem. Eur. J.* **2001**, *7*, 2245–2253.
- (289) Sautter, A.; Thalacker, C.; Würthner, F. *Angew. Chem., Int. Ed.* **2001**, *40*, 4425–4428.
- (290) Struijk, C. W.; Sieval, A. B.; Dakhorst, J. E. J.; van Dijk, M.; Kimkes, P.; Koehorst, R. B. M.; Donker, H.; Schaafsmma, T. J.; Picken, S. J.; van de Craats, A. M.; Warman, J. M.; Zuilhof, H.; Sudholter, E. J. R. *J. Am. Chem. Soc.* **2000**, *122*, 11057–11066.
- (291) Katz, H. E.; Lovering, A. J.; Johnson, J.; Kloc, C.; Siegrist, T.; Li, W.; Lin, Y.-Y.; Dodabalapur, A. *Nature* **2000**, *404*, 478–480.
- (292) Guan, Y.; Zakrevskyy, Y.; Stumpe, J.; Antonietti, M.; Faul, C. F. *J. Chem. Commun.* **2003**, 894–895.
- (293) Facchetti, A.; Mushrush, M.; Katz, H. E.; Marks, T. J. *Adv. Mater.* **2003**, *15*, 33–38.
- (294) Facchetti, A.; Yoon, M.-H.; Stern, C. L.; Katz, H. E.; Marks, T. J. *Angew. Chem., Int. Ed.* **2003**, *42*, 3900–3903.
- (295) Lee, C.-H.; Yamamoto, T. *Mol. Cryst. Liq. Cryst. Sci. Technol., Sect A* **2002**, *378*, 13–21.
- (296) Lee, C. H.; Yamamoto, T. *Tetrahedron Lett.* **2001**, *42*, 3993–3996.
- (297) Attias, A.-J.; Cavalli, C.; Donnio, B.; Guillot, D.; Hapiot, P.; Malthete, J. *Chem. Mater.* **2002**, *14*, 375–384.
- (298) Pieterse, K.; Lauritsen, A.; Schenning, A. P. H. J.; Vekemans, J. A. J. M.; Meijer, E. W. *Chem. Eur. J.* **2003**, *9*, 5597–5604.
- (299) Bock, H.; Babeau, A.; Seguy, I.; Jolinat, P.; Destreul, P. *Chem. Phys. Chem.* **2002**, *3*, 532–535.
- (300) Kestemont, G.; de Halleux, V.; Lehmann, M.; Ivanov, D. A.; Watson, M.; Geerts, Y. H. *Chem. Commun.* **2001**, 2074–2075.
- (301) Pieterse, K.; van Hal, P. A.; Kleppinger, R.; Vekemans, J. A. J. M.; Janssen, R. A. J.; Meijer, E. W. *Chem. Mater.* **2001**, *13*, 2675–2679.
- (302) Kumar, S.; Wachtel, E. J.; Keinan, E. *J. Org. Chem.* **1993**, *58*, 3821–3827.
- (303) Boden, N.; Borner, R. C.; Bushby, R. J.; Clements, J. *J. Am. Chem. Soc.* **1994**, *116*, 10807–10808.
- (304) Kumar, S.; Shankar Rao, D. S.; Krishna Prasad, S. *J. Mater. Chem.* **1999**, *9*, 2751–2754.
- (305) Gearba, R. I.; Lehmann, M.; Levin, J.; Ivanov, D. A.; Koch, M. H. J.; Barbera, J.; Debije, M. G.; Piris, J.; Geerts, Y. H. *Adv. Mater.* **2003**, *15*, 1614–1618.
- (306) Chuard, T.; Deschenaux, R. *Helv. Chim. Acta* **1996**, *79*, 736–741.
- (307) Chuard, T.; Deschenaux, R.; Hirsch, A.; Schönberger, H. *Chem. Commun.* **1999**, 2103–2104.
- (308) Tirelli, N.; Cardullo, F.; Habicher, T.; Suter, U. W.; Diederich, F. *J. Chem. Soc., Perkin Trans.* **2000**, *2*, 193–198.
- (309) Felder, D.; Heinrich, B.; Guillot, D.; Nicoud, J. F.; Nierengarten, J. F. *Eur. J. Org. Chem.* **2000**, *6*, 3501–3507.
- (310) Dardel, S.; Guillot, D.; Heinrich, B.; Deschenaux, R. *J. Mater. Chem.* **2001**, *11*, 2814–2831.
- (311) (a) Chuard, T.; Deschenaux, R. *J. Mater. Chem.* **2002**, *12*, 1944–1951. (b) Sawamura, M.; Kawai, K.; Matsuo, Y.; Kanie, K.; Kato, T.; Nakamura, E. *Nature* **2002**, *419*, 702–705.
- (312) Terech, P.; Weiss, R. G. *Chem. Rev.* **1997**, *97*, 3133–3159.
- (313) Van Esch, J. H.; Feringa, B. L. *Angew. Chem., Int. Ed.* **2000**, *39*, 2263–2266.
- (314) Ito, S.; Wehmeier, M.; Brand, J. D.; Kubel, C.; Epsch, R.; Rabe, J. P.; Müllen, K. *Chem. Eur. J.* **2000**, *6*, 4327–4342.
- (315) Grimsdale, A. C.; Bauer, R.; Weil, T.; Tchebotareva, N.; Wu, J. S.; Watson, M.; Müllen, K. *Synthesis* **2002**, 1229–1238.
- (316) Reitzel, N.; Hassenkam, T.; Balashev, K.; Jensen, T. R.; Howes, P. B.; Kjaer, K.; Fechtenkötter, A.; Tchebotareva, N.; Ito, S.; Müllen, K.; Bjørnholm, T. *Chem. Eur. J.* **2001**, *7*, 4894.
- (317) Kubowicz, S.; Pietsch, U.; Watson, M. D.; Tchebotareva, N.; Müllen, K.; Thünemann, A. F. *Langmuir* **2003**, *19*, 5036–5041.
- (318) Thünemann, A. F.; Ruppelt, D.; Ito, S.; Müllen, K. *J. Mater. Chem.* **1999**, *9*, 1055–1057.
- (319) Thünemann, A. F.; Ruppelt, D.; Burger, C.; Müllen, K. *J. Mater. Chem.* **2000**, *10*, 1325–1329.
- (320) Faul, C. F. J.; Antonietti, M. *Adv. Mater.* **2003**, *15*, 673–683.
- (321) Mizoshita, N.; Monobe, H.; Inoue, M.; Ukon, M.; Watanabe, T.; Shimizu, Y.; Hanabusa, K.; Kato, T. *Chem. Commun.* **2002**, 428–429.
- (322) Thünemann, A. F.; Kubowicz, S.; Burger, C.; Watson, M. D.; Tchebotareva, N.; Müllen, K. *J. Am. Chem. Soc.* **2003**, *125*, 352–356.
- (323) Desvergne, J.-P.; Brotin, T.; Meerschaut, D.; Clavier, G.; Placine, F.; Pozzo, J.-L.; Bouas-Laurent, H. *New J. Chem.* **2004**, *28*, 234–243.
- (324) Terech, P.; Meerschaut, D.; Desvergne, J. P.; Colomes, M.; Bouas-Laurent, H. *J. Colloid Interface Sci.* **2003**, *261*, 441–450.
- (325) Placine, F.; Desvergne, J. P.; Belin, C.; Buffeteau, T.; Desbat, B.; Ducasse, L.; Lassegues, J.-C. *Langmuir* **2003**, *19*, 4563–4572.
- (326) Kato, T.; Kutsuna, T.; Yabuuchi, K.; Mizoshita, N. *Langmuir* **2002**, *18*, 7086–7088.
- (327) Pozzo, J.-L.; Desvergne, J.-P.; Clavier, G. M.; Bouas-Laurent, H.; Jones, P. G.; Perlstein, J. *J. Chem. Soc., Perkin Trans. 2* **2001**, 824–826.
- (328) Placine, F.; Desvergne, J. P.; Lassegues, J. C. *Chem. Mater.* **2001**, *13*, 117–121.
- (329) Terech, P.; Bouas-Laurent, H.; Desvergne, J.-P. *J. Colloid Interface Sci.* **1995**, *174*, 258–263.
- (330) Brotin, T.; Utermohlen, R.; Fages, F.; Bouas-Laurent, H.; Desvergne, J. P. *J. Chem. Soc., Chem. Commun.* **1991**, 416–418.
- (331) Kawano, S.-i.; Tamaru, S.-i.; Fujita, N.; Shinkai, S. *Chem. Eur. J.* **2004**, *10*, 343–351.
- (332) Shirakawa, M.; Kawano, S.; Fujita, N.; Sada, K.; Shinkai, S. *J. Org. Chem.* **2003**, *68*, 5037–5044.
- (333) Hatano, T.; Takeuchi, M.; Ikeda, A.; Shinkai, S. *Chem. Lett.* **2003**, *32*, 314–315.
- (334) Hatano, T.; Takeuchi, M.; Ikeda, A.; Shinkai, S. *Org. Lett.* **2003**, *5*, 1395–1398.
- (335) Tamaru, S.-i.; Uchino, S.-y.; Takeuchi, M.; Ikeda, M.; Hatano, T.; Shinkai, S. *Tetrahedron Lett.* **2002**, *43*, 3751–3755.

- (336) Tamaru, S.-i.; Takeuchi, M.; Sano, M.; Shinkai, S. *Angew. Chem., Int. Ed.* **2002**, *41*, 853–856.
- (337) Tamaru, S.-i.; Nakamura, M.; Takeuchi, M.; Shinkai, S. *Org. Lett.* **2001**, *3*, 3631–3634.
- (338) Arimori, S.; Takeuchi, M.; Shinkai, S. *Supramol. Sci.* **1998**, *5*, 1–8.
- (339) de Witte, P. A. J.; Castricano, M.; Cornelissen, J. J. L. M.; Scolaro, L. M.; Nolte, R. J. M.; Rowan, A. E. *Chem. Eur. J.* **2003**, *9*, 1775–1781.
- (340) Lensen, M. C.; Castricano, M.; Coumans, R. G. E.; Foekema, J.; Rowan, A. E.; Scolaro, L. M.; Nolte, R. J. M. *Tetrahedron Lett.* **2002**, *43*, 9351–9355.
- (341) Samori, P.; Engelkamp, H.; de Witte, P.; Rowan, A. E.; Nolte, R. J. M.; Rabe, J. P. *Angew. Chem., Int. Ed.* **2001**, *40*, 2348–2350.
- (342) van der Boom, T.; Hayes, R. T.; Zhao, Y.; Bushard, P. J.; Weiss, E. A.; Wasielewski, M. R. *J. Am. Chem. Soc.* **2002**, *124*, 9582–9590.
- (343) Lensen, M. C.; Takazawa, K.; Elemans, J. A. A. W.; Jeukens, C. R. L. P. N.; Christianen, P. C. M.; Maan, J. C.; Rowan, A. E.; Nolte, R. J. M. *Chem. Eur. J.* **2004**, *10*, 831–839.
- (344) De La Escosura, A.; Martinez-Diaz, M. V.; Thordarson, P.; Rowan, A. E.; Nolte, R. J. M.; Torres, T. *J. Am. Chem. Soc.* **2003**, *125*, 12300–12308.
- (345) Boamfa, M. I.; Christianen, P. C. M.; Maan, J. C.; Engelkamp, H.; Nolte, R. J. M. *Physica B* **2001**, *294&295*, 343–346.
- (346) Engelkamp, H.; Middelbeek, S.; Nolte, R. J. M. *Science* **1999**, *284*, 785–788.
- (347) van Nostrum, C. F.; Picken, S. J.; Schouten, A.-J.; Nolte, R. J. M. *J. Am. Chem. Soc.* **1995**, *117*, 9957–9965.
- (348) Blanzat, B.; Barthou, C.; Tercier, N.; Andre, J. J.; Simon, J. J. *Am. Chem. Soc.* **1987**, *109*, 6193–6194.
- (349) Zlatkin, A.; Yudin, S.; Simon, J.; Hanack, M.; Lehman, H. *Adv. Mater. Opt. Electron.* **1995**, *5*, 259–263.
- (350) Engel, M. K.; Bassoul, P.; Bosio, L.; Lehmann, H.; Hanack, M.; Simon, J. *Liq. Cryst.* **1993**, *15*, 709–722.
- (351) Sirlin, C.; Bosio, L.; Simon, J. *J. Chem. Soc., Chem. Commun.* **1988**, 236–237.
- (352) Sirlin, C.; Bosio, L.; Simon, J.; Ahsen, V.; Yilmazer, E.; Bekaroglu, O. *Chem. Phys. Lett.* **1987**, *139*, 362–364.
- (353) Würthner, F.; Yao, S.; Beginn, U. *Angew. Chem., Int. Ed.* **2003**, *42*, 3247–3250.
- (354) von Berlepsch, H.; Böttcher, C.; Dähne, L. *J. Phys. Chem. B* **2000**, *104*, 8792–8799.
- (355) Würthner, F.; Yao, S.; Beginn, U. *Angew. Chem., Int. Ed.* **2003**, *42*, 3247–3250.
- (356) Würthner, F.; Yao, S. *J. Org. Chem.* **2003**, *68*, 8943–8949.
- (357) Wortmann, R.; Rosch, U.; Redi-Abshiro, M.; Würthner, F. *Angew. Chem., Int. Ed.* **2003**, *42*, 2080–2083.
- (358) Würthner, F.; Yao, S.; Debaerdemaecker, T.; Wortmann, R. *J. Am. Chem. Soc.* **2002**, *124*, 9431–9447.
- (359) Würthner, F.; Yao, S.; Schilling, J.; Wortmann, R.; Redi-Abshiro, M.; Mecher, E.; Gallego-Gomez, F.; Meerholz, K. *J. Am. Chem. Soc.* **2001**, *123*, 2810–2824.
- (360) Würthner, F.; Yao, S.; Heise, B.; Tschierske, C. *Chem. Commun.* **2001**, 2260–2261.
- (361) Prins, L. J.; Thalacker, C.; Würthner, F.; Timmerman, P.; Reinoudt, D. N. *PNAS* **2001**, *98*, 10042–10045.
- (362) Würthner, F.; Yao, S. *Angew. Chem., Int. Ed.* **2000**, *39*, 1978–1981.
- (363) Babu, P.; Sangeetha, N. M.; Vijaykumar, P.; Maitra, U.; Risisanen, K.; Raju, A. R. *Chem. Eur. J.* **2003**, *9*, 1922–1932.
- (364) Geiger, C.; Stanescu, M.; Chen, L.; Whitten, D. G. *Langmuir* **1999**, *15*, 2241–2245.
- (365) Chen, H.; Farahat, M. S.; Law, K.-Y.; Whitten, D. G. *J. Am. Chem. Soc.* **1996**, *118*, 2584–2594.
- (366) Chen, H.; Law, K.-Y.; Perlstein, J.; Whitten, D. G. *J. Am. Chem. Soc.* **1995**, *117*, 7257–7258.
- (367) Wang, R.; Geiger, C.; Chen, L.; Swanson, B.; Whitten, D. G. *J. Am. Chem. Soc.* **2000**, *122*, 2399–2400.
- (368) Whitten, D. G.; Chen, L.; Geiger, H. C.; Perlstein, J.; Song, X. *J. Phys. Chem. B* **1998**, *102*, 10098–10111.
- (369) Ajayaghosh, A.; George, S. *J. J. Am. Chem. Soc.* **2001**, *123*, 5148–5149.
- (370) Schoonbeek, F. S.; Van Esch, J. H.; Wegewijs, B.; Rep, D. B. A.; De Haas, M. P.; Klapwijk, T. M.; Kellogg, R. M.; Feringa, B. L. *Angew. Chem., Int. Ed. Engl.* **1999**, *38*, 1393–1397.
- (371) Rep, D. B. A.; Roelfsema, R.; Van Esch, J. H.; Schoonbeek, F. S.; Kellogg, R. M.; Feringa, B. L.; Palstra, T. T. M.; Klapwijk, T. M. *Adv. Mater.* **2000**, *12*, 563–566.
- (372) Gesquière, A.; Abdel-Mottaleb, M. M. S.; De Feyter, S.; De Schryver, F. C.; Schoonbeek, F.; van Esch, J.; Kellogg, R. M.; Feringa, B. L.; Calderone, A.; Lazzaroni, R.; Brédas, J.-L. *Langmuir* **2000**, *16*, 10385–10391.
- (373) Gesquière, A.; De Feyter, S.; De Schryver, F. C.; Schoonbeek, F.; van Esch, J.; Kellogg, R. M.; Feringa, B. L. *Nano Lett.* **2001**, *1*, 201–206.
- (374) El-Ghayoury, A.; Schenning, A. P. H. J.; Meijer, E. W. *J. Polym. Sci., Part A: Polym. Chem.* **2002**, *40*, 4020–4023.
- (375) Dobrawa, R.; Würthner, F. *Chem. Commun.* **2002**, 1878–1879.
- (376) Havinga, E. E.; Rotte, I. *Mol. Cryst. Liq. Cryst.* **1992**, *218*, 1–3.
- (377) DiCésare, N.; Belletête, M.; Marrano, C.; Leclerc, M.; Durocher, G. *J. Phys. Chem. A* **1999**, *103*, 795–802.
- (378) Martin, S. J.; Cadby, A. J.; Lane, P. A.; Bradley, D. D. C. *Synth. Met.* **1999**, *101*, 665–666.
- (379) Pope, M.; Swenberg, C. E. *Electronic Processes in Organic Crystals*; Clarendon Press: Oxford, 1982.
- (380) Davydov, A. S. *Theory of Molecular Excitons*; McGraw-Hill: New York, 1962.
- (381) Malenfant, P. R. L.; Groenendaal, L.; Fréchet, J. M. J. *J. Am. Chem. Soc.* **1998**, *120*, 10990–10991.
- (382) Jestin, I.; Levillain, E.; Roncali, J. *Chem. Commun.* **1998**, 2655–2656.
- (383) Miller, L. L.; Zinger, B.; Schlechte, J. S. *Chem. Mater.* **1999**, *11*, 2313–2315.
- (384) Miller, L. L.; Schlechte, J. S.; Zinger, B.; Burrell, C. J. *Chem. Mater.* **2002**, *14*, 5081–5089.
- (385) Apperloo, J. J.; Janssen, R. A. J.; Malenfant, P. R. L.; Fréchet, J. M. J. *Macromolecules* **2000**, *33*, 7038–7043.
- (386) Apperloo, J. J.; Malenfant, P. R. L.; Fréchet, J. M. J.; Janssen, R. A. J. *Synth. Met.* **2001**, *121*, 1259–1260.
- (387) Apperloo, J. J.; Janssen, R. A. J.; Malenfant, P. R. L.; Fréchet, J. M. J. *J. Am. Chem. Soc.* **2001**, *123*, 6916–6924.
- (388) Lee, M.; Jeong, Y.-S.; Cho, B.-K.; Oh, N.-K.; Zin, W.-C. *Chem. Eur. J.* **2002**, *8*, 876–883.
- (389) Locklin, J.; Youk, J. H.; Xia, C.; Park, M.-K.; Fan, X.; Advincula, R. C. *Langmuir* **2002**, *18*, 877–883.
- (390) Xia, C.; Locklin, J.; Youk, J. H.; Fulghum, T.; Advincula, R. C. *Langmuir* **2002**, *18*, 955–957.
- (391) Schenning, A. P. H. J.; Jonkheijm, P.; Hofkens, J.; De Feyter, S.; Asavel, T.; Cotlet, M.; De Schryver, F. C.; Meijer, E. W. *Chem. Commun.* **2002**, 1264–1265.
- (392) Sandberg, H.; Henze, O.; Kilbinger, A. F. M.; Sirringhaus, H.; Feast, W. J.; Friend, R. H. *Synth. Met.* **2003**, *137*, 885–886.
- (393) Leclère, Ph.; Surin, M.; Jonkheijm, P.; Henze, O.; Schenning, A. P. H. J.; Biscarini, F.; Grimsdale, A. C.; Feast, W. J.; Meijer, E. W.; Müllen, K.; Brédas, J.-L.; Lazzaroni, R. *Eur. Polym. J.* **2004**, *40*, 885–892.
- (394) Schenning, A. P. H. J.; Kilbinger, A. F. M.; Biscarini, F.; Cavallini, M.; Cooper, H. J.; Derrick, P. J.; Feast, W. J.; Lazzaroni, R.; Leclère, Ph.; McDonnell, L. A.; Meijer, E. W.; Meskers, S. C. J. *J. Am. Chem. Soc.* **2002**, *124*, 1269–1275.
- (395) Kilbinger, A. F. M.; Schenning, A. P. H. J.; Goldoni, F.; Feast, W. J.; Meijer, E. W. *J. Am. Chem. Soc.* **2000**, *122*, 1820–1821.
- (396) Kilbinger, A. F. M.; Feast, W. J.; Cooper, H. J.; McDonnell, L. A.; Derrick, P. J.; Schenning, A. P. H. J.; Meijer, E. W. *Chem. Commun.* **2000**, *383*–384.
- (397) Jiang, L.; Hughes, R. C.; Sasaki, D. Y. *Chem. Commun.* **2004**, 1028–1029.
- (398) Arnaud, A.; Belleneij, J.; Boue, F.; Bouteiller, L.; Carrot, G.; Wintgens, V. *Angew. Chem., Int. Ed.* **2004**, *43*, 1718–1721.
- (399) Gaylord, B. S.; Wang, S.; Heeger, A. J.; Bazan, G. C. *J. Am. Chem. Soc.* **2001**, *123*, 6417–6418.
- (400) Xiong, H.; Qin, L.; Sun, J.; Zhang, X.; Shen, J. *Chem. Lett.* **2000**, *35*, 586–587.
- (401) Jonkheijm, P.; Fransen, M.; Schenning, A. P. H. J.; Meijer, E. W. *J. Chem. Soc., Perkin Trans. 1* **2001**, 1280–1286.
- (402) Peeters, E.; Janssen, R. A. J.; Meskers, S. C. J.; Meijer, E. W. *Polym. Prepr.* **1999**, *40*, 519–520.
- (403) Yoo, Y.-S.; Choi, J.-H.; Song, J.-H.; Oh, N.-K.; Zin, W.-C.; Park, S.; Chang, T.; Lee, M. *J. Am. Chem. Soc.* **2004**, *126*, 6294–6300.
- (404) Brunsdorf, L.; Folmer, B. J. B.; Meijer, E. W.; Sijbesma, R. P. *Chem. Rev.* **2001**, *101*, 4071–4097.
- (405) El-Ghayoury, A.; Schenning, A. P. H. J.; Van Hal, P. A.; Van Duren, J. K. J.; Janssen, R. A. J.; Meijer, E. W. *Angew. Chem., Int. Ed.* **2001**, *40*, 3660–3663.
- (406) El-Ghayoury, A.; Peeters, E.; Schenning, A. P. H. J.; Meijer, E. W. *Chem. Commun.* **2000**, 1969–1970.
- (407) Sivakova, S.; Rowan, S. *J. Chem. Commun.* **2003**, 2428–2429.
- (408) Balogh, D. T.; Dhanabalan, A.; Dynarowicz-Latka, P.; Schenning, A. P. H. J.; Oliveira, O. N., Jr.; Meijer, E. W.; Janssen, R. A. J. *Langmuir* **2001**, *17*, 3281–3285.
- (409) Jonkheijm, P.; Miura, A.; Zdanowska, M.; Hoeben, F. J. M.; De Feyter, S.; Schenning, A. P. H. J.; De Schryver, F. C.; Meijer, E. W. *Angew. Chem., Int. Ed.* **2004**, *43*, 74–78.
- (410) Kimizuka, N.; Kunitake, T. *J. Am. Chem. Soc.* **1989**, *111*, 3758–3759.
- (411) Kimizuka, N.; Kawasaki, T.; Hirata, K.; Kunitake, T. *J. Am. Chem. Soc.* **1995**, *117*, 6360–6361.
- (412) Würthner, F.; Thalacker, C.; Sautter, A. *Adv. Mater.* **1999**, *11*, 754–758.
- (413) Würthner, F.; Thalacker, C.; Sautter, A.; Schartl, W.; Ibach, W.; Hollricher, O. *Chem. Eur. J.* **2000**, *6*, 3871–3886.
- (414) Thalacker, C.; Würthner, F. *Adv. Funct. Mater.* **2002**, *12*, 209–218.
- (415) Sijbesma, R. P.; Meijer, E. W. *Curr. Opin. Colloid Interface Sci.* **1999**, *4*, 24–32.

- (416) Jonkheijm, P.; Hoeben, F. J. M.; Kleppinger, R.; Van Herrikhuizen, J.; Schenning, A. P. H. J.; Meijer, E. W. *J. Am. Chem. Soc.* **2003**, *125*, 15941–15949.
- (417) Schenning, A. P. H. J.; Jonkheijm, P.; Peeters, E.; Meijer, E. W. *J. Am. Chem. Soc.* **2001**, *123*, 409–416.
- (418) Herz, L. M.; Daniel, C.; Silva, C.; Hoeben, F. J. M.; Schenning, A. P. H. J.; Meijer, E. W.; Friend, R. H.; Phillips, R. T. *Phys. Rev. B* **2003**, *68*, 045203/1–045203/7.
- (419) Daniel, C.; Herz, L. M.; Silva, C.; Hoeben, F. J. M.; Jonkheijm, P.; Schenning, A. P. H. J.; Meijer, E. W. *Phys. Rev. B* **2003**, *68*, 235212/1–235212/9.
- (420) Hirschberg, J. H. K. K.; Brunsved, L.; Ramzi, A.; Vekemans, J. A. J. M.; Sijbesma, R. P.; Meijer, E. W. *Nature* **2000**, *407*, 167–170.
- (421) Sessler, J. L.; Wang, B.; Harriman, A. *J. Am. Chem. Soc.* **1995**, *117*, 704–714.
- (422) Beckers, E. H. A.; van Hal, P. A.; Schenning, A. P. H. J.; El-Ghazouri, A.; Peeters, E.; Rispens, M. T.; Hummelen, J. C.; Meijer, E. W.; Janssen, R. A. J. *J. Mater. Chem.* **2002**, *12*, 2054–2060.
- (423) Rispens, M. T.; Sanchez, L.; Beckers, E. H. A.; van Hal, P. A.; Schenning, A. P. H. J.; Abdulkrim, E.-G.; Peeters, E.; Meijer, E. W.; Janssen, R. A. J.; Hummelen, J. C. *Synth. Met.* **2003**, *135*–136, 801–803.
- (424) Würthner, F.; Sautter, A. *Org. Biomol. Chem.* **2003**, *1*, 240–243.
- (425) Araki, K.; Losco, P.; Engelmann, F. M.; Winnischöfer, H.; Toma, H. E. *J. Photochem. Photobiol. A* **2001**, *142*, 25–30.
- (426) Di Casa, M.; Fabbrizzi, L.; Licchelli, M.; Poggi, A.; Russo, A.; Taglietti, A. *Chem. Commun.* **2001**, 825–826.
- (427) Dixon, I. M.; Collin, J.-P.; Sauvage, J.-P.; Flamigni, L. *Inorg. Chem.* **2001**, *40*, 5507–5517.
- (428) Guldi, D. M.; Da Ros, T.; Braiuca, P.; Prato, M.; Alessio, E. *J. Mater. Chem.* **2002**, *12*, 2001–2008.
- (429) Loiseau, F.; Marzannini, G.; Quici, S.; Indelli, M. T.; Campagna, S. *Chem. Commun.* **2003**, 286–287.
- (430) Kohn, F.; Hofkens, J.; Wiesler, U.-M.; Cotlet, M.; van der Auweraer, M.; Müllen, K.; de Schryver, F. C. *Chem. Eur. J.* **2001**, *7*, 4126–4133.
- (431) Stork, M.; Gaylord, B. S.; Heeger, A. J.; Bazan, G. C. *Adv. Mater.* **2002**, *14*, 361–366.
- (432) Yamazaki, T.; Yamazaki, I.; Osuka, A. *J. Phys. Chem. B* **1998**, *102*, 7858–7865.
- (433) Grieser, F.; Thistletonwaite, P.; Triandos, P. *Langmuir* **1987**, *3*, 1173–1175.
- (434) Shimomura, M.; Karthaus, O.; Ijiro, K. *Synth. Met.* **1996**, *81*, 251–257.
- (435) Komatsu, T.; Moritake, M.; Tsuchida, E. *Chem. Eur. J.* **2003**, *9*, 4626–4633.
- (436) Schenning, A. P. H. J.; Peeters, E.; Meijer, E. W. *J. Am. Chem. Soc.* **2000**, *122*, 4489–4495.
- (437) Beeck, W. J. E.; Janssen, R. A. J. *Adv. Funct. Mater.* **2002**, *12*, 519–525.
- (438) Montalti, M.; Prodi, L.; Zuccheroni, N.; Zattoni, A.; Reschiglian, P.; Falini, G. *Langmuir* **2004**, *20*, 2989–2991.
- (439) Gfeller, N.; Calzaferri, G. *J. Phys. Chem. B* **1997**, *101*, 1396–1408.
- (440) Bongiovanni, G.; Botta, C.; Di Silvestro, G.; Loi, M. A.; Mura, A.; Tubino, R. *Chem. Phys. Lett.* **2001**, *345*, 386–394.
- (441) Calzaferri, G.; Pauchard, M.; Maas, H.; Huber, S.; Khatyr, A.; Schaafsma, T. *J. Mater. Chem.* **2002**, *12*, 1–13.
- (442) Yonezawa, Y. *Rec. Res. Dev. Pure Appl. Chem.* **1998**, *2*, 157–178.
- (443) van Burgel, M.; Wiersma, D. A.; Duppen, K. *J. Chem. Phys.* **1995**, *102*, 20–33.
- (444) Moll, J.; Dähne, S.; Durrant, J. R.; Wiersma, D. A. *J. Chem. Phys.* **1995**, *102*, 6362–6370.
- (445) Sakomura, M.; Takagi, T.; Nakayama, H.; Sawada, R.; Fujihira, M. *Colloid Surf., A* **2002**, *198*–*200*, 769–775.
- (446) Yonezawa, Y.; Fukumoto, H. *Synth. Met.* **1997**, *91*, 147–150.
- (447) Kometani, N.; Nakajima, H.; Asami, K.; Yonezawa, Y.; Kajimoto, O. *Chem. Phys. Lett.* **1998**, *294*, 619–624.
- (448) Kometani, N.; Nakajima, H.; Asami, K.; Yonezawa, Y.; Kajimoto, O. *J. Phys. Chem. B* **2000**, *104*, 9630–9637.
- (449) Bliznyuk, V.; Möhwald, H. *Thin Solid Films* **1995**, *261*, 275–279.
- (450) Yonezawa, Y.; Ishizawa, H. *J. Lumin.* **1996**, *69*, 141–150.
- (451) Pescatore, J. A., Jr.; Yamazaki, I. *J. Phys. Chem.* **1996**, *100*, 13333–13337.
- (452) Ishizawa, H.; Sato, T.; Sluch, M. I.; Vitukhnovsky, A. G.; Yonezawa, Y. *Thin Solid Films* **1996**, *284*–*285*, 134–137.
- (453) Yonezawa, Y.; Ishizawa, H. *J. Lumin.* **1997**, *72*–*74*, 555–556.
- (454) Murata, K.; Shin, H.-K.; Saito, K.; Kuroda, S.-i. *Thin Solid Films* **1998**, *327*–*329*, 446–449.
- (455) Franco, L.; Pasimeni, L.; Ponterini, G.; Ruzzi, M.; Segre, U. *Phys. Chem. Chem. Phys.* **2001**, *3*, 1736–1742.
- (456) Gil, A.; Aristegui, I.; Suarez, A.; Sandez, I.; Möbius, D. *Langmuir* **2002**, *18*, 8527–8534.
- (457) Jones, R. M.; Lu, L.; Helgeson, R.; Bergstedt, T. S.; McBranch, D. W.; Whitten, D. G. *PNAS* **2001**, *98*, 14769–14772.
- (458) Lu, L.; Jones, R. M.; McBranch, D.; Whitten, D. *Langmuir* **2002**, *18*, 7706–7713.
- (459) Pawlik, A.; Ouart, A.; Kirstein, S.; Abraham, H.-W.; Dähne, S. *Eur. J. Org. Chem.* **2003**, 3065–3080.
- (460) Herz, A. H. *Adv. Colloid Interface Sci.* **1977**, *8*, 237–298.
- (461) Kawasaki, M.; Aoyama, S. *Chem. Commun.* **2004**, 988–989.
- (462) Desiraju, G. R. *Crystal Engineering*; Elsevier: Amsterdam, 1989.
- (463) Bock, H.; Seitz, W.; Sievert, M.; Kleine, M.; Bats, J. W. *Angew. Chem., Int. Ed. Engl.* **1996**, *35*, 2244–2246.
- (464) Greer, M. L.; Duncan, J. R.; Duff, J. L.; Blackstock, S. C. *Tetrahedron Lett.* **1997**, *38*, 7665–7668.
- (465) Colonna, B.; Menzer, S.; Raymo, F. M.; Stoddart, J. F.; Williams, D. J. *Tetrahedron Lett.* **1998**, *39*, 5155–5158.
- (466) Ego, C.; Marsitzky, D.; Becker, S.; Zhang, J.; Grimsdale, A. C.; Müllen, K.; MacKenzie, J. D.; Silva, C.; Friend, R. H. *J. Am. Chem. Soc.* **2003**, *125*, 437–443.
- (467) Jiang, B.; Yang, S.-W.; Jones, W. E., Jr. *Chem. Mater.* **1997**, *9*, 2031–2034.
- (468) Jiang, B.; Jones, W. E., Jr. *Macromolecules* **1997**, *30*, 5575–5581.
- (469) Neuteboom, E. E.; Meskers, S. C. J.; Van Hal, P. A.; Van Duren, J. K. J.; Meijer, E. W.; Janssen, R. A. J.; Dupin, H.; Pourtois, G.; Cornil, J.; Lazzaroni, R.; Brédas, J.-L.; Beljonne, D. *J. Am. Chem. Soc.* **2003**, *125*, 8625–8638.
- (470) Romaner, L.; Pogantsch, A.; Scandiucci de Freitas, P.; Scherf, U.; Gaal, M.; Zoyer, E.; List, E. J. W. *Adv. Funct. Mater.* **2003**, *13*, 597–601.
- (471) Iqbal, R.; Moratti, S. C.; Holmes, A. B.; Yahioglu, G.; Milgrom, L. R.; Cacialli, F.; Morgado, J.; Friend, R. H. *J. Mater. Sci. Mater. El.* **2000**, *11*, 97–103.
- (472) Russell, D. M.; Arias, A. C.; Friend, R. H.; Silva, C.; Ego, C.; Grimsdale, A. C.; Müllen, K. *Appl. Phys. Lett.* **2002**, *80*, 2204–2206.
- (473) Belletête, M.; Rivera, E.; Giasson, R.; Zhu, X. X.; Durocher, G. *Synth. Met.* **2004**, *143*, 37–42.
- (474) Sanda, F.; Nakai, T.; Kobayashi, N.; Masuda, T. *Macromolecules* **2004**, *37*, 2703–2708.
- (475) Stalmach, U.; de Boer, B.; Videlot, C.; van Hutten, P. F.; Hadzioannou, G. *J. Am. Chem. Soc.* **2000**, *122*, 5464–5472.
- (476) de Boer, B.; Stalmach, U.; Melzer, C.; Hadzioannou, G. *Synth. Met.* **2001**, *121*, 1541–1542.
- (477) Gong, X.; Ostrowski, J. C.; Moses, D.; Bazan, G. C.; Heeger, A. J. *Adv. Funct. Mater.* **2003**, *13*, 439–444.
- (478) Gong, X.; Ma, W.; Ostrowski, J. C.; Bazan, G. C.; Moses, D.; Heeger, A. J. *Adv. Mater.* **2004**, *16*, 615–619.
- (479) D'Andrade, B. W.; Holmes, R. J.; Forrest, S. R. *Adv. Mater.* **2004**, *16*, 624–628.
- (480) Morgado, J.; Cacialli, F.; Iqbal, R.; Moratti, S. C.; Holmes, A. B.; Yahioglu, G.; Milgrom, L. R.; Friend, R. H. *J. Mater. Chem.* **2001**, *11*, 278–283.
- (481) Brunner, K.; van Haare, J. A. E. H.; Langeveld-Voss, B. M. W.; Schoo, H. F. M.; Hofstraat, J. W.; van Dijken, A. *J. Phys. Chem. B* **2002**, *106*, 6834–6841.
- (482) Welter, S.; Brunner, K.; Hofstraat, J. W.; De Cola, L. *Nature* **2003**, *421*, 54–57.
- (483) Tew, G. N.; Pralle, M. U.; Stupp, S. I. *Angew. Chem., Int. Ed.* **2000**, *39*, 517–521.
- (484) Chen, A. C. A.; Culligan, S. W.; Geng, Y.; Chen, S. H.; Klubek, K. P.; Vaeth, K. M.; Tang, C. W. *Adv. Mater.* **2004**, *16*, 783–788.
- (485) Geng, Y.; Chen, A. C. A.; Ou, J. J.; Chen, S. H.; Klubek, K.; Vaeth, K. M.; Tang, C. W. *Chem. Mater.* **2003**, *15*, 4352–4360.
- (486) Schmidt-Mende, L.; Fechtenköetter, A.; Müllen, K.; Moons, E.; Friend, R. H.; MacKenzie, J. D. *Science* **2001**, *293*, 1119–1122.
- (487) Markovitsi, D.; Rigaut, F.; Moualem, M.; Malthéte, J. *Chem. Phys. Lett.* **1987**, *135*, 236–242.
- (488) Markovitsi, D.; Thu Hoa Tran, T.; Briois, V.; Simon, J.; Ohta, K. *J. Am. Chem. Soc.* **1988**, *110*, 2001–2002.
- (489) Markovitsi, D.; Lécuyer, I.; Simon, J. *J. Phys. Chem.* **1991**, *95*, 3620–3626.
- (490) Ecoffet, C.; Markovitsi, D.; Jallabert, C.; Strzelecka, H.; Veber, M. *J. Chem. Soc., Faraday Trans.* **1992**, *88*, 3007–3011.
- (491) Gregg, B. A.; Fox, M. A.; Bard, A. J. *J. Phys. Chem.* **1989**, *93*, 4227–4234.
- (492) Boden, N.; Bushby, R. J.; Clements, J.; Movaghfar, B.; Fonobsn, K. J.; Kreouzis, T. *Phys. Rev. B* **1995**, *52*, 13274–13280.
- (493) Boden, N.; Bushby, R. J.; Clements, J.; Jesudason, M. V.; Knowles, P. F.; Williams, G. *Chem. Phys. Lett.* **1988**, *152*, 94–99.
- (494) Blasse, G.; Dirksen, G. J.; Meijerink, A.; Van der Pol, J. F.; Neeleman, E.; Drenth, W. *Chem. Phys. Lett.* **1989**, *154*, 420–424.
- (495) Kobayashi, N.; Higashi, R.; Ishii, K.; Hatsusaka, K.; Ohta, K. *Bull. Chem. Soc. Jpn.* **1999**, *72*, 1263–1271.
- (496) Markovitsi, D.; Lécuyer, I.; Lianos, P.; Malthéte, J. *J. Chem. Soc., Faraday Trans.* **1991**, *87*, 1785–1790.
- (497) Markovitsi, D.; Bengs, H.; Ringsdorf, H. *J. Chem. Soc., Faraday Trans.* **1992**, *88*, 1275–1279.

- (498) Markovitsi, D.; Marguet, S.; Gallos, L. K.; Sigal, H.; Millié, P.; Argyrakis, P.; Ringsdorf, H.; Kumar, S. *Chem. Phys. Lett.* **1999**, *306*, 163–167.
- (499) Markovitsi, D.; Marguet, S.; Bondkowski, J.; Kumar, S. *J. Phys. Chem. B* **2001**, *105*, 1299–1306.
- (500) Markovitsi, D.; Pfeffer, N.; Charra, F.; Nunzi, J. M.; Bengs, H.; Ringsdorf, H. *J. Chem. Soc., Faraday Trans.* **1993**, *89*, 37–42.
- (501) Sigal, H.; Markovitsi, D.; Gallos, L.; Argyrakis, P. *J. Phys. Chem.* **1996**, *100*, 10999–11004.
- (502) Weck, M.; Dunn, A. R.; Matsumoto, K.; Coates, G. W.; Lobkovsky, E. B.; Grubbs, R. H. *Angew. Chem., Int. Ed.* **1999**, *38*, 2741–2745.
- (503) Bengs, H.; Ebert, M.; Karthaus, O.; Kohne, B.; Praefcke, K.; Ringsdorf, H.; Wendorff, J. H.; Wüstefeld, R. *Adv. Mater.* **1990**, *2*, 141–144.
- (504) Gallivan, J. P.; Schuster, G. B. *J. Org. Chem.* **1995**, *60*, 2423–2429.
- (505) Green, M. M.; Ringsdorf, H.; Wagner, J.; Wüstefeld, R. *Angew. Chem., Int. Ed. Engl.* **1990**, *29*, 1478–1481.
- (506) Janietz, D.; Goldmann, D.; Schmidt, C.; Wendorff, J. H. *Mol. Cryst. Liq. Cryst. A* **1999**, *332*, 2651–2658.
- (507) Goldmann, D.; Janietz, D.; Schmidt, C.; Wendorff, J. H. *Angew. Chem., Int. Ed.* **2000**, *39*, 1851–1854.
- (508) Goldmann, D.; Janietz, D.; Schmidt, C.; Wendorff, J. H. *J. Mater. Chem.* **2004**, *14*, 1521–1525.
- (509) Hassheider, T.; Benning, S. A.; Kitzerow, H.-S.; Achard, M.-F.; Bock, H. *Angew. Chem., Int. Ed.* **2001**, *40*, 2060–2063.
- (510) Tam-Chang, S.-W.; Seo, W.; Rove, K.; Casey, S. M. *Chem. Mater.* **2004**, *16*, 1832–1834.
- (511) Percec, V.; Glodde, M.; Bera, T. K.; Miura, Y.; Shiyanskaya, I.; Singer, K. D.; Balagurusamy, V. S. K.; Heiney, P. A.; Schnell, I.; Rapp, A.; Spiess, H. W.; Hudson, S. D.; Duan, H. *Nature* **2002**, *419*, 384–387.
- (512) Shiyanskaya, I.; Singer, K. D.; Percec, V.; Bera, T. K.; Miura, Y.; Glodde, M. *Phys. Rev. B* **2003**, *67*, 035204/1–035204/7.
- (513) Janietz, D. *J. Mater. Chem.* **1998**, *8*, 265–274.
- (514) Janietz, D. *Chem. Commun.* **1996**, 713–714.
- (515) Goldmann, D.; Mahlstedt, S.; Janietz, D.; Busch, P.; Schmidt, C.; Stracke, A.; Wendorff, J. H. *Liq. Cryst.* **1998**, *24*, 881–890.
- (516) Stracke, A.; Wendorff, J. H.; Janietz, D.; Mahlstedt, S. *Adv. Mater.* **1999**, *11*, 667–670.
- (517) Mahlstedt, S.; Janietz, D.; Stracke, A.; Wendorff, J. H. *Chem. Commun.* **2000**, 15–16.
- (518) Frese, T.; Wendorff, J. H.; Janietz, D.; Cozan, V. *Chem. Mater.* **2003**, *15*, 2146–2152.
- (519) Manickam, M.; Belloni, M.; Kumar, S.; Varshney, S. K.; Shankar Rao, D. S.; Ashton, P. R.; Preece, J. A.; Spencer, N. *J. Mater. Chem.* **2001**, *11*, 2790–2800.
- (520) Samori, P.; Severin, N.; Simpson, C. D.; Müllen, K.; Rabe, J. P. *J. Am. Chem. Soc.* **2002**, *124*, 9454–9457.
- (521) Tchebotareva, N.; Yin, X.; Watson, M. D.; Samori, P.; Rabe, J. P.; Müllen, K. *J. Am. Chem. Soc.* **2003**, *125*, 9734–9739.
- (522) (a) Samori, P.; Yin, X.; Tchebotareva, N.; Wang, Z.; Pakula, T.; Jaekel, F.; Watson, M. D.; Venturini, A.; Müllen, K.; Rabe, J. P. *J. Am. Chem. Soc.* **2004**, *126*, 3567–3575. (b) Wu, J.; Baumgarten, M.; Debije, M. G.; Warman, J. M.; Müllen, K. *Angew. Chem., Int. Ed.* **2004**, *43*, 5331–5335.
- (523) Laursen, B. W.; Nørgaard, K.; Reitzel, N.; Simonsen, J. B.; Nielsen, C. B.; Als-Nielsen, J.; Bjørnholm, T.; Sølling, T. I.; Nielsen, M. M.; Bunk, O.; Kjaer, K.; Tchebotareva, N.; Watson, M. D.; Müllen, K.; Piris, J. *Langmuir* **2004**, *20*, 4139–4146.
- (524) Peeters, E.; Van Hal, P. A.; Meskers, S. C. J.; Janssen, R. A. J.; Meijer, E. W. *Chem. Eur. J.* **2002**, *8*, 4470–4474.
- (525) Kimura, M.; Narikawa, H.; Ohta, K.; Hanabusa, K.; Shirai, H.; Kobayashi, N. *Chem. Mater.* **2002**, *14*, 2711–2717.
- (526) (a) Campidelli, S.; Deschenaux, R.; Eckert, J.-F.; Guillon, D.; Nierengarten, J.-F. *Chem. Commun.* **2002**, 656–657. (b) Armaroli, N.; Accorsi, G.; Gisselbrecht, J.-P.; Gross, M.; Krasnikov, V.; Tsamouras, D.; Hadzioannou, G.; Gómez-Escalona, M. J.; Langa, F.; Eckert, J.-F.; Nierengarten, J.-F. *J. Mater. Chem.* **2002**, *12*, 2077–2087. (c) Campidelli, S.; Deschenaux, R. *Helv. Chim. Acta* **2001**, *84*, 589–593. (d) Wang, H.; Ng, M.-K.; Wang, L.; Yu, L.; Lin, B.; Meron, M.; Xiao, Y. *Chem. Eur. J.* **2002**, *8*, 3246–3253.
- (527) Estroff, L. A.; Hamilton, A. D. *Chem. Rev.* **2004**, *104*, 1201–1217.
- (528) (a) Murata, K.; Aoki, M.; Nishi, T.; Ikeda, A.; Shinkai, S. *J. Chem. Soc., Chem. Commun.* **1991**, 1715–1718. (b) Murata, K.; Aoki, M.; Suzuki, T.; Harada, T.; Kawabata, H.; Komori, T.; Ohseto, F.; Ueda, K.; Shinkai, S. *J. Am. Chem. Soc.* **1994**, *116*, 6664–6676.
- (529) van der Laan, S.; Feringa, B. L.; Kellogg, R. M.; van Esch, J. *Langmuir* **2002**, *18*, 7136–7140.
- (530) Moriyama, M.; Mizoshita, N.; Yokota, T.; Kishimoto, K.; Kato, T. *Adv. Mater.* **2003**, *15*, 1335–1338.
- (531) Swager, T. M.; Gil, C. J.; Wrighton, M. S. *J. Phys. Chem.* **1995**, *99*, 4886–4893.
- (532) Huang, W. Y.; Matsuoka, S.; Kwei, T. K.; Okamoto, Y. *Macromolecules* **2001**, *34*, 7166–7171.
- (533) Ajayaghosh, A.; George, S. J.; Praveen, V. K. *Angew. Chem., Int. Ed.* **2003**, *42*, 332–335.
- (534) Ihara, H.; Yamada, T.; Nishihara, M.; Sakurai, T.; Takafuji, M.; Hachisako, H.; Sagawa, T. *J. Mol. Liq.* **2004**, *111*, 73–76.
- (535) Maitra, U.; Vijay Kumar, P.; Chandra, N.; D'Souza, L. J.; Prasanna, M. D.; Raju, A. R. *Chem. Commun.* **1999**, 595–596.
- (536) Nakashima, T.; Kimizuka, N. *Adv. Mater.* **2002**, *14*, 1113–1116.
- (537) Sugiyasu, K.; Fujita, N.; Shinkai, S. *Angew. Chem., Int. Ed.* **2004**, *43*, 1229–1233.
- (538) Liu, Y.; Xiao, S.; Li, H.; Li, Y.; Liu, H.; Lu, F.; Zhuang, J.; Zhu, D. *J. Phys. Chem. B* **2004**, *108*, 6256–6260.
- (539) de la Escosura, A.; Martinez-Diaz, M. V.; Thordarson, P.; Rowan Alan, E.; Nolte Roeland, J. M.; Torres, T. *J. Am. Chem. Soc.* **2003**, *125*, 12300–12308.
- (540) (a) Ahrens, M. J.; Sinks, L. E.; Rybtchinski, B.; Liu, W.; Jones, B. A.; Giaimo, J. M.; Gusev, A. V.; Goshe, A. J.; Tiede, D. M.; Wasielewski, M. R. *J. Am. Chem. Soc.* **2004**, *126*, 8284–8294. (b) Li, X.; Sinks, L. E.; Rybtchinski, B.; Wasielewski, M. R. *J. Am. Chem. Soc.* **2004**, *126*, 10810–10811.
- (541) Lewis, F. D.; Letsinger, R. L.; Wasielewski, M. R. *Acc. Chem. Res.* **2001**, *34*, 159–170.
- (542) Kelley, S. O.; Barton, J. K. *Science* **1999**, *283*, 375–381.
- (543) Yu, Z. G.; Song, X. *Phys. Rev. Lett.* **2001**, *86*, 6018–6021.
- (544) Ratner, M. *Nature* **1999**, *397*, 480–481.
- (545) Meggers, E.; Michel-Beyerle, M. E.; Giese, B. *J. Am. Chem. Soc.* **1998**, *120*, 12950–12955.
- (546) Pasternack, R. F.; Bustamante, C.; Collings, P. J.; Giannetto, A.; Gibbs, E. J. *J. Am. Chem. Soc.* **1993**, *115*, 5393–5399.
- (547) Brun, A. M.; Harriman, A. *J. Am. Chem. Soc.* **1994**, *116*, 10383–10393.
- (548) Pasternack, R. F.; Goldsmith, J. I.; Szep, S.; Gibbs, E. J. *Biophys. J.* **1998**, *75*, 1024–1031.
- (549) Pasternack, R. F.; Gibbs, E. J.; Collings, P. J.; dePaula, J. C.; Turzo, L. C.; Terracina, A. *J. Am. Chem. Soc.* **1998**, *120*, 5873–5878.
- (550) Gurrieri, S.; Aliffi, A.; Bellacchio, E.; Lauceri, R.; Purrello, R. *Inorg. Chim. Acta* **1999**, *286*, 121–126.
- (551) Far, S.; Kossanyi, A.; Verchere-Beaur, C.; Gresh, N.; Taillandier, E.; Perree-Fauvet, M. *Eur. J. Org. Chem.* **2004**, 1781–1797.
- (552) Smith, J. O.; Olson, D. A.; Armitage, B. A. *J. Am. Chem. Soc.* **1999**, *121*, 2686–2695.
- (553) Seifert, J. L.; Connor, R. E.; Kushon, S. A.; Wang, M.; Armitage, B. A. *J. Am. Chem. Soc.* **1999**, *121*, 2987–2995.
- (554) Wang, M.; Silva, G. L.; Armitage, B. A. *J. Am. Chem. Soc.* **2000**, *122*, 9977–9986.
- (555) Garoff, R. A.; Litzinger, E. A.; Connor, R. E.; Fishman, I.; Armitage, B. A. *Langmuir* **2002**, *18*, 6330–6337.
- (556) Wang, M.; Dilek, I.; Armitage, B. A. *Langmuir* **2003**, *19*, 6449–6455.
- (557) Amann, N.; Pandurski, E.; Fiebig, T.; Wagenknecht, H.-A. *Chem. Eur. J.* **2002**, *8*, 4877–4883.
- (558) Tong, A. K.; Jockusch, S.; Li, Z.; Zhu, H. R.; Akins, D. L.; Turro, N. J.; Ju, J. *J. Am. Chem. Soc.* **2001**, *123*, 12923–12924.
- (559) Malakhov, A. D.; Skorobogaty, M. V.; Prokhorenko, I. A.; Gontarev, S. V.; Kozhich, D. T.; Stetsenko, D. A.; Stepanova, I. A.; Shenkarev, Z. O.; Berlin, Y. A.; Korshun, V. A. *Eur. J. Org. Chem.* **2004**, 1298–1307.
- (560) Heilemann, M.; Tinnefeld, P.; Sanchez Mosteiro, G.; Garcia Parajo, M.; Van Hulst, N. F.; Sauer, M. *J. Am. Chem. Soc.* **2004**, *126*, 6514–6515.
- (561) Lewis, F. D.; Wu, Y.; Zhang, L. *Chem. Commun.* **2004**, 636–637.
- (562) Bevers, S.; O'Dea, T. P.; McLaughlin, L. W. *J. Am. Chem. Soc.* **1998**, *120*, 11004–11005.
- (563) Bevers, S.; Schutte, S.; McLaughlin, L. W. *J. Am. Chem. Soc.* **2000**, *122*, 5905–5915.
- (564) Lewis, F. D.; Wu, Y.; Hayes, R. T.; Wasielewski, M. R. *Angew. Chem., Int. Ed.* **2002**, *41*, 3485–3487.
- (565) Lewis, F. D.; Wu, Y.; Liu, X. *J. Am. Chem. Soc.* **2002**, *124*, 12165–12173.
- (566) Rahe, N.; Rinn, C.; Carell, T. *Chem. Commun.* **2003**, 2120–2121.
- (567) Wang, W.; Wan, W.; Zhou, H.-H.; Niu, S.; Li, A. D. Q. *J. Am. Chem. Soc.* **2003**, *125*, 5248–5249.
- (568) Wang, S.; Liu, B.; Gaylord, B. S.; Bazan, G. C. *Adv. Funct. Mater.* **2003**, *13*, 463–467.
- (569) Gaylord, B. S.; Heeger, A. J.; Bazan, G. C. *J. Am. Chem. Soc.* **2003**, *125*, 896–900.
- (570) Liu, B.; Baudrey, S.; Jaeger, L.; Bazan, G. C. *J. Am. Chem. Soc.* **2004**, *126*, 4076–4077.
- (571) Liu, B.; Bazan, G. C. *J. Am. Chem. Soc.* **2004**, *126*, 1942–1943.
- (572) Wang, S.; Gaylord, B. S.; Bazan, G. C. *J. Am. Chem. Soc.* **2004**, *126*, 5446–5451.
- (573) Nagata, N.; Kugimiya, S.-i.; Kobuke, Y. *Chem. Commun.* **2000**, 1389–1390.
- (574) Tamiaki, H.; Miyatake, T.; Tanikaga, R.; Holzwarth, A. R.; Schaffner, K. *Angew. Chem., Int. Ed. Engl.* **1996**, *35*, 772–774.
- (575) Miyatake, T.; Tamiaki, H.; Holzwarth, A. R.; Schaffner, K. *Helv. Chim. Acta* **1999**, *82*, 797–810.

- (576) Miyatake, T.; Tamiaki, H.; Holzwarth, A. R.; Schaffner, K. *Photochem. Photobiol.* **1999**, *69*, 448–456.
- (577) Prokhorenko, V. I.; Holzwarth, A. R.; Müller, M. G.; Schaffner, K.; Miyatake, T.; Tamiaki, H. *J. Phys. Chem. B* **2002**, *106*, 5761–5768.
- (578) Sagawa, T.; Fukugawa, S.; Yamada, T.; Ihara, H. *Langmuir* **2002**, *18*, 7223–7228.
- (579) Syamakumari, A.; Schenning, A. P. H. J.; Meijer, E. W. *Chem. Eur. J.* **2002**, *8*, 3353–3361.
- (580) Yamaguchi, T.; Ishii, N.; Tashiro, K.; Aida, T. *J. Am. Chem. Soc.* **2003**, *125*, 13934–13935.
- (581) Tashiro, K.; Aida, T.; Zheng, J.-Y.; Kinbara, K.; Saigo, K.; Sakamoto, S.; Yamaguchi, K. *J. Am. Chem. Soc.* **1999**, *121*, 9477–9478.
- (582) Schenning, A. P. H. J.; van Herrikhuyzen, J.; Jonkheijm, P.; Chen, Z.; Würthner, F.; Meijer, E. W. *J. Am. Chem. Soc.* **2002**, *124*, 10252–10253.
- (583) Würthner, F.; Chen, Z.; Hoeben, F. J. M.; Osswald, P.; You, C.-C.; Jonkheijm, P.; van Herrikhuyzen, J.; Schenning, A. P. H. J.; van der Schoot, P. P. A. M.; Meijer, E. W.; Beckers, E. H. A.; Meskers, S. C. J.; Janssen, R. A. J. *J. Am. Chem. Soc.* **2004**, *126*, 10611–10618.
- (584) Hoeben, F. J. M.; Herz, L. M.; Daniel, C.; Jonkheijm, P.; Schenning, A. P. H. J.; Silva, C.; Meskers, S. C. J.; Beljonne, D.; Phillips, R. T.; Friend, R. H.; Meijer, E. W. *Angew. Chem., Int. Ed.* **2004**, *43*, 1976–1979.
- (585) (a) O'Neill, M. A.; Becker, H.-C.; Wan, C.; Barton, J. K.; Zewail, A. H. *Angew. Chem., Int. Ed.* **2003**, *42*, 5896–5900. (b) O'Neill, M. A.; Barton, J. K. *J. Am. Chem. Soc.* **2004**, *126*, 11471–11483.
- (586) Huisman, B.-H.; Valeton, J. J. P.; Nijssen, W.; Lub, J.; ten Hoeve, W. *Adv. Mater.* **2003**, *15*, 2002–2005.
- (587) McCulloch, I.; Zhang, W.; Heeney, M.; Bailey, C.; Giles, M.; Graham, D.; Shkunov, M.; Sparrowe, D.; Tierney, S. *J. Mater. Chem.* **2003**, *13*, 2436–2444.
- (588) Hecht, S.; Khan, A. *Angew. Chem., Int. Ed.* **2003**, *42*, 6021–6024.
- (589) Murphy, A. R.; Fréchet, J. M. J.; Chang, P.; Lee, J.; Subramanian, V. *J. Am. Chem. Soc.* **2004**, *126*, 1596–1597.
- (590) Stutzmann, N.; Friend, R. H.; Sirringhaus, H. *Science* **2003**, *299*, 1881–1885.
- (591) van Herrikhuyzen, J.; Syamakumari, A.; Schenning, A. P. H. J.; Meijer, E. W. *J. Am. Chem. Soc.* **2004**, *126*, 10021–10027.
- (592) Joachim, C.; Gimzewski, J. K.; Aviram, A. *Nature* **2000**, *408*, 541–548.
- (593) Hill, J. P.; Jin, W.; Kosaka, A.; Fukushima, T.; Ichihara, H.; Shimomura, T.; Ito, K.; Hashizume, T.; Ishii, N.; Aida, T. *Science* **2004**, *304*, 1481–1483.

CR030070Z